Galactokinase is a Novel Modifier of Calcineurin-Induced Cardiomyopathy in *Drosophila*

by

Teresa Ena Lee

Department of Cell Biology
Duke University

Date:_____

Approved:

_____
Howard A. Rockman, Supervisor

_____
Kenneth D. Poss, Chair

_____
Douglas A. Marchuk

_____
Bernard Mathey Prevot

_____
Nina T. Sherwood

Dissertation submitted in partial fulfillment of
the requirements for the degree of Doctor
of Philosophy in the Department of
Cell Biology in the Graduate School
of Duke University

2014

ABSTRACT

Galactokinase is a Novel Modifier of Calcineurin-Induced Cardiomyopathy in *Drosophila*

by

Teresa Ena Lee

Department of Cell Biology
Duke University

Date:_____

Approved:

_____
Howard A. Rockman, Supervisor

_____
Kenneth D. Poss, Chair

_____
Douglas A. Marchuk

_____
Bernard Mathey-Prevot

_____
Nina T. Sherwood

An abstract of a dissertation submitted in partial
fulfillment of the requirements for the degree
of Doctor of Philosophy in the Department of
Cell Biology in the Graduate School of
Duke University

2014

Abstract

Calcineurin is both necessary and sufficient to induce cardiac hypertrophy, an independent risk factor for arrhythmia, dilated cardiomyopathy, heart failure, and sudden cardiac death. However, current knowledge of the downstream effectors of calcineurin is limited. My study utilizes *Drosophila melanogaster* to 1) establish a reliable model for discovering novel modifiers of calcineurin-induced cardiomyopathy; and 2) discover and characterize novel modifiers of calcineurin-induced cardiomyopathy.

In this study, I generated sensitized *Drosophila* lines expressing constitutively active calcineurin ($CanA^{act}$) that was either fused to yellow fluorescent protein (YFP) or a Flag epitope (Flag-tagged) specifically in the heart using the cardiac-specific *tinC* driver (*tinC-CanA*^{act}). These sensitized lines displayed significant cardiac enlargement as assayed via optical coherence tomography (OCT), histology, and confocal microscopy. The feasibility of this method was established by testing *Drosophila* expressing deficiency of a known calcineurin modifier, *Mef*2.

Employing a targeted deficiency screen informed by calcineurin modifier screens in the eye and mesoderm, *Galactokinase* (*Galk*) was discovered as a novel modifier of calcineurin-induced cardiomyopathy in the fly through 1) genetic deficiencies, transposable elements, and RNAi disrupting Galk expression rescued *tinC-CanA*^{act}-induced cardiomyopathy; and 2) transposable element in Galk rescued *tinC-CanA*^{act}-induced decreased life span. Further characterization identified that the genetic

disruption of *Galk* rescued CanA^{act}-induced phenotypes driven in the posterior wing, but not ectodermaly, mesodermaly, or ubiquitously driven phenotypes. In a separate region, genetic disruption of the galactoside-binding lectin, galectin, was also found to rescue *tinC-CanA^{act}*-induced cardiac enlargement.

Together, these results characterize *tinC-CanA^{act}*-induced cardiac enlargement in the fly, establish that the *tinC-CanA^{act}* sensitized line is a reliable model for discovering novel calcineurin regulators and suggest that galactokinase and galectin-regulated glycosylation is important for calcineurin-induced cardiomyopathy. These results have the potential to provide insight into new treatments for cardiac hypertrophy.

Dedication

This dissertation is dedicated to my amazing family and Science. My parents, Shuo-Jen Lee and Huei-Ju Lee, your relentless sacrifices have sustained me greatly and shaped me throughout the years. My sisters, Johanna Eting Lee and Cynthia Eshiuan Lee, your cheerful support and encouragement are always worth looking forward to. Science Lee, you have always been there to accompany me and bring me joy throughout the dissertation process.

Contents

List of Tables

List of Figures

List of Abbreviations

CanA	Calcineurin
$CanA^{act}$	Constitutively active calcineurin
EDD	End-diastolic dimension
ESD	End-systolic dimension
$FCanA^{act}$	Flag-tagged constitutively active calcineurin
FS	Fractional shortening
Galk	Galactokinase
H&E	Hematoxylin and eosin
Mef2	Myocyte enhancer factor 2
NFAT	Nuclear factor of activated T cells
OCT	Optical coherence tomography
tinC	tinman enhancer element C
UAS	Upstream activation sequence
$YCanA^{act}$	Yellow fluorescent protein-tagged constitutively active calcineurin
YFP	Yellow fluorescent protein

Acknowledgements

Too many individuals have been helpful and supportive of me in my dissertation. I am especially grateful to my mentor, Howard Rockman, for the time, effort, support and encouragement you have invested in me. Thank you for your emphasis on research integrity, critical thinking, and positive attitude pushing me forward. Matthew Wolf has been exceptionally resourceful and a main contributor to my project. Thank you for your guidance throughout my project, providing me with many fly stocks and support, and going through my paper and dissertation with meticulous edits. Thank you to Ken Poss for serving as my committee chair, your constructive comments, and helping me establish a broader view to my project. Thank you to Doug Marchuk for your encouragement, helpfulness, and bringing the aspect of human genetics to my research. Thank you to Bernard Mathey-Prevot for your extensive knowledge in *Drosophila* research and thoughtful comments on my project. Thank you to Nina Sherwood for your help regarding *Drosophila* genetics and your tips and encouragement for my dissertation and defense.

From the Rockman lab, thank you to Dennis Abraham for giving me helpful comments regarding my research and reading over my dissertation. Michelle Casad and Il-man Kim have been especially helpful by teaching me about techniques in fruitfly research. Jialu Wang was a good friend and coworker, always helpful with cell experiments and Westerns. Josh Watson was resourceful in cardiology research and

everything else from paper publishing to computer problems. Sam Yu offered support, comments, and suggestions as a friend and labmate. Thank you to Lan, Weili, Cheryl, Barbara, Sima, Angad, Rachel, Gianluigi, Wei, and Kenji for your help and encouragement. Karen has been especially helpful by being on top of lab-related issues from ordering to fixing lab equipment with her magic hands. From the Wolf lab, Lin has been a great friend and neighbor, giving me thoughtful input on *Drosophila* research and life in general. Joe has provided much *Drosophila* knowledge and fly stocks. From the Chen lab, Wei has been good encouraging friend and neighbor, and generous with lending lab equipment. Bill assisted me with real time PCR.

Stephanie has helped me greatly as my dissertation spouse, providing me with food, encouragement, help, and making sure I celebrate my accomplishments. Gladys is an encouraging and helpful housemate. Thank you Weisong for your insightful comments and helping me with dissertation defense preparations. Mimi is an amazing friend and tuned in to my defense practice from Texas. Thank you Amber, Jinhu, Chenhui, Kelly, Wenshuan, Jack, Tiffany, Chunchi, Alex, Yifan, Guanwen, Wenyu, and Chienkuang for your friendship, help, and suggestions on my dissertation defense. Thank you Joann, Howard, Renee, Eric, Shuchuan, and Randy for praying for and with me earnestly. Last but not least, thank you to Devin Singh for being my personal psychiatrist and boyfriend, showing me love and support with your strong shoulders and Duke blue sweater that I have dried my tears on many times.

Chapter 1. Background and Introduction

My study aims to 1) establish a reliable model for discovering novel modifiers of calcineurin-induced cardiomyopathy using *Drosophila melanogaster*; 2) discover and characterize novel modifiers of calcineurin-induced cardiomyopathy. This research utilizes an efficient *Drosophila* model and provides insight into treating the detrimental effects of calcineurin and cardiac hypertrophy.

1.1 Calcineurin: structure and function

Calcineurin acts as a calcium/calmodulin-dependent protein phosphatase that consists of two subunits: a large CanA subunit (60 kD), and a small CanB subunit (19 kD). In the mouse, there are three *CanA* genes (*Ppp3ca*, *Ppp3cb*, and *Ppp3cc*) and two *CanB* genes (*Ppp3r1* and *Ppp3r2*), only *Ppp3ca*, *Ppp3cb* and *Ppp3r1* are expressed in the heart; in the fly, there are three *CanA* genes (*CanA1*, *CanA-14F*, and *Pp2B-14D*) and two *CanB* genes (*CanB* and *CanB2*), *CanA1*, *CanA-14F*, and *CanB* have low expression while *Pp2B-14D* and *CanB2* have moderate to high expression in the fly heart. (NCBI Gene: http://www.ncbi.nlm.nih.gov/gene) The coding sequences for calcineurin subunits are highly conserved between mammals and flies: 73-78% identical for CanA [1, 2] and 88% identical for CanB [3-5] with the catalytic regions close to completely conserved between species.

The large CanA subunit has phosphatase activity and consists of several domains: the catalytic domain, which regulates protein dephosphorylation [6], the CanB binding domain [7], the calcium/calmodulin binding domain, and the autoinhibitory domain [8]. In the inactive state, the autoinhibitory domain inhibits the catalytic domain. Binding of calcium/calmodulin activates calcineurin by alleviating this autoinhibition. A constitutively active calcineurin ($CanA^{act}$) is generated by eliminating the autoinhibitory domain, and has been used in previous studies to investigate calcineurin signaling [9-11]. Expression of constitutively active calcineurin ($CanA^{act}$) has

been found to induce cardiac hypertrophy [9], skeletal muscle hypertrophy [12, 13] and slow twitch skeletal muscle specification [14, 15]. The smaller subunit (CanB) is constitutively bound to CanA and is required for maintaining calcineurin expression [16-18]. Deficiency of CanB results in significant cardiomyopathy, including impaired cardiomyocyte growth, impaired contractility, and lethality after birth [19, 20]. In addition to cardiac and skeletal muscle hypertrophy, calcineurin is involved in many diverse processes: T cell activation [21], chondrogenesis [22], synaptic plasticity [23, 24], apoptosis [25], and cardiovascular development [26, 27].

1.1.1 NFAT as a modifier of calcineurin-induced cardiomyopathy

NFAT (Nuclear factor of activated T-cells) is well characterized as a major downstream effector of calcineurin signaling, and is both necessary and sufficient to induce cardiac hypertrophy [5, 28]. There are 5 vertebrate NFAT genes, NFATc1-5, while only the NFATc5 orthologue, not regulated by calcineurin [29, 30], exists in *Drosophila*. NFATc1-4 consist of several domains: the DNA binding domain which is highly conserved between the NFAT proteins, the NFAT homology region which binds calcineurin and is absent from NFATc5, the N-terminus transcriptional activation domain, and the C-terminus transcriptional activation domain which are largely variable between the NFAT genes [31]. The different NFAT genes are found to be expressed in most tissues with distinct temporal and spatial patterns [31].

NFAT-induced transcription is regulated at multiple levels: dephosphorylation of NFAT by calcineurin induces translocation into the nucleus and increases DNA binding affinity [32]; phosphorylation of NFAT by glycogen synthase kinase (GSK-3), protein kinase A (PKA), p38, JNK, and caseine kinase deactivates NFAT, facilitating cytoplasmic localization [33-36]; and NFAT induces transcription in cooperation with other transcription factors including AP-1, Mef2, and GATA4 [9, 14, 37]. NFAT regulates the expression of many genes, including interleukin-2,3,4 (IL-2,3,4), cyclooxygenase-2, (Cox-2), tumor necrosis factor-α (TNF-α), atrial natriuretic factor (ANF), b-type natriuretic peptide (BNP), myosin heavy chain (MHC), MCIP-1, endothelin 1 (ET-1), and troponin I, many of which are up-regulated in cardiac hypertrophy [9, 38-43]. This suggests that NFAT induces cardiac hypertrophy by activating gene expression. In addition, expressing constitutively active NFAT in the heart was sufficient to induce concentric cardiac hypertrophy, suggesting that NFAT is a major pathway in calcineurin-induced cardiomyopathy [9].

Calcineurin regulation of NFAT was first characterized in T-cell activation [21] and later discovered to regulate many processes including chondrogenesis [22], thymic development [44], cardiac morphogenesis [26], and vascular development [27]. Calcineurin-regulated NFAT is not present in the fly. However, a study used *Drosophila* S2 cells to identify a novel regulator of calcineurin-induced NFAT translocation [45],

indicating that the molecules involved in regulating NFAT downstream of calcineurin are present in the fly.

1.1.2 Mef2 as a modifier of calcineurin-induced cardiomyopathy

Myocyte enhancer factor (Mef2) is a well-known NFAT-independent pathway that has been implicated in calcineurin-mediated cardiac hypertrophy [15, 46]. In vertebrates, there are four *Mef2* genes: *Mef2a*, *Mef2b*, *Mef2c*, and *Mef2d*. There is only one Mef2 family member in the fly. Each Mef2 consists of several subdomains: a DNA binding and activation domain (including a MADS box domain and a Mef2 domain), and a transcriptional activation domain. The MADS domain is conserved 90-95% between vertebrate and *Drosophila* Mef2; the Mef2 domain is conserved 68-87% between vertebrate and *Drosophila* Mef2; the transcriptional activation domain is more variable, and is only conserved 6-16% between the vertebrate and *Drosophila* Mef2 [47]. *Drosophila* Mef2 is most highly conserved with mammalian Mef2c. The expression pattern of the different vertebrate Mef2 isoforms is distinct but overlapping, both spatially and temporally. Mef2c is the first transcript to be expressed, starting embryonic day 7.5 in the heart in mesothelial cells in the anterior heart while Mef2a and Mef2d are expressed highly after day 8.5 in the heart [47, 48]. Somatic precursors and limb buds also express *Mef2* genes starting with Mef2c expression at day 8.5 and Mef2a and Mef2d at embryonic day 9.5. These differences suggest differing functionality for each of the *Mef2*

genes. *Drosophila* Mef2 is expressed throughout the mesoderm since gastrulation and maintains expression in all precursors and differentiated muscle [49]. Mef2 is regulated through many diverse mechanisms: Mef2 functions as either homo- or heterodimers [50-53], is repressed by histone deacetylases (HDACs) [54, 55], recruits activator proteins such as mastermind-like (MAML) and ERK5 [56, 57], and post-translational modification through phosphorylation [58, 59].

Calcineurin-mediated Mef2 signaling has been investigated in many studies. Cardiac calcineurin expression has been shown to activate Mef2 reporter activity [60]. The expression of a dominant-negative Mef2 inhibited $CanA^{act}$-induced cardiac enlargement and overexpressing Mef2 caused cardiac chamber dilation [61]. In skeletal muscle, calcineurin activates Mef2 with exercise [46, 62]. Mechanistically, calcineurin was found to co-immunoprecipitate with Mef2 and induce activation of Mef2 through dephosphorylation [46]. The binding of Mef2 and calcineurin is mediated by the scaffolding protein mAKAP [63].

Although no studies have examined the role of Mef2 downstream of calcineurin in the *Drosophila* heart, preliminary studies using *Drosophila* flight muscle showed that mutation of *Mef2* modified lethality with mesodermally-expressed constitutively active calcineurin [11]. Mutating *Mef2* in *Drosophila* results in the failure to induce myosin heavy chain expression and form differentiated muscle of all lineages, including cardiac, somatic, and visceral [64-66]. Both null-mutations in *Mef2* and overexpressing Mef2

mesodermally result in late embryonic lethality [64, 67]. Similarly, the phenotype observed in flies overexpressing mesodermal constitutively active calcineurin is late pupal stage lethal with the inability for flight muscle differentiation and myosin heavy chain expression [11] and *CanB* null mutation also results in late pupal lethality [10, 11]. This is consistent with the notion that Mef2 acts downstream of calcineurin and suggests that appropriate regulation of Mef2 by calcineurin is required for normal muscle differentiation.

1.1.3 Other modifiers of calcineurin-induced cardiomyopathy

In addition to the above mentioned effectors inducing cardiac hypertrophy downstream of calcineurin, many additional proteins have been discovered to modify calcineurin-induced cardiac hypertrophy and signaling.

The myocyte-enriched calcineurin-interacting protein-1 (MCIP1) [68], calcineurin inhibitor protein (Cain) [69], and AKAP79 [70] inhibit calcineurin by direct binding and modify calcineurin-induced cardiac hypertrophy [71, 72]. There are no *Drosophila* homologues of MCIP1, cain, or AKAP79.

To date, no prior studies have focused on modifiers of calcineurin-induced cardiomyopathy in the fly. Instead, screens in the fly have focused on changes in the fly eye or lethality related to mesodermal calcineurin expression. One screen for modifiers

of calcineurin in the eye discovered *sprouty*, *CanB2*, and *Mef2* as modifiers of calcineurin-induced rough eye [10]. *Sprouty* is a negative regulator of EGFR signaling.

An additional independent suppressor screen of mesodermally expressed calcineurin-induced lethality was performed and identified *CanB2* and *Mef2* as modifiers of calcineurin-induced lethality [11]. These prior investigations underscore the importance of Mef2 in calcineurin signaling and highlight the observation that other as-yet-unidentified modifiers exist that potentially impact calcineurin signaling.

1.2 Calcineurin and cardiomyopathy

Numerous studies have concluded that calcineurin is both necessary and sufficient to induce cardiac hypertrophy [9, 72-76]. Expressing constitutively active calcineurin ($CanA^{act}$) in the mouse heart results in a cardiac hypertrophy phenotype characterized by a thicker heart wall and an enlarged cardiac chamber, which progressed to heart failure and sudden premature death [9]. Inhibiting calcineurin with the calcineurin inhibitors cyclosporin A or FK506 attenuated cardiomyopathy in mice with mutations in tropomodulin, myosin light chain-2, or fetal β-tropomyosin (genes associated with familial cardiac hypertrophy) in the heart. In the same study, FK506 calcineurin inhibition was also found to attenuate cardiac hypertrophy caused by pressure overload in rats [76]. Calcineurin mRNA and protein levels are increased in rat cardiomyocytes upon stimulation with hypertrophic agents such as angiotensin II,

phenylephrine, and 1% fetal bovine serum. Genetic inhibition by expressing the calcineurin inhibition proteins Cain and AKAP79 with adenovirus attenuated angiotensin II, phenylephrine, and 1% fetal bovine serum-induced hypertrophy in cultured rat cardiomyocytes [72]. Calcineurin null mice have decreased heart size and do not display cardiac hypertrophy after provocation by pressure overload, or angiotensin II or isoproterynol stimulation [73]. Activated calmodulin-bound calcineurin is upregulated 4 fold in failing human heart tissue [75]. Angiotensin II-induced cardiac hypertrophy in rats was suppressed by cyclosporine (CsA), a calcineurin inhibitor [74, 77].

To summarize the above findings, calcineurin has been proven to be important for cardiomyopathy on multiple levels: 1) expressing constitutively active calcineurin ($CanA^{act}$) in the heart causes cardiac hypertrophy; 2) calcineurin activity is increased with hypertrophic stimulation; 3) inhibiting calcineurin genetically and pharmacologically attenuates genetic or induced cardiac hypertrophy.

Current knowledge of calcineurin signaling leading to cardiac hypertrophy is summarized in Figure 1. Calcineurin signaling in mammals involves calcineurin-dependent dephosphorylation of nuclear factor of activated T cells (NFAT) transcription factors [9, 78]. The calcineurin/NFAT pathway was initially discovered in T-cell activation and is the most well studied pathway downstream of calcineurin activation [79]. In contrast, *Drosophila* do not contain calcineurin-regulated isoforms of NFAT and

use NFAT-independent pathways [80]. As such, whether calcineurin will induce a cardiac phenotype in *Drosophila* remains to be investigated.

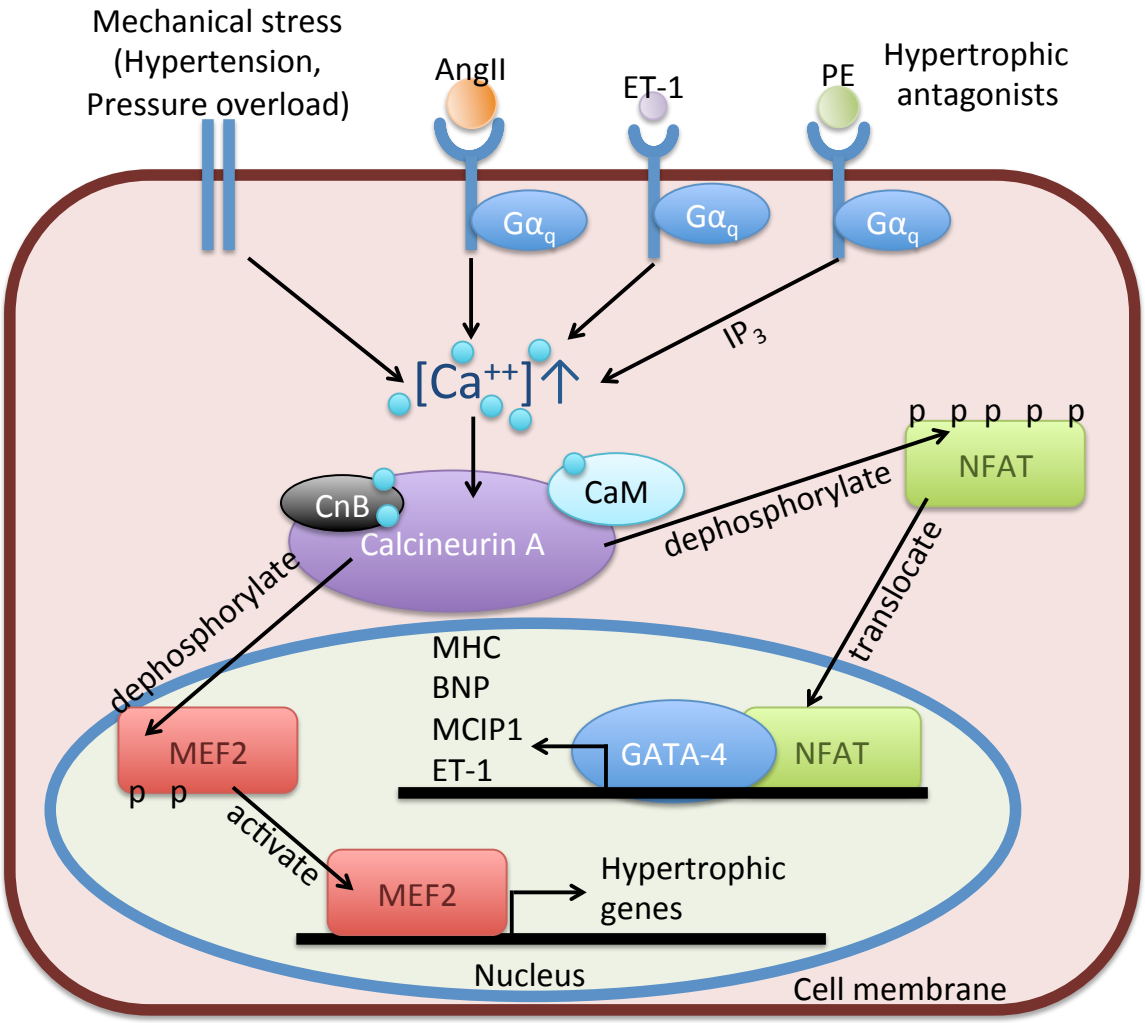

Figure 1: Known pathways regulated by calcineurin signaling.

Currently known signaling pathways related to calcineurin signaling. With upstream activation by hypertrophic signals such as angiotensin II (AngII), endothelin-1

(ET-1), phenylephrine (PE), or mechanical stress, intracellular calcium concentration is increased, triggering the activation of the calcineurin complex by calcium/calmodulin (CaM) and binding with the CanB subunit. Activated calcineurin then dephosphorylates NFAT, leading to nuclear translocation and downstream hypertrophic gene transcription. Another known pathway downstream of calcineurin activation is dephosphorylation and activation of Mef2, leading to activation of downstream hypertrophic signaling. Adapted from [81].

In contrast to the above-mentioned pathological cardiac hypertrophy, cardiac hypertrophy stimulated by exercise is physiological, is not typically associated with abnormal cardiac function, and does not stimulate calcineurin/NFAT signaling [82]. These findings further support that calcineurin negatively impacts cardiac function and understanding calcineurin downstream signaling factors is important for our understanding of cardiac disease. In addition, current inhibitors (cyclosporin A and FK501) of calcineurin exert side effects with immunosuppression, nephrotoxicity, and off-target effects, further demanding the need for insight into calcineurin signaling for treatment of cardiac hypertrophy.

1.3 Cardiac hypertrophy: progression and signaling

Cardiovascular disease is the leading cause of mortality in the United States of America. Pathological cardiac hypertrophy is a response initiated by multiple factors including stress (neuroendocrine factors), hypertension (pressure overload), valve dysfunction (volume overload), and familial mutations in sarcomeric or calcium handling genes. Initially, this response compensates for cardiac function by increasing cardiac muscle. However, prolonged cardiac hypertrophy is a known independent risk factor for arrhythmia, dilated cardiomyopathy, heart failure, and sudden death [83-86]. These results indicate that intervention and treatment of cardiac hypertrophy is an important aspect of treating cardiac disease.

Pathological cardiac hypertrophy shows many morphological and biochemical changes. Based on morphology of the cardiac wall, two types of cardiac hypertrophy are characterized: 1) concentric hypertrophy, where sarcomeres are added in parallel and cause the cardiac wall to thicken [87], and 2) eccentric hypertrophy, where sarcomeres added in series induce an increase in the radius of the wall [88, 89]. Biochemically, many changes to protein and gene expression have been shown. The adult onset of a fetal gene program is elicited: atrial natriuretic factor (ANF) is induced in both pressure-overload-induced concentric hypertrophy and volume-overload-induced eccentric hypertrophy while skeletal muscle α-actin and β-myosin heavy chain are induced with pressure-overload [90]. Expression of sarcoplasmic (endoplasmic)

reticulum calcium-ATPase 2A (SERCA) is decreased, which leads to abnormal calcium regulation and contractility of the heart. In addition to an increase in cardiomyocyte size, fibrosis, arrhythmia, and myofibrillar disarray are also characteristics of pathological cardiac hypertrophy.

In addition to the aforementioned calcineurin-related pathways, several branches of signaling pathways have been found in induced cardiac hypertrophy. These pathways form a complex network of regulation involving crosstalk at multiple points [91]. One major pathway regulating cardiac hypertrophy involves neuroendocrine factors such as endothelin (ET-1), angiotensin II (AngII), and catecholamines binding to G protein coupled receptors (GPCRs associated with Gαq/11) which signal through phospholipase C (PLC) to increase calcium concentration, activation of protein kinase C (PKC), calcium/calmodulin activated kinase (CaMK), export of histone deacetylases (HDAC), and activation of Mef2 [92, 93]. The increase in calcium also activates calcineurin through binding of calcium/calmodulin [94].

Another major pathway in cardiac hypertrophy is the mitogen-activated protein kinase (MAPK) signaling pathway: GPCRs (ET-1, AngII), receptor tyrosine kinases (IGF-1, FGF receptors), receptor serine/threonine kinases (TGFβ), reactive oxygen species (ROS), and mechanical stretch activate the MAPK signaling cascade, signaling to ERK, JNK, or p38-MAPK [91, 95]. Interestingly, expressing activated MEK1, which directly activates ERK, induced a compensated cardiac hypertrophy that is not associated with

heart failure [96], while overexpressing a constitutively active form of the upstream activator Ras, which activates ERK, JNK, and PI3K [97], induced a pathological phenotype [98]. Several studies have also indicated that ERK plays a protective role in inhibiting apoptosis [99, 100] while also activating *NFAT* gene expression [101]. The distinct roles of these pathways and their involvement in eccentric vs. concentric hypertrophy are currently unclear. Recent studies in transgenic mice suggest that activating the MEK1/ERK1/2 pathway promotes concentric hypertrophy [96] while MEK5/ERK5 activation promotes eccentric hypertrophy [102]. To add to the complexity of signals underlying cardiac hypertrophy, a study examining different mouse models that display cardiac hypertrophy (further discussed in the next section) discovered that the upregulated genes did not completely overlap. In this study, gene upregulation was analyzed for mice expressing protein kinase C-ε activating peptide (ΨεRACK), calsequestrin (CSQ), calcineurin, and Gαq using microarray. These results indicate that a similar phenotype of cardiac hypertrophy can be elicited from distinct sets of gene expression [103]. These studies suggest that pathological cardiac hypertrophy results from a balance of multiple intracellular signaling pathways that remain to be elucidated.

Hypertrophy of the heart can also be triggered in the form of genetically inherited disease, familial hypertrophic cardiomyopathy. Familial hypertrophic cardiomyopathy manifests as thickening of the cardiac wall, myofibrillar disarray, and fibrosis [104]. It is characterized as a monogenic Mendelian-inherited disease resulting

from 1,400 known mutations in 20 genes, affecting 0.2% of the population [105]. Even though many afflicted are asymptomatic, up to 25% will develop detrimental symptoms or sudden death. A majority of the mutations are in sarcomeric genes including β-myosin heavy chain (MYH7), myosin binding protein-C (MYBPC3), cardiac troponin T (TNNT2), myosin light chain (MYL2), cardiac α-actinin (ACTC), and titin (TTN) [106, 107]. Two genes account for the majority of familial hypertrophic cardiomyopathy cases: MYH7 mutations account for 35-50%, MYBPC3 mutations account for 20-35%. The mechanisms behind induction of hypertrophy from genetic mutations are controversial. The genetic mutations that occur correlate to calcium-binding domains, which may alter the ability of the cardiac muscle to contract, increasing stress and downstream signaling. However, this has not been empirically demonstrated, and studies show inconsistencies as to whether the mutations enhance or decrease calcium sensitivity [108, 109]. Mutations in calcineurin have not been implicated in familial hypertrophic cardiomyopathy. However, it is conceivable that calcineurin may be activated due to the alterations in calcium availability.

In addition to the previously mentioned classification of cardiac hypertrophy into concentric and eccentric types according to dimensional changes in the cardiac chamber, cardiac hypertrophy is also commonly classified into pathological or physiological types according to whether the observed remodeling is maladaptive in nature. Physiological cardiac hypertrophy occurs during growth in childhood, exercise,

and pregnancy [110-113]. Physiological cardiac hypertrophy is not associated with fibrosis, arrhythmia, or heart failure, and is regulated by a distinct yet overlapping set of signaling factors [91, 112]. IGF-I signaling through downstream effectors including Ga/q PI3K, AKT, mTOR and GSK3β regulates physiological cardiac hypertrophy [114]. In addition to having distinct signaling pathways and phenotypes, physiological cardiac hypertrophy does not appear to activate the fetal gene program or calcineurin-NFAT signaling [82, 115].

Current treatment for cardiac hypertrophy includes an array of pharmacological inhibitors of the underlying hypertension which also show efficacy in reducing hypertrophy, including angiotensin-converting enzyme blockers, angiotensin receptor blockers, β-adrenergic receptor blockers, and calcium channel blockers [88, 116, 117]. However, not all patients are responsive to current treatment and the disease often progresses even in the responsive patients [118]. More effective treatment is needed to target multiple aspects of this complex disease involving numerous signaling pathways, which may differ from patient to patient. In addition, investigating the factors involved in pathological versus physiological cardiac hypertrophy, such as calcineurin, will provide insight into combinations of molecules within the pathway that should be either enhanced or suppressed for guiding the intricate balance between overlapping effects of individual signaling pathways towards the most beneficial phenotype. Since calcineurin is strongly associated with pathological cardiac hypertrophy, discovering novel

mechanisms involved in calcineurin downstream function has high potential to generate novel therapeutic targets.

1.4 Animal models of cardiac hypertrophy

Animal models have the advantage of the ability to set up proper control experiments, to have enough animals in each experimental group to perform rigorous statistical analysis, and to genetically or pharmacologically manipulate to rigorously test specific molecular pathways. Many animal models have been used to facilitate the study of cardiac hypertrophy.

1.4.1 Mouse (*Mus musculus*)

The mouse model has been extensively used to study cardiac hypertrophy. A large community of researchers and tools are available, including transgenic mice with gene knock-out or overexpression under inducible and constitutive promoters. The generation time of the mouse is 5-8 weeks. The mouse heart is similar to the human heart developmentally and structurally, consisting of four cardiac chambers, left and right atria and ventricles. The genes expressed controlling cardiac development and the components of the sarcomeric structure are highly conserved [119]. Of note, one major discrepancy between the mouse and human hearts is the neonatal versus adult myosin heavy chain (MHC) isoforms expressed: the mouse expresses predominantly β-MHC

embryonically with a complete switch to α-MHC after birth [120] while humans do not undergo this switch and express primarily β-MHC in the adult ventricles [121, 122]. Even so, both mice and humans display an increase in β-MHC percentage with hypertrophy (3% to 25% in mice and 75% to 95% in humans) [123, 124].

The most commonly-utilized method for pressure-overload cardiac hypertrophy is by using transverse aortic constriction (TAC), mimicking the cardiac hypertrophy response of human patients [125]. Many studies have utilized this model to discover genes that are necessary for cardiac hypertrophy. Inhibition of cyclic GMP phosphodiesterase 5A (PDE5A) was found to inhibit TAC-induced cardiac hypertrophy, including heart weight/tibia length, fractional shortening, and fibrosis. Other genes found to mediate TAC-induced cardiac hypertrophy include calcium/calmodulin-dependent protein kinase II (CaMKII) [126], phosphoinositide 3-kinase (PI3K) [127], and growth factor receptor-bound protein 2 (Grb2) [128]. Pharmacological stimulation including the adrenergic receptor agonists phenylephrine (PE) and isoproterenol [129], and angiotensin II [130] have also been used to simulate stress conditions and cardiac hypertrophy.

Cardiac hypertrophy in mice has been induced genetically. Genetic models have been produced to express molecules in the multiple signaling pathways inducing cardiac hypertrophy. One of these molecules is Gαq. Gαq activates signaling downstream of GPCRs and many agonists that induce cardiac hypertrophy such as ET-1

and AngII described in the previous section [91]. Mice overexpressing Gαq in the heart display significant cardiac hypertrophy, reduced fractional shortening, but no fibrosis or myofibrillar disarray [131]. Another molecule is the calcium storage protein, calsequestrin. Calcium handling is significantly altered during cardiac hypertrophy [132]. Overexpression of calsequestrin in mice results in cardiac hypertrophy and fetal gene expression [133]. Protein kinase C (PKC) regulates angiotensin-induced gene activation [134], and overexpression of the PKCβ2 and ε isoforms induce cardiac hypertrophy while only the PKC isoform mediates contractile dysfunction [135, 136]. In this respect, expression of a small 8 a.a. peptide encoding the region on the receptor of activated PKC (ΨεRACK), which acts as a PKCε agonist, induced a minor hypertrophy with decreased fractional shortening [137]. Genetic manipulations, though not able to represent the full scale of alterations in a clinical setting, are useful in delineating the regulation of individual pathways.

1.4.2 Rat (*Rattus norvegicus*)

The rat model has been extensively used to study cardiac hypertrophy, taking advantage of the larger size for making hemodynamic measurements. Like the mouse heart, the rat heart is also similar to the human heart in structure. The rat generation time is longer than that of the mouse (8-12 weeks). Hypertrophy models for rats include aortic banding [138, 139] and norepinephrine stimulation [140], and have been useful in

determining molecular and cellular aspects of cardiac hypertrophy [141-143]. Due to their larger size and longer generation time compared to mice, transgenic rats are more difficult to generate though tools are available [144]. Transgenic rats expressing renin, upstream to the generation of angiotenisin II, develop cardiac hypertrophy without signs of heart failure [145].

1.4.3 Other animal models

Many other larger mammalian models have been used to study cardiac hypertrophy. These include aortic constriction or pulmonary artery constriction in rabbits, hamsters, dogs, cats, pigs, ferrets, and sheep. These models have the advantage of being closer in size and electrophysiology to humans, with disadvantages of longer generation times and less widespread genetic tools [146].

The zebrafish heart also possesses high conservation in developmental and structural genes compared to humans [147]. The zebrafish heart undergoes similar early morphologic changes during development without septation, resulting in a 2 chamber heart with one atrium and one ventricle. Zebrafish have the advantages of ease of care, low generation time, high yield, and well-developed genetic manipulation tools [148]. Although extensive research has investigated cardiac development and regeneration in zebrafish [148-150], fewer studies have been performed regarding cardiac hypertrophy. Knocking down the MYBPC homologue, which causes familial hypertrophic

cardiomyopathy in humans, results in significant cardiac hypertrophy with increased wall thickness, decreased diastolic relaxation rate, and impaired calcium reuptake [151]. Anemic fish with a mutation in erythrocyte-specific transmembrane protein band 3 (*tr265*) resulted in significant cardiac hypertrophy with increased heart size, proliferation, myofibrillar disarray, and fetal gene activation [152].

The model used for my study, the fruitfly (*Drosophila melanogaster*), is the smallest and most efficient system for performing genetic studies with a visible heart, and will be discussed in detail in the following chapters.

1.5 Drosophila as a model system

Drosophila is well adapted for genetic studies: it has a relatively short generation time (2 weeks), well developed genetic manipulation methods, and well developed genetic resources, including mutation stocks and vectors for making transgenics [153-155].

The Gene Disruption Project (GDP) and Exelixis collections have focused efforts on generating at least one gene disruption for every gene [156] and maximal coverage of the entire *Drosophila* genome with deficiency lines [157, 158]. Genetic disruptions include many different transposable element insertion lines, large stretches of DNA with inverted repeats on either end that are recognized by specific transposase, allowing integration into the genome. The first transposable element discovered and utilized in

the fruitfly was the *P*-element, recognized by the P protein transposase [159, 160]. The piggyBac element, discovered in the cabbage looper moth *Trichoplusia ni* [161], and the Minos element, discovered in *Drosophila hydei* [162], have also subsequently been utilized for gene disruption. Each of these transposable elements have insertion site preferences, making it necessary to utilize different elements for maximal coverage of the genome. Deficiency stocks are generated by introducing Flp-FRT sites and Flp recombinase to induce recombination between two inserted elements, deleting the portion of the chromosome between the two elements in progeny [157].

Many systems are also available to generate knock-down or knock-out of gene expression including RNAi, CRISPR, and TALEN systems. The emerging CRISPR system allows for specific gene targeting with a short guide RNA and has been utilized in several studies and reported to have less off-target effects than RNAi [163-165]. The TALEN system is more specific but requires more specialized techniques [166-168]. CRISPR and TALEN systems can also be utilized for site-specific mutagenesis and genetic knock-in [166, 169, 170].

In addition to gene disruption, transposable element constructs are also widely utilized for making transgenic flies expressing a gene of interest and for enhancer or protein trapping. A transposable element insertion carrying a promoter sequence driving a specific gene of interest generates an overexpression transgenic fly. The Gal4/UAS system greatly enhanced the efficiency and versatility of gene expression.

Gal4 is a transcription factor that specifically recognizes the UAS (Upstream Activation Sequence) promoter, driving expression. By using a bipartite system, a gene of interest downstream to a UAS promoter can be crossed to different driver-Gal4 lines to efficiently express a gene of interest in different tissues or express different genes with the same driver without going through the lengthy process of embryo injection, propagation, and mapping [171]. Enhancer trapping involves transposable elements carrying a reporter gene, often lacZ or GFP fused to a minimal promoter, which can utilize enhancer elements [172]. Protein trapping involves an insertion without a minimal promoter in an artificial exon to examine the expression of GFP fusion proteins [173, 174]. The above applications are only part of the many strategies and techniques that have been developed and utilized in *Drosophila* research.

1.6 The Drosophila heart

The *Drosophila melanogaster* heart consists of a tube-like structure running along the center of the abdominal dorsal cuticle (Figure 2). This structure is formed by a single layer of 52 pairs of *tin*-expressing (104 total) cells, one on each side of the cardiac tube [175]. At the intersection of each abdominal segment, a pair of valve-like cells, ostia, allow hemolymph to enter the cardiac tube from the abdomen with contraction of the cardiac tube. The beating heart plays multiple important roles in maintaining vitality of the fly: hemolymph carries nutrients [176, 177], and immune cells (hemocytes) [178];

hemoglobins carry oxygen (intracellular to tracheal and fat body cells) [179], and displacement of hemolymph in the abdominal cavity assists with airflow in the tracheal system for ventilation [180, 181]. In a *Drosophila* RNAi screen, cardiac-specific knock-down of regulators of heart function have been shown to induce early death [182], demonstrating that cardiac function is important for survival of the fly.

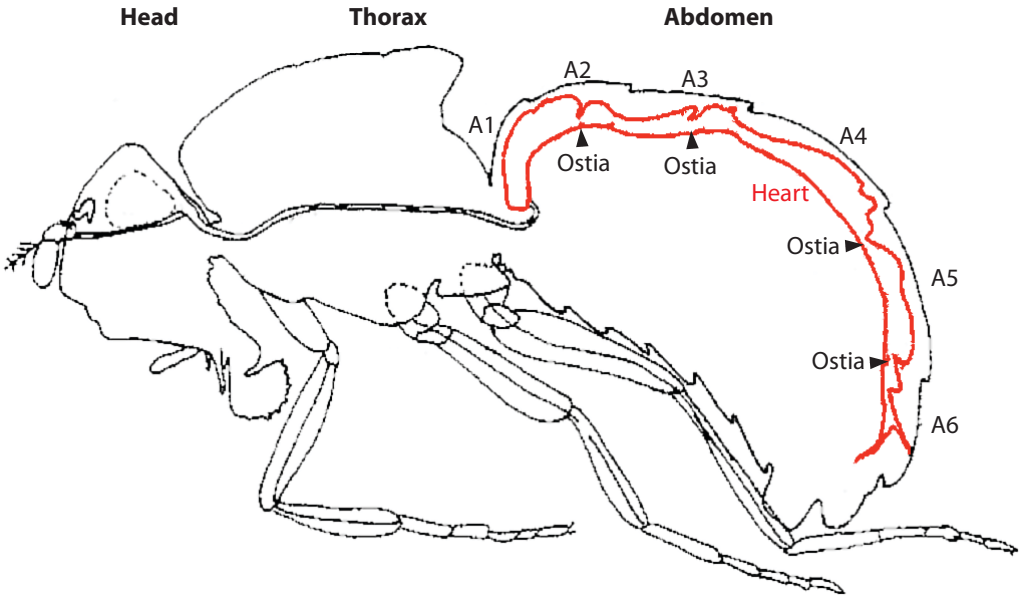

Figure 2: The *Drosophila melanogaster* circulatory system.

A longitudinal view of the *Drosophila melanogaster* circulatory system is shown. The heart (dorsal vessel) is a tube, shown in red, lying underneath the cuticle, adjacent to the dorsal side of the abdomen. Abdominal segments A1-A6 are also labeled

according to the cuticle pattern. Corresponding ostia (valve-like structures that allow hemolymph to come through) are also labeled. [154]

Several methods have been employed by different groups to study cardiac morphology and function. The fine structure of the *Drosophila* heart can be visualized by a number of approaches: paraffin sectioning with H&E stain, transmission electron microscopy, and visualization under a fluorescence microscope after dissection by exposing the heart from the abdominal side with immunostaining [183, 184]. These methods can visualize the structure and morphology of the heart in detail, but can not provide functional data. The beating heart can be monitored by dissecting the heart of the adult fly or by immobilizing the larva (the beating heart is visible under the transparent cuticle) and recording of transmitted light under a dissection microscope [185]. Software programs record the beating heart through time, producing an efficient way to visualize and monitor heart rate [186]. However, this method only detects heart rate and does not allow for analysis of function. The semi-automated optical heartbeat analysis (SOHA) method involves two software programs and allows for monitoring of heart rate and cardiac dimensions and contractile function on the left-right axis over time [187]. However, this method involves careful dissection of the heart to avoid damage and the heart rate is significantly altered from loss of neuronal input [188].

Optical coherence tomography (OCT) is used to efficiently monitor intact awake *Drosophila* heart [189]. Real-time monitoring allows for detection of the size of the cardiac lumen through the cardiac cycle, from end-diastole (the heart at its most relaxed state) to end-systole (the heart at its most constricted state) (Figure 3). Therefore, OCT has been utilized in my study for making cardiac measurements.

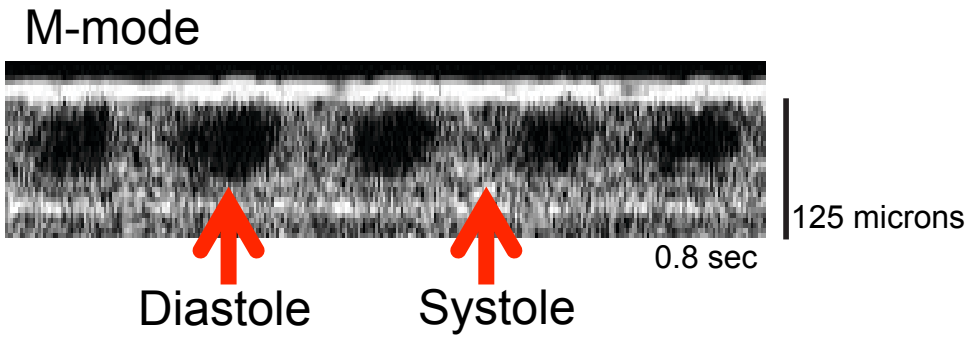

Figure 3: Visualizing the beating *Drosophila* heart with OCT in intact, awake flies.

The adult *Drosophila* heart can be monitored in real time using OCT. M-mode images are captured by collecting data from one straight line through the transverse section of the heart through time. End diastolic dimensions (the heart at its most relaxed state) and end systolic dimensions (the heart at its most constricted state) are easily visualized (red arrows).

Drosophila is a good model for investigating the heart. Many pathways are conserved among mammalian and *Drosophila* cardiac development [153, 190-193]. These include cardioblast specification genes like *Drosophila* tinman (*tin*) (homologous to mouse Nkx2.5), *Drosophila* decapentaplegic (*dpp*) (homologous to mouse BMP), and cardiomyocyte differentiation genes like *Mef2*, which are conserved in *Drosophila* and mammals. In addition, the main machinery for muscle contraction including actin, myosin heavy chain, myosin light chain, and tropomyosin, are also conserved between *Drosophila* and mammals. In fact, strategies based on fly genetics have been used to identify genes that cause or modify cardiomyopathies [182, 189, 194]. Many studies have analyzed genes causing cardiac dilation [184, 189, 195-197] or arrhythmia [188, 198-200], while cardiac hypertrophy has been less investigated. One study found that expressing constitutively active EGFR or Ras in the heart induces cardiac wall thickness in the fly [194].

In addition to the above advantages, since *Drosophila* do not express calcineurin-regulated NFAT [80], this increases the possibility of discovering novel genes downstream of calcineurin activation. Therefore, we conducted studies using fly genetics to identify novel modifiers of cardiac calcineurin-induced cardiomyopathy.

1.7 Calcineurin screens in the fly

Previously, two independent screens have been conducted to identify modifiers of calcineurin phenotypes in tissues other than the heart [10, 11]. The deficiency regions identified are summarized in Table 1. Sullivan and Rubin performed a dominant modifier screen in the *Drosophila* eye and found five suppressor and four enhancer loci [10]. Two modifier genes, *CanB2* and *sprouty* were identified. However, modifier genes within the seven other broadly mapped loci remained uncharacterized. Gajewski *et al* found seven different deletion intervals that suppressed the lethal phenotype of constitutively active calcineurin driven by the general mesodermal driver 24B [11]. Interestingly, only one interval overlapped between these two studies on chromosome 3L, cytolocation 66F5 (gray, Table 1). This is the region where I initiated my study.

Table 1: Suppressor regions in previous calcineurin screens.

Chr	Cytolocation	Region	Driver	Overlapping
2L	21A1-21B8	326.5 kbp, 56 genes	Mesoderm	No
2R	43E16, CanB2	Modifier gene found, *CanB2*	Eye Mesoderm	Yes
2R	46A-46C	351 kbp, 51 genes Modifier gene found, *Mef2* (preliminary)	Mesoderm	No
2R	59A1-59D4	609 kbp, 109 genes	Mesoderm	No
3L	60E2-60E12	221 kbp, 40 genes	Mesoderm	No
3L	63D2, Sty	Modifier gene found, *sty*	Eye	No
3L	65E-68C	4,621 kbp, >500 genes	Eye	Yes
3L	66F5	28.43 kbp, 4 genes	Mesoderm	Yes
3L	76B1-76B5	158 kbp, 23 genes	Mesoderm	No
3R	86A-89B	6,374 kbp, >500 genes	Eye	No

1.8 Specific aims

Calcineurin plays an important regulatory role in cardiac hypertrophy. Cardiac hypertrophy is a deleterious condition which pends novel targets for therapy. The *Drosophila melanogaster* is an efficient model for performing screens to discover novel modifier genes.

Accordingly, the specific aims I have accomplished in this study are as follows:

1) Establish a reliable model for discovering novel modifiers of calcineurin-induced cardiomyopathy in the *Drosophila melanogaster* heart.

2) Discover and characterize novel modifiers of calcineurin-induced cardiomyopathy in the *Drosophila melanogaster* heart.

Chapter 2. Materials and methods

2.1 Drosophila stocks

The following *Drosophila* stocks were obtained from the Bloomington *Drosophila* Stock Center: w^{1118}, *Df(3L)ED4416*, *Df(3L)ED4421*, *Df(3L)ED4414*, *Df(3L)ED4415*, *Df(3L)ED4413*, *Df(3L)BSC130*, *Df(3L)BSC170*, *Df(3L)BSC390*, $Df(2R)X1,Mef2^{X1}/CyOAdh^{nB}$, $sty^{\Delta 5}/TM3,P\{35UZ\}2$, $P\{EP\}CanB2^{EP774}$, $PBac\{PB\}Galk^{c03848}$, $Mi\{ET1\}Galk^{MB10638}$, $P\{wHy\}galectin^{DG25505}$, *P{GD4334}v16746*(Doc1 RNAi), *P{TRiP.JF02222}attP2* (Doc1 RNAi), *P{GD4335}v37634* (Doc2 RNAi), *P{TRiP.JF02223}attP2* (Doc3 RNAi), $sna^{Sco}/SM6a$, *P{hsILMiT}2.4*, *P{en2.4-Gal4}e16E* (*e16E-Gal4*), *P{GAL4-dpp.blk1}40C.6* (*dpp-Gal4*), *P{Act5C-GAL4}25FO1* (*Act5C-Gal4*), *P{GAL4-Mef2.R}3* (*mef2-Gal4*). The *Drosophila* stock $PBac\{PB\}Argk^{f05255}$ was obtained from the Exelixis Collection at Harvard Medical School. The following *Drosophila* stocks were obtained from the Vienna *Drosophila* RNAi Center: *P{KK107841}VIE-260B* (*Galk* RNAi), *P{GD4334}v16747* (*Doc1* RNAi), *P{GD4335}v37634* (*Doc2* RNAi). The double balancer line *WR135* was kindly provided by Dr. Robin Wharton. The *P{tinC-Gal4}* line was kindly provided by Dr. Manfred Frasch [201]. The *UAS-Mef2* line was kindly provided by Dr. Michael Taylor [64, 202]. The *TnI* mutant *hdp2* was a kind gift from Dr. Jim Vigoreaux and had previously been shown to induce flight muscle [203] and cardiac enlargement [189] phenotypes. The *P{tinC-GFP}* (*tinC-GFP*) line was generated as previously described by inserting the 304 bp *tinC* genetic sequence into the pGreen-H-Pelican vector [184, 201, 204] and the construct injected at the Duke University Model Systems Genomics Facility. The $tinC\text{-}YCanA^{act}$, *tinC-*

FCanA^{act}, and *UAS-YCanA^{act} Drosophila* lines were generated at the Duke University Model Systems Genomics Facility by injecting the corresponding constructs into *Drosophila* embryos.

2.2 Cloning

The *tinC-YCanA^{act}*, *tinC-FCanA^{act}*, *UAS-YCanA^{act}*, and *UAS-Galk* constructs for transgenic expression were generated using standard procedures. Constitutively active calcineurin (CanA^{act}) was generated from *Drosophila* cDNA as previously described by amplifying *Pp2B-14D* with corresponding primers, excluding the c-terminus auto-inhibitory domain [10]. The following primers were used: ATG TCT TCG AAT AAC CAG AGC AGC AG (forward) and TCA GTT GCG TAT CAC CTC CTT GCG CA (reverse). The amplified product was blunt-end ligated into TOPO vector (Invitrogen, Inc.) and subsequently amplified with corresponding restriction enzyme sites. The YFP tag was added to the N-terminus of CanA^{act} by cutting with the corresponding restriction enzyme sites and ligating into the pEYFP-C1 vector. For the Flag tag, the full-length sequence of the tag was added on the amplification primer to directly generate a tagged sequence. For the *tinC-CanA^{act}* constructs, the tagged sequence of either YFP-tagged CanA^{act} (YCanA^{act}) or Flag-tagged CanA^{act} (FCanA^{act}) were then cut and ligated into the pCaSpeR5 *Drosophila* expression vector. This vector contained the *tinC-hsp70* promoter to the N-terminus as previously described [184]. The *UAS-YCanA^{act}* construct

was generated by cutting and ligating the tagged YCanA^{act} sequence with restriction enzyme sites into a pUAST *Drosophila* vector. This vector consists of the UAS-promoter, which drives expression of the transgene upon binding of the Gal4 transcription factor. The catalytic activity of N-terminal YFP-tagged *CanA^{act}* has been confirmed in studies by a number of investigators, using well characterized NFAT reporter assays [205, 206], NFAT phosphorylation assays [205], and NF-κB reporter assays [207].

2.3 Histology

Histology was performed according to standard procedures [208]. 3 - 5 day old flies of the corresponding genotypes were collected and washed briefly with 70% ethanol to clean the surface and facilitate infiltration of the fixative and fixes the fly hearts at the most relaxed state, end-diastole. To assess this, OCT images were measured and compared between alive *w^{1118}* end-diastolic dimension (46.37 ± 4.91 microns, N=9) and the size of the heart after EtOH fixation (50.19 ± 6.09 microns, N=9), P=N.S., student's t test. Flies were then fixed in formalin at 4°C overnight. The next day, flies were washed in PBS and subsequently through an ethanol gradient up to a solution consisting of 95% ethanol with 5% glycerol to soften the cuticle and facilitate the sectioning process. The flies were then submerged in xylene, and then incubated at 60°C with one 40 minute paraffin wax wash followed by incubation overnight under vacuum in liquid wax. Samples were then positioned in molds and the wax allowed to harden.

8 μm sections were cut using a standard microtome and adhered to poly-L-lysine-coated glass slides. After drying overnight on a 37°C slide warmer, slides were collected for staining. Standard hematoxylin and eosin (H&E) staining procedures were performed. Slides were warmed vertically at 50°C for 30 minutes and subsequently submerged in xylene before going into an ethanol gradient to rehydrate into water before performing hematoxylin & eosin staining according to standard procedures. The slides were then dehydrated through an ethanol gradient into xylene and mounted in Cytoseal XYL mounting medium (Thermo Fisher Scientific Inc.). Slides were then allowed to harden overnight at 37°C. Images were captured using the PAXcam ARC camera connected to the Olympus IX70 inverted microscope and quantified for lumen area and perimeter in imageJ, calibrated with a hemocytometer measuring 50 μm. Locating the position along the cardiac tube for measurement was determined as previously described by examining the portion of the sections where an *en face* section of the cardiac tube was visible and measuring three consecutive sections three sections (24μm) posterior to this section [184].

2.4 Optical coherence tomography (OCT)

End-diastolic dimension and end-systolic dimension were measured using optical coherence tomography (OCT) (Bioptigen, Inc. Durham, NC) as previously described [189]. Briefly, 7-10 days post-eclosion, female *Drosophila* were placed in

GelWax medium and allowed to awaken. M-mode images through the conical chamber were collected for immobilized awake *Drosophila*. End-diastolic and end-systolic dimensions were measured in ImageJ, calibrated to a 125μm thick glass slide. Fractional shortening was calculated as (End-diastolic dimension minus end-systolic dimension/End-diastolic dimension) x 100% and used as a measure of cardiac contractility.

Several types of controls were used and compared for our study: w^{1118} used routinely in our lab as a control (Flybase ID: FBst0003605), w^{1118} used to create transgenics from the Duke University Model Systems Genetics Facility (Flybase ID: FBst0006326), *tinC-Gal4*, *tinC-Gal4* heterozygous with w^{1118}, *tinC-GFP* and *tinC-GFP* heterozygous with w^{1118}. We performed a one-way ANOVA comparing OCT measurements between all control groups and showed that none were significantly different from each other (Figure 4).

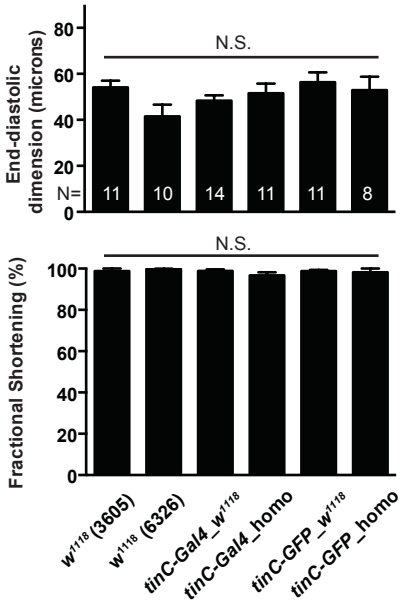

Figure 4: End-diastolic dimensions and fractional shortenings are not different among control flies used in this study

Quantitative results from OCT images for several control lines used in this study: w^{1118} (FBst0003605) control, w^{1118} (FBst0006326) from the Duke University Model System Genomics Facility for generation of transgenic flies, *tinC-Gal4* heterozygous from cross with w^{1118} (FBst0003605), homozygous *tinC-Gal4*, *tinC-GFP* heterozygous from cross with w^{1118} (FBst0003605), and homozygous *tinC-GFP*. End-diastolic dimensions and fractional shortenings were not significantly different among the control lines used in this study. One-way ANOVA with Bonferroni correction. Numbers on each bar represent number of flies in each group. Data represent mean ±SEM.

2.5 Confocal microscopy

Flies that harbored *tinC-GFP* or *tinC-YCanA^{act}* were collected 1-2 days after eclosion, and dissected as previously described [184] by removing the ventral side of the abdomen and exposing the heart tube. Immunohistochemistry was performed according to standard procedures as previously described [184] using 5% BSA in TBS as the blocking reagent with a rabbit anti-GFP antibody (Invitrogen, Inc.), and Alexa Fluor488 goat anti-rabbit secondary antibody (Invitrogen, Inc.). After immuno-staining, the *Drosophila* heart was visualized under a Zeiss LSM510 confocal microscope. Consecutive Z-stacks were taken at 1μm intervals, and projected to form a 3D image in the LSM image browser software.

For capturing images of stage 16 embryos, *tinC-GFP* or *tinC-YCanA^{act}* flies were collected and allowed to lay eggs on apple juice agar plates for 2 hours. 14-16 hours after egg laying, embryos were collected in an embryo collection apparatus by first dechorionating embryos in 50% bleach and washing with distilled water. Embryos were then imaged in VECTASHIELD® (Vector Laboratories, Inc.) under the Zeiss LSM510 confocal microscope.

2.6 Fluorescence microscopy for determining nuclei number in Drosophila hearts

tinC-GFP or *tinC-YCanA^{act}* flies were crossed with *tinC-Gal4*, *UAS*-nuclear RFP flies and the offspring were collected 1-2 days after eclosion. Hearts were exposed by

dissection as previously described for confocal microscopy and imaged without staining under the confocal microscope [184]. Nuclei from visualization of RFP were counted visually to determine the number of cardiomyocytes present in each heart. Ostia cells and cuticle patterning were used to determine the abdominal segment boundaries and nuclei number was counted for abdominal segments 2 and 3 because the first and last couple abdominal segments were often damaged in the dissection process.

2.7 Precise excision of the Minos insertion in galactokinase

The Minos insertion in *Galk, Mi{ET1}Galk^{MB10638}*, was excised precisely according to standard transposable element excision procedures [162, 209]. Briefly, the *Mi{ET1}Galk^{MB10638}* males were crossed to virgin females containing the Minos transposase *sna^{Sco}/SM6a*, *P{w^{+mC}=hsILMiT}2.4*. After three days, adult flies were removed, and the embryos were heat shocked for 1 hour in a 37°C water bath for 4 consecutive days. Male progeny were selected for the presence of the Minos insertion and the Minos transposase according to eye color (the Minos element expresses GFP, and Minos transposase expresses a red eye color from *mini-white* in the insertion) and crossed to the double balancer fly stock *WR135*. Male progeny were selected for the absence of GFP and *mini-white*, indicating a successful excision, and crossed again to *WR135* virgin females. Progeny harboring excisions were crossed to each other to make a homozygous

stock. These stocks were assayed for the presence of a precise excision using primers sequencing through the affected genomic region.

2.8 Real-time RT-PCR

Real-time RT-PCR was performed to determine the expression level of genes. *Drosophila* were collected 3-5 days after eclosion and 5 whole flies were collected or 10-15 fly hearts were dissected for each group. RNA was extracted using RNA-Bee RNA isolation reagent (Amsbio) according to the manufacturer's protocol. SuperScript II (Invitrogen) reverse transcription according to the manufacturer's protocol was followed by real-time PCR analysis using taqman probes (probe: Dm01801608_g1, Applied Biosystems, Inc.).

2.9 Life span

Drosophila were collected 1-2 days after eclosion. 10 males and 10 females were kept in the same vial and food changed every 2-3 days. A total of 6 vials were monitored for each group. The number of remaining flies was monitored daily. Data was analyzed using GraphPad Prism software and statistical analysis was performed with a Mantel-Cox test for significance.

2.10 Wing vein phenotype

Drosophila from the respective crosses were collected at 3-5 days after eclosion. The wings were detached using forceps and the ventral surface was placed face down on GelWax plates. The wings were examined for abnormalities under a dissection microscope at 40x or imaged under a Leica M165FC Fluorescence stereo microscope equipped with a Leica DFC310FX camera at 50x. A range of wing vein abnormalities were observed, which were divided into normal, abnormalities of the posterior crossvein (PCV), or abnormalities of both the PCV and the longitudinal vein 5 (L5). The number of wings under each category of wing vein phenotype were counted for each group and the percentage of total wings counted was calculated. Statistical significance to detect for a rescue of the abnormal wing vein phenotype (pooling the two different types of wing vein abnormalities) with the *Df(3L)ED4416* deficiency was determined using Fisher's exact test. Tissue-specific expression of $CanA^{act}$ with *dpp-Gal4*, *Act5C-Gal4*, and *mef2-Gal4* was analyzed similarly by counting the number of progeny with the respective phenotypes according to the crosses and genotypes described in the figure legend.

2.11 Cell Culture

H9c2 rat embryonic cardiomyoblasts and NIH-3T3 mouse fibroblasts were obtained from ATCC and maintained according to standard procedures. H9c2 cells

were maintained in DMEM medium while NIH-3T3 mouse fibroblasts were maintained in RPMI medium. Cells were passaged regularly by detaching with 0.25% trypsin-EDTA solution. Transfection with NFAT-GFP was performed with lipofectamin® 2000 (Life Technologies, Inc.) according to manufacturer's protocols. After 24 hours of lipofectamine® transfection, cells were detached from the plate and replated onto poly-L-lysine coated, collagen pretreated glass bottom confocal dishes, allowed to attach, and transfected with predesigned siRNA to Galk1 (Life Technologies, Inc.) with GeneSilencer® (Genlantis) according to manufacturer's protocol. Cells were serum starved for 24 hours, treated with or without 0.1 μM ionomycin for 1 hour. After washing with PBS, fixation with 4% paraformaldehyde followed by another PBS wash (3 times, 10 minutes each), cells were kept in VECTASHIELD® (Vector Laboratories, Inc.) before imaging under the Zeiss LSM510 confocal microscope.

2.12 Statistical analysis

All statistical analysis was performed using GraphPad Prism software. One-way ANOVA with Bonferroni correction was used to determine significance for multiple comparisons and student's t test was used for single comparisons. Mantel-Cox rank test was used to compare survival curves, two-way ANOVA was used to compare the progression of *Drosophila* heart function with age, and Fisher's exact test was used to determine rescue for wing and lethality phenotypes.

Chapter 3. Generating and characterizing the calcineurin fly

In order to use deficiency screening to discover novel calcineurin modifiers, I generated sensitized *Drosophila* lines expressing constitutively active calcineurin ($CanA^{act}$) by expressing $CanA^{act}$ directly under control of the cardiac-specific driver *tinC*- (*tinC-CanA*^{act}) or under control of the *UAS* driver (*UAS-CanA*^{act}). Driving *CanA*^{act} in the heart induces a significant cardiac enlargement phenotype.

3.1 Making the sensitized CanA^{act} Drosophila line

3.1.1 The cardiac-specific constitutively active calcineurin (CanA^{act}) construct

Several components were utilized in the vector to make the transgenic fly: 1) constitutively active calcineurin (CanA^{act}); 2) a tag for detecting transgene expression; and 3) a cardiac-specific promoter to express this transgene specifically in the fly heart (Figure 5). Each of these components are described in detail below:

3.1.1.1 Constitutively active calcineurin (CanA^{act})

Calcineurin acts as a calcium/calmodulin-dependent protein phosphatase. The large CanA subunit has phosphatase activity and consists of several domains: the catalytic domain, which regulates protein dephosphorylation [6], the CanB binding domain [7], the calcium/calmodulin binding domain, and the autoinhibitory domain [8], summarized in Figure 5. Binding of calcium/calmodulin activates calcineurin by alleviating autoinhibition. A constitutively active calcineurin (CanA^{act}) was generated as previously described, using *Drosophila* cDNA, amplifying only up to the calcium/calmodulin binding domain and eliminating the autoinhibitory domain [9-11]. This results in a protein that is constitutively active by alleviating autoinhibition.

3.1.1.2 Tags (YFP or Flag)

I generated CanA^{act} according to previous studies, adding either a YFP- or a Flag-tag to the N-terminus to facilitate detection of the transgene (Figure 5B-C). The YFP tag facilitates convenient visualization of the transgene using fluorescence microscopy with the possibility of the larger YFP molecule (238 aminio acids, 26.4 kDa) to interfere with or exert effects independent of CanA^{act}. Of note, the catalytic activity of N-terminal YFP-tagged *CanA^{act}* has been confirmed in studies by a number of investigators, using well characterized NFAT reporter assays [205, 206], NFAT phosphorylation assays [205], and NF-κB reporter assays [207]. In contrast, Flag is a short 8 amino acid sequence (1 kDa) that is less likely to interfere with CanA^{act} activity but requires additional immuno-staining techniques for detection. Both transgenic flies were generated and analyzed to rule out any effects that may result from the interference of the tag or transgene insertion site.

3.1.1.3 Cardiac-specific promoter (*tinC-*)

In order to create a *Drosophila* line expressing CanA^{act} in the heart, I used the *tinC-* promoter, a 304 bp intronic region within the *tinman* gene that controls cardiac-specific gene expression in conjunction with a minimal *hsp70* promoter (*tinC-CanA^{act}*) [189, 210, 211].

The *tinman* gene is a key regulatory gene for all mesodermal development, including that of the heart, visceral, and somatic muscle. Even though the tinman gene is expressed in the entire mesoderm at early stages of development, by stage 12, expression is confined to all cardiac muscle cells, excluding the sevenup (svp)-expressing ostia cells. This expression pattern is controlled by multiple enhancer elements in the tinman gene. The enhancer element I used in my study, *tinC-*, specifically drives later expression in cardiac cells after embryonic stage 12 [211].

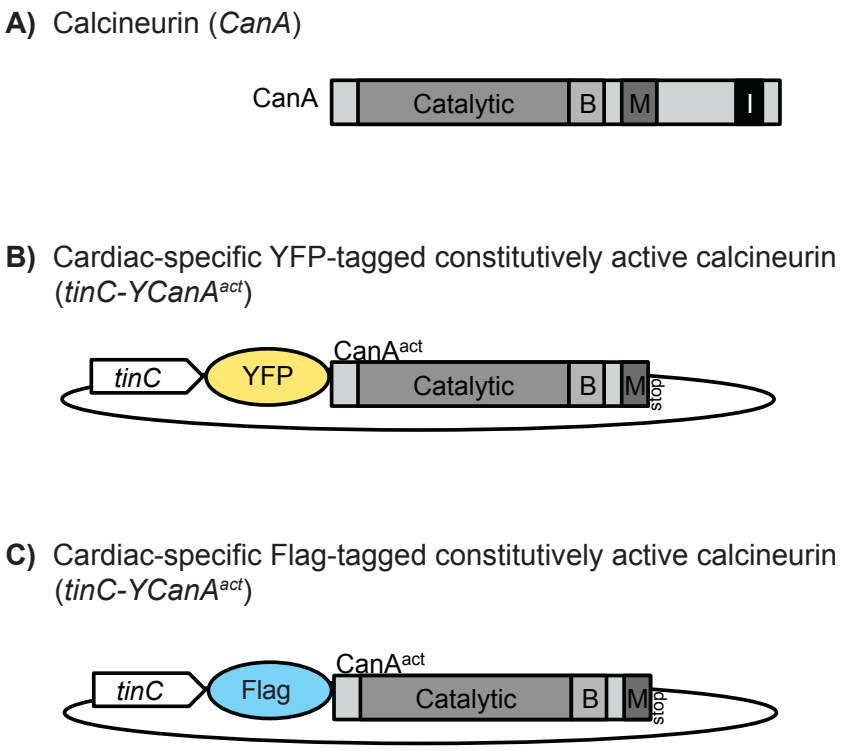

Figure 5: The structure of calcineurin and CanA^{act} constructs.

A) Domain structure of calcineurin (CanA), including the catalytic domain (Catalytic), the CanB-binding domain (B), the calmodulin-binding domain (M), and the autoinhibitory domain (I). B) Domain structure of the YFP-tagged constitutively active calcineurin (*tinC-YCanA*^{act}) construct, excluding the autoinhibitory domain (I, Figure 5A), inserting a premature stop codon, and showing the YFP N-terminal tag and cardiac-specific *tinC*- promoter. C) Domain structure of the Flag-tagged constitutively active calcineurin (*tinC-FCanA*^{act}) construct. (Referencing [8].)

3.1.2 Expression of cardiac-specific *CanA*^{act} in the fly

After injecting the *tinC-YCanA*^{act} construct into *Drosophila* embryos, identifying germline transmission of the transgene, mapping the chromosomal insertion, and establishing stable stocks, fluorescence microscopy was used to confirm expression of the transgene (Figure 6). Cardiac-specific YFP is detected in stage 16 embryos and 1-2 day old adult flies. This confirmed that the transgene was expressed as expected in the fly heart. In addition, it is also observed that the fly heart is already visibly larger at an embryonic state.

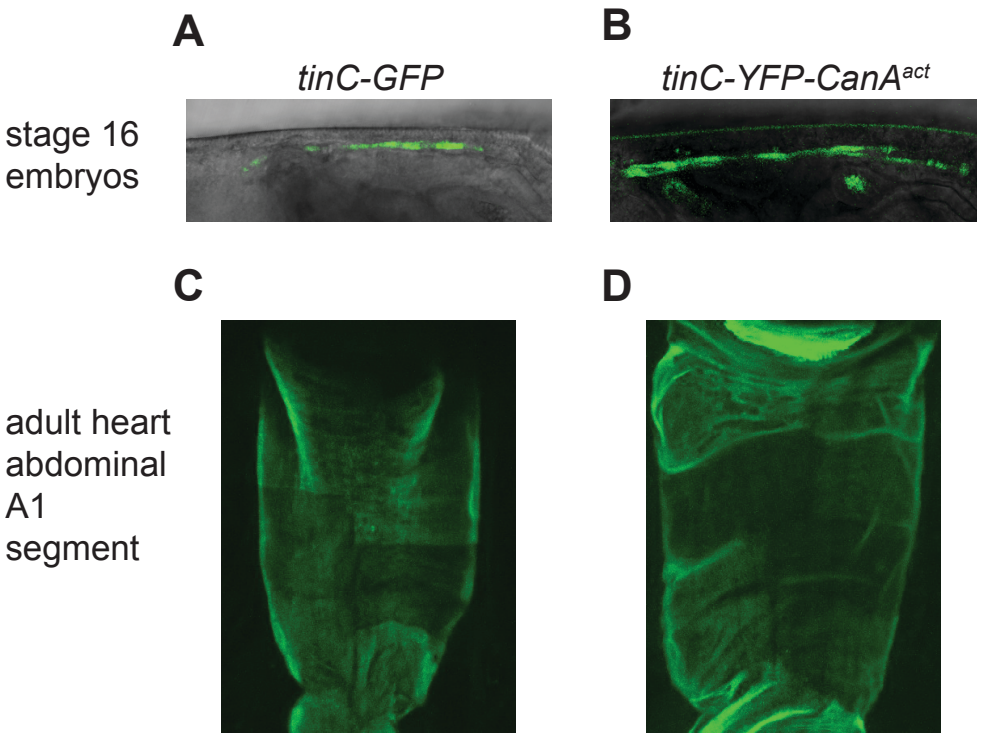

Figure 6: *tinC-YCanA^{act}* fly hearts express cardiac YFP-tagged CanA^{act} and are larger than *tinC-GFP* control fly hearts

Confocal microscopy detecting the GFP or YFP tag in stage 16 embryos or the A1 abdominal segment of adult flies in A, C) *tinC-GFP* or B, D) *tinC-YCanA^{act}* flies. C, D) Adult flies were dissected to reveal the heart from the ventral side. Images detect transgene expression and reveal that fly hearts are visibly larger in stage 16 embryos and adults.

3.2 Expressing CanA^{act} in the heart induced a cardiac enlargement phenotype

After the CanA^{act}-expressing fly, lines were established, multiple methods were employed to phenotype cardiac structure and function, as described in the sections below.

3.2.1 Optical coherence tomography (OCT)

I performed optical coherence tomography (OCT) on both *tinC-YCanA^{act}* and *tinC-FCanA^{act}* flies. This allowed for real-time imaging of the beating heart in alive, awake adult flies. Several transgenic lines were generated and tested for both *tinC-YCanA^{act}* and *tinC-FCanA^{act}* insertions, including lines where the transgenic insertion site was mapped to the first, second, or third chromosomes (Figure 7A-B). Results showed that several independent transgenic lines induced significant cardiac enlargement (increased end-diastolic dimension). In addition to examining end-diastolic dimension (EDD), the size of the cardiac chamber at its most relaxed state, fractional shortening (FS) was also calculated as a measurement of cardiac contractility for heterozygous *tinC-YCanA^{act}* and *tinC-FCanA^{act}* flies. Results show a significant increase in EDD and a significant decrease in FS in both *tinC-YCanA^{act}* and *tinC-FCanA^{act}* flies, signifying that CanA^{act} in the heart induces the cardiac chamber to enlarge and cardiac contractility to decline (Figure 7C-D). There was a 15% decrease in fractional shortening in CanA^{act} flies. In humans, normal fractional shortening ranges from 25-45%, where a 15%

reduction corresponds to severe abnormality [61]. All further screening and suppressor studies were of flies with the transgene in a heterozygous state.

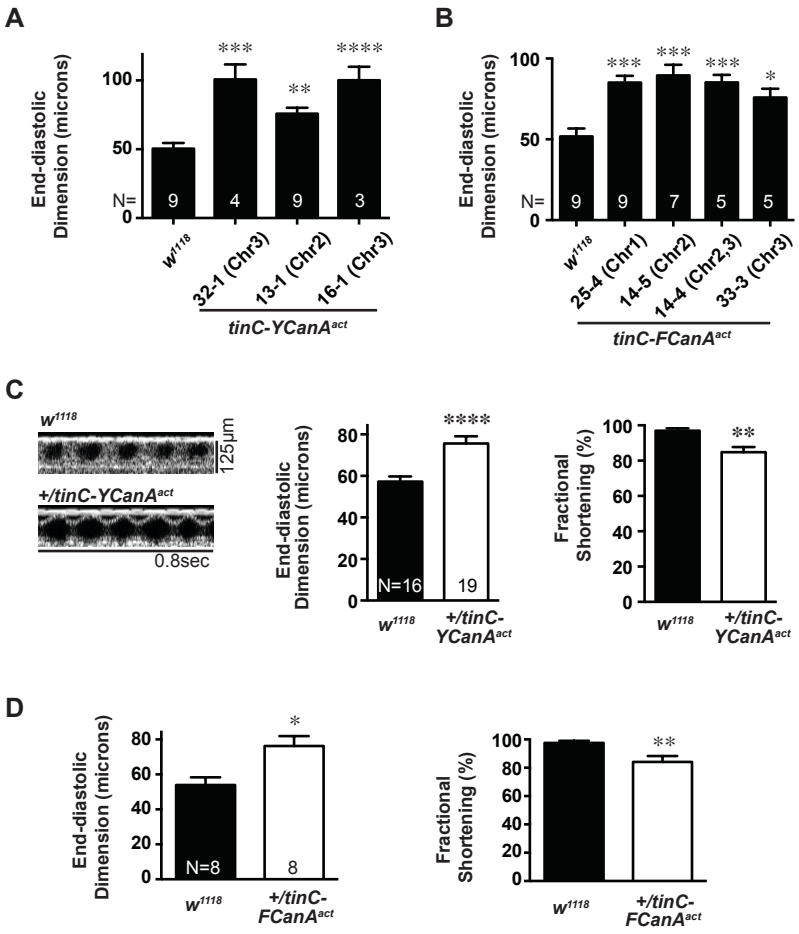

Figure 7: CanA^{act} induced cardiac enlargement and decreased contractility assayed using optical coherence tomography (OCT)

Quantitative results from OCT images of A) homozygous *tinC-YCanA^{act}* and B) *tinC-FCanA^{act}* fly hearts compared to *w^{1118}* control. Each number denotes an independent line generated from embryo injection of the respective constructs, either *tinC-YCanA^{act}* or *tinC-FCanA^{act}*, followed by the chromosome the corresponding insertion was mapped to.

C-D) Representative OCT images and quantitated results for heterozygous C) *tinC-YCanA^{act}* or D) *tinC-FCanA^{act}* flies compared to *w^{1118}* control. Expressing either YCanA^{act} or FCanA^{act} in the fly heart resulted in cardiac enlargement and diminished contractility. (*P<0.05, **P<0.01, ***P<0.001, ****P<0.0001. One-way ANOVA with Bonferroni correction (A-B). Student t test (C-D). Data represent mean ±SEM.)

3.2.2 Histology

Cardiac enlargement and the fly heart were also examined more closely using paraffin sectioning and hematoxylin and eosin (H&E) staining (Figure 8). Either control (*tinC-GFP* or *w^{1118}*) or CanA^{act} (*tinC-YCanA^{act}* or *tinC-FCanA^{act}*) flies were embedded in paraffin, sectioned 8μm thick, and stained with hematoxylin and eosin (H&E). Lumen area and perimeter of *tinC-CanA^{act}* fly hearts were significantly enlarged compared to control. Interestingly, abnormalities in cardiac wall thickness or musculature structure in these histological sections were not observed, which is distinct from the mouse phenotype [9]. These results corroborate the feasibility of using *tinC-CanA^{act}* flies as a sensitized line for genetic screening.

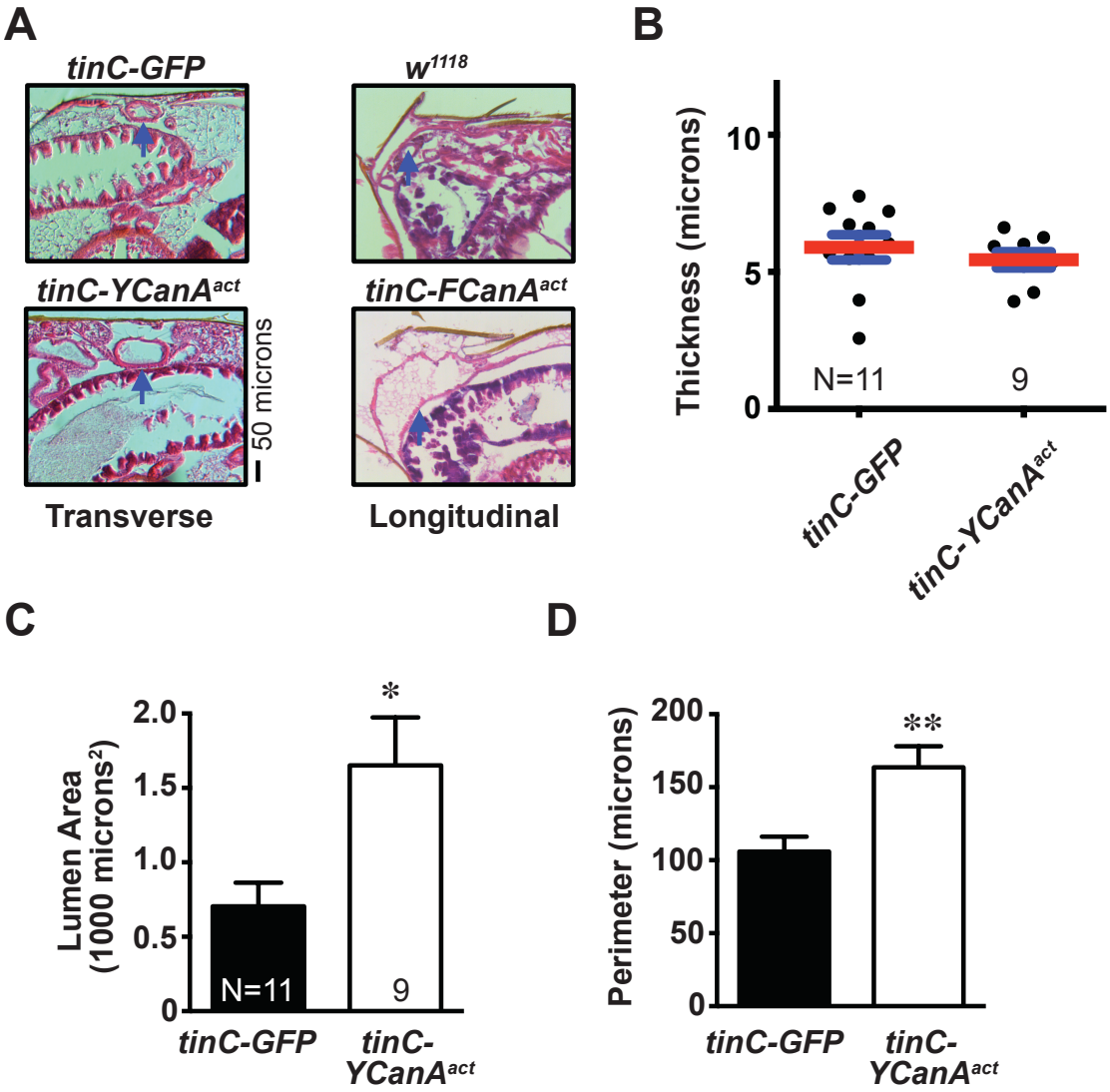

Figure 8: Histological sections showed that CanA^{act} induced cardiac enlargement

Histological sections from paraffin sectioning and hematoxylin and eosin (H&E) staining was performed on homozygous *tinC-YCanA^{act}* or *tinC-FCanA^{act}* flies (A). Blue arrows point to the heart, located underneath the dorsal abdominal cuticle. Quantitative analysis with multiple images was performed in imageJ, measuring B) heart wall thickness, C) cardiac lumen area, and D) cardiac lumen perimeter for homozygous *tinC-*

YCanA^{act} flies. CanA^{act} caused significant increase in cardiac lumen area and perimeter, but not cardiac wall thickness. (*P<0.01; **P<0.0001, student t test. Data represent mean ±SEM.)

3.3 CanA^{act}-induced cardiac enlargement persisted with age

I also examined cardiac enlargement and contractility up to 5 weeks (35 days) post-eclosion (Figure 9). As the results show, *tinC-FCanA*^{act} flies display sustained cardiac enlargement and decreased contractility compared to control w^{1118} 1 to 5 weeks after eclosion. Control and *tinC-FCanA*^{act} flies also had an increase in end-diastolic dimension throughout aging. I further determined whether CanA^{act} induced an age-dependent increase in cardiac enlargement. There was no interaction between the control and CanA^{act} lines by ANOVA, indicating that CanA^{act} did not exacerbate the rate of cardiac enlargement with age.

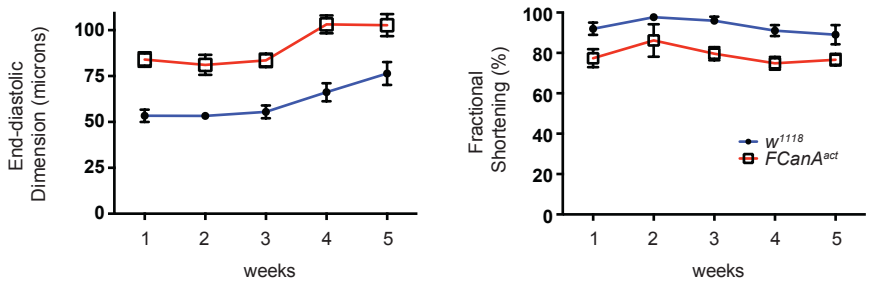

Figure 9: Cardiac enlargement of CanA^{act} flies persists with age

Control w^{1118} or *tinC-FCanA*^{act} flies were collected after eclosion and assayed using optical coherence tomography (OCT). Throughout 5 weeks of age, *tinC-FCanA*^{act} flies displayed significant cardiac enlargement (two-way ANOVA, $P<0.0001$) and decreased contractility (two-way ANNOVA, $P<0.0001$). End-diastolic dimension increased with age (two-way ANOVA, $P<0.0001$). No significant interaction was detected using two-way ANOVA, indicating that the cardiac dimensions enlarge with age, but CanA^{act} does not increase the rate of enlargement. (N=7-17 in each group.)

3.4 CanA^{act}-induced cardiac enlargement was not due to increase in cell number

To further analyze the nature of CanA^{act}-induced cardiac enlargement, I examined whether the increase in heart size was a result of increased myocyte number or hypertrophy of individual cells. This was addressed by expressing cardiac-specific nuclear RFP (*tinC-Gal4>nuclear RFP*) in the context of *tinC-GFP* or *tinC-YCanA*^{act} (Figure 10). The number of cardiac cells present in the abdominal segments A2 and A3 was not altered in *tinC-YCanA*^{act} flies. These results show that the cardiac enlargement is not due to proliferation. Studies to directly measure individual cell size will provide quantitative evidence to confirm the notion that cardiac enlargement involves the increase of individual cell size.

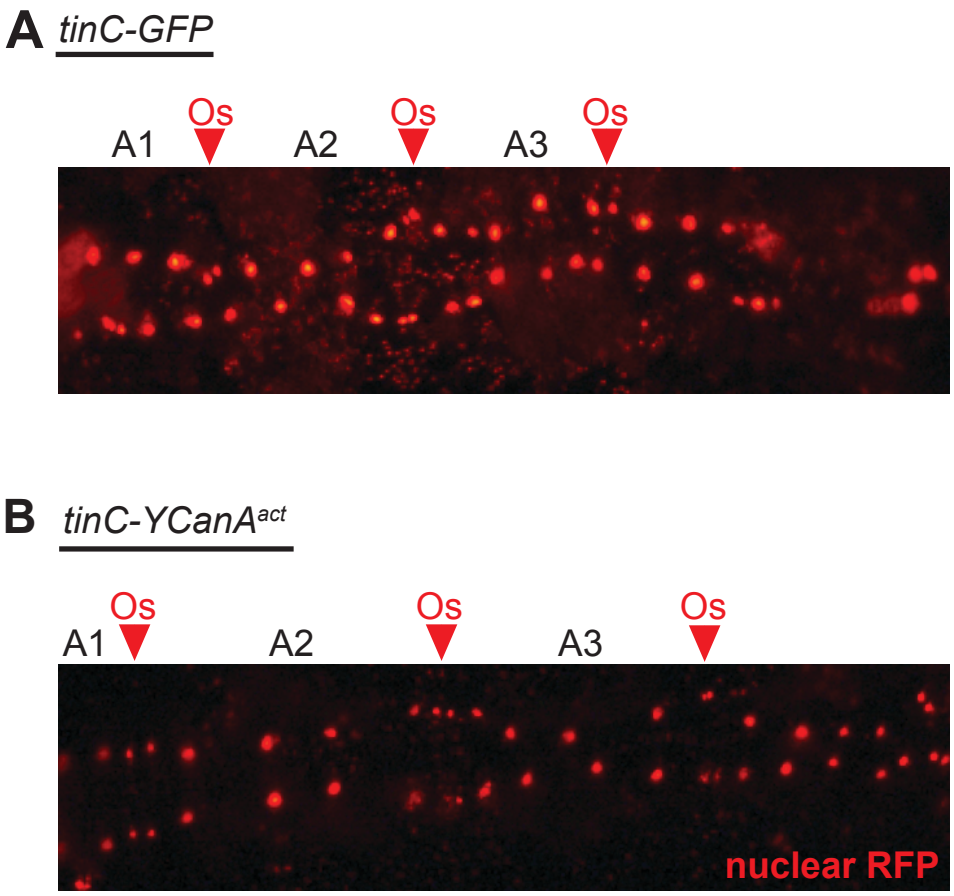

Figure 10: CanA^{act} fly hearts do not have an increased number of cells.

Nuclei of A) control *tinC-GFP/tinC-Gal4>UAS-nuclear RFP* and B) tinC-*YCanA^{act}/tinC-Gal4>UAS-nuclear RFP* flies. Abdominal segments A1-A3 were determined by presence of ostial cells and the pattern of the dorsal abdominal cuticle. *tinC-GFP* and *tinC-YCanA^{act}* flies both have 4 cardiac cells in the A2-A3 segments apart from the ostial cells, indicating that the increased cardiac size is not due to proliferation.

Chapter 4. Performing a deficiency screen using the *tinC-CanA^{act}* fly as a sensitized line

After identifying a significant phenotype in flies that expressed cardiac-specific CanA^{act}, I tested the feasibility of using the *tinC-CanA^{act}* fly as a sensitized line to perform genetic screening. The approach was validated by examining effects of a known calcineurin modifier, *Mef2*. Then, a deficiency screen was performed to determine a suppressor region containing genes that modify CanA^{act}. From this screen, I identified *Galactokinase* as a novel modifier of CanA^{act}-induced cardiac enlargement.

4.1 Deficiency of the known CanA^{act} modifier, Mef2, suppressed CanA^{act}-induced cardiac enlargement

In order to establish the feasibility of finding a modifier of the heart phenotype, a known downstream regulator of calcineurin signaling [11, 61] was analyzed. Two main direct targets of calcineurin are currently known: NFAT and Mef2. Since *Drosophila* do not express the NFAT regulated by calcineurin [80], it is conceivable that a main downstream regulator of calcineurin is Mef2. To test the hypothesis that Mef2 was important for generating a cardiac phenotype downstream of CanA^{act}, the cardiac phenotype of CanA^{act} was examined in the context of *Mef2* deficiency. The *tinC-FCanA^{act}* line was used as a sensitized line and crossed to *Df(2R)X1,Mef2^{X1}* flies (a fly line that is haploinsufficient for *Mef2*), resulting in a fly with half the normal amount of *Mef2*. +/*tinC-FCanA^{act}*;+/*Df(2R)X1,Mef2^{X1}* flies had improved chamber dimensions compared to +/*tinC-FCanA^{act}* (Figure 11), demonstrating that deficiency of a modifier can rescue cardiac enlargement of the sensitized line.

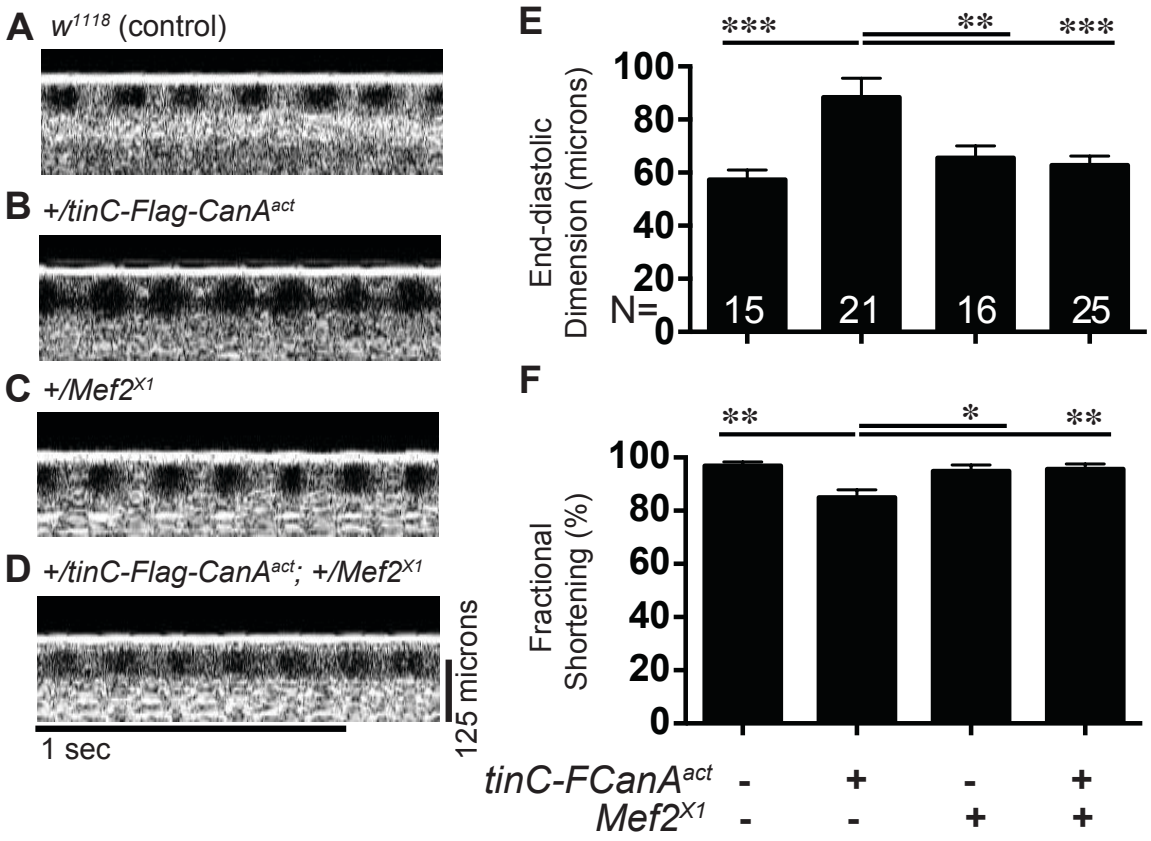

Figure 11: Deficiency in the known CanA^{act} modifier, *Mef2*, rescued CanA^{act}-induced cardiac enlargement.

A-D) Representative OCT images of control w^{1118}, heterozygous +/*tinC-FCanA*^{act}, heterozygous deficiency in +/*Mef2* (*Mef2*^{X1}), and heterozygous +/*tinC-FCanA*^{act}; +/*Mef2*^{X1}. E,F) Quantification of OCT images from multiple flies of E) end-diastolic dimension and F) fractional shortening. Deficiency in *Mef2* rescued CanA^{act}-induced cardiac enlargement. (*P<0.05, **P<0.01, ***P<0.0001, One-way ANOVA with Bonferroni correction. Data represent mean ±SEM.)

4.2 A deficiency screen determines a suppressor region that rescued CanA^{act}-induced cardiac enlargement.

Having generated a sensitized line that displays a significant cardiac enlargement phenotype, a deficiency screen was performed, starting with regions previously identified to modify phenotypes from CanA^{act} overexpression in the eye and mesoderm.

4.2.1 Selecting a region to initiate deficiency screening

Deficiency stocks cover 98.4% of the *Drosophila* euchromatic genome (flystocks.bio.indiana.edu) [212]. The Bloomington *Drosophila* Stock Center offers a deficiency kit composed of 462 fly stocks that cover the genetic material maximally. The high number of stocks calls for the need to prioritize a region to start screening. In order to maximize the probability of discovering a novel modifier gene, I referenced two previous screens for modifiers of CanA^{act} [10, 11].

Previously, two independent screens had been conducted to identify modifiers of calcineurin phenotypes in tissues other than the heart [10, 11]. The suppressor regions from these two studies are summarized in Table 1. Sullivan and Rubin performed a dominant modifier screen in the *Drosophila* eye and found five suppressor and four enhancer loci [10]. Gajewski *et al* found seven different deletion intervals that suppressed the lethal phenotype of constitutively active calcineurin driven by the general mesodermal driver *24B* [11]. Importantly, only one interval overlapped between these two studies on chromosome 3L, cytolocation 66F, emphasized in gray shading in

Table 1. Therefore, I initiated a deficiency screen to identify modifiers of CanA^{act}-induced cardiac enlargement based on the concordant findings of these two prior studies.

4.2.2 A deficiency screen reveals a suppressor region for CanA^{act}-induced cardiac enlargement

I initiated a deficiency screen according to the overlapping region between the Sullivan and Rubin and Gajewski *et al*. screens described in the previous section. Eight deficiency lines were obtained from the Bloomington *Drosophila* Stock Center (Figure 12A). All deficiency lines were crossed to either w^{1118} control or *tinC-YCanA*^{act} flies. Using optical coherence tomography (OCT) to determine end-diastolic dimension (EDD) and fractional shortening (FS), I compared these cardiac dimensions between control w^{1118}, the sensitized line heterozygous *tinC-YCanA*^{act}, the heterozygous deficiency alone, and *tinC-YCanA*^{act} in the context of a heterozygous deficiency. If the region encompassed by a deficiency line included a gene that influences any step downstream of calcineurin activation, presence of the deficiency will rescue the *tinC-YCanA*^{act} phenotype. Out of the 8 lines screened, only two, *Df(3L)ED4416* and *Df(3L)BSC130*, modified CanA^{act}-induced cardiac enlargement (Figure 12B-C). One of the deficiency lines, *Df(3L)ED4421*, displayed cardiac enlargement alone without CanA^{act} and was not included in determining the suppressor region (Figure 12C). Delineated from these

results, I determined a region in between the two dotted lines (Figure 12A) which contains a gene that modifies CanA^{act}-induced cardiac enlargement. This region spans a total of 13 genes as shown in the expanded view in Figure 12A.

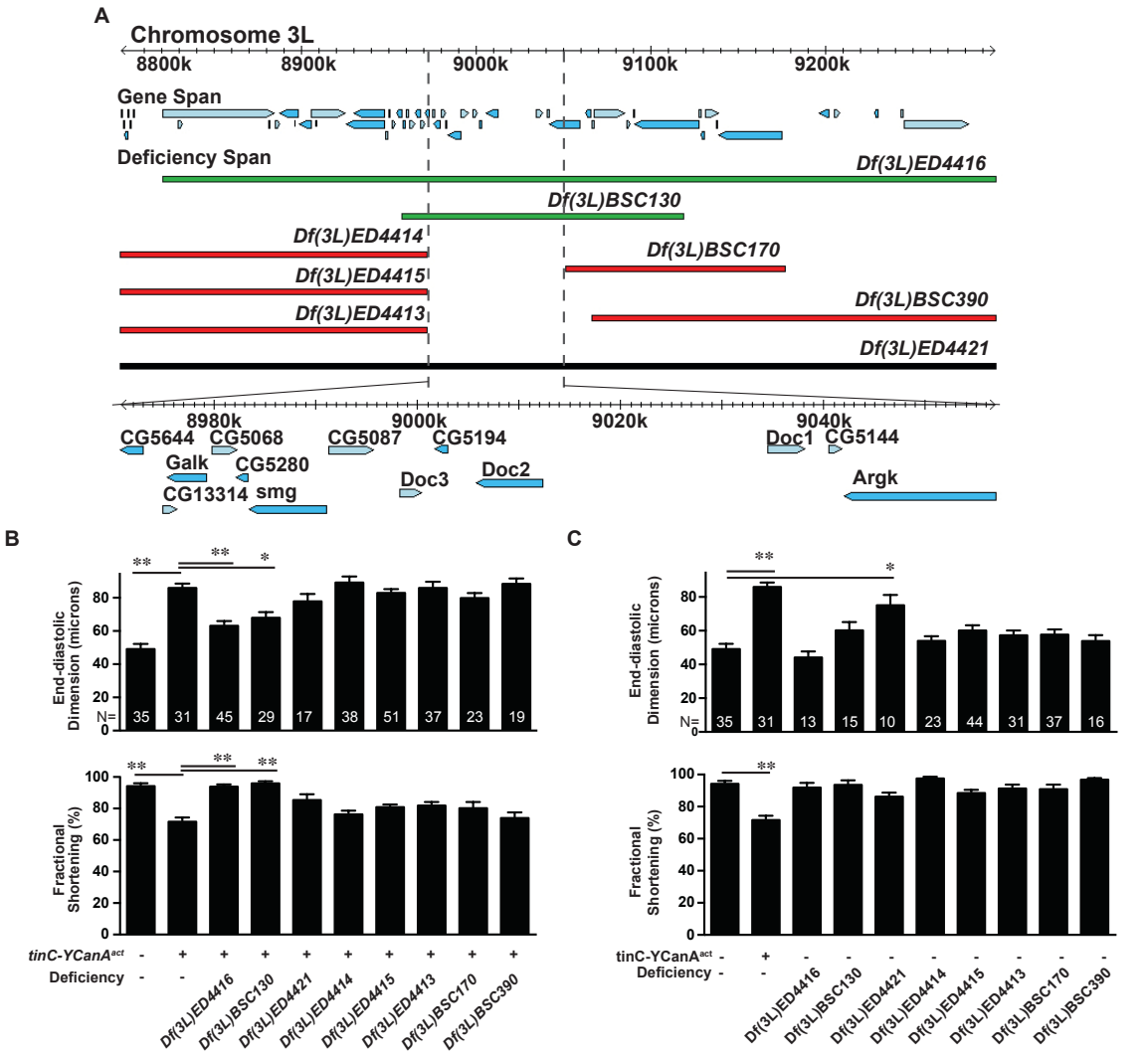

Figure 12: A deficiency region that rescues CanA^{act}-induced cardiac enlargement

A) Genetic map of deficiency stocks tested and depiction of the chromosomal region that rescues CanA^{act}-induced cardiac enlargement. (Adapted from Gbrowse, http://flybase.org/cgi-bin/gbrowse/dmel). Dotted lines indicate the suppressor region. Genes within the suppressor region are shown in the magnified view below. (Green bars= rescuing deficiencies. Red bars= non-rescuing deficiencies. Black bar= deficiency that causes cardiomyopathy on its own.) (B-C) Summary data for end-diastolic dimensions and fractional shortenings of *tinC-YCanA^{act}* alone and in the context of molecularly-defined genomic deficiencies shown in (A). All deficiencies were tested in the heterozygous states. Two deficiency lines rescued the *tinC-YCanA^{act}* phenotype, *Df(3L)ED4416* and *Df(3L)BSC130*, narrowing down the original suppressor region to the region in between the dotted lines in (A). C) End-diastolic dimensions and fractional shortenings for *w^{1118}* control, *tinC-YCanA^{act}*, or *Drosophila* lines utilized in the deficiency screen without *YCanA^{act}*. Note that *Df(3L)ED4421* covers the deficiency region but was dilated on its own without CanA^{act} expression, and was not considered in defining the deficiency region. (One-way ANOVA with Bonferroni correction. *P<0.01, **P<0.0001. Data represent mean ±SEM.)

4.3 Using RNAi or transposable element insertion stocks to determine the causal genes in the suppressor region

Results in the previous section determined a suppressor region which encompassed genes that modulate $CanA^{act}$-induced cardiac enlargement. There are 13 genes in this region; Table 2 outlines the properties of these genes (flybase.org, flyatlas.org). Out of these genes, a couple stood out: 1) the dorsocross (Doc) genes, Doc1, Doc2, and Doc3 are known to regulate cardiac development; 2) galactokinase (Galk) and arginine kinase (Argk) have high expression in the adult fly heart. Subsequent studies followed accordingly to determine the causative modifier gene within the smaller region identified.

Table 2: Genes within the suppressor region

Gene	Possible function	Human orthologue	Expression in adult heart
CG5644	CHK kinase-like	none	Unknown
CG13314	unknown	none	Unknown
CG5288	galactokinase activity.	galactokinase 2	High
CG5068	catalytic activity.	protein phosphatase methylesterase 1	No
smg	protein binding; translation repressor activity	none	Low
CG5087	ubiquitin-protein ligase activity.	ubiquitin protein ligase E3B	Low
Doc3	transcription factor activity, cardiac development	T-box 6	Low
Doc2	transcription factor activity, cardiac	none	No

	development		
Doc1	transcription factor activity, cardiac development	T-box 6	No
CG5144	arginine kinase activity.	none	No
Argk	arginine kinase activity.	none	High
CG4911	unknown	F-box protein 33	No
CG4942	unknown	COX18 cytochrome c oxidase assembly homolog	Low

Gene information obtained from flybase.org; gene expression obtained from flyatlas.org.

4.3.1 The *dorsocross* (*Doc*) genes

There are three *dorsocross* genes, *Doc1*, *Doc2* and *Doc3*. The *Doc* genes are required for specification of cardioblasts during cardiac development. Cardioblasts and pericardial cells do not form in embryos with a deletion of all three *Doc* genes and overexpressing *Doc2* induces ectopic cardioblast specification. In addition, Doc genes interact with the cardiac developmental genes *tinman* (*tin*, mammalian Nkx-2.5 protein) and *pannier* (*pnr*, mammalian Gata protein) during cardiac specification [213]. *Doc* genes have been implicated in the regulation of cardiac specification by maintaining *tin* expression and activating *pnr*. Due to the regulation of cardiac development by *Doc* genes, it is plausible that the causal gene in the $CanA^{act}$ cardiac enlargement suppressor region may be a *Doc* gene.

I examined the *Doc* genes in the context of the $CanA^{act}$-induced cardiac enlargement phenotype. I made a fly that expressed *tinC-FCanA*^{act} and *tinC-Gal4*

through genetic recombination and then crossed this fly line with flies that expressed RNAi to *Doc1* (*P{GD4334}v16746 and P{TRiP.JF02222}*), *Doc2* (*P{GD4335}v37634*), or *Doc3* (*P{TRiP.JF02223}attP2*). The knock-down of *Doc2* or *Doc3* genes caused cardiac enlargement independent of $CanA^{act}$ expression. Furthermore, $CanA^{act}$-induced cardiac enlargement was not rescued in the context of RNAi to *Doc* genes (Figure 13). These results suggested that the *Doc* genes were not responsible for the suppression of $CanA^{act}$-induced cardiac enlargement.

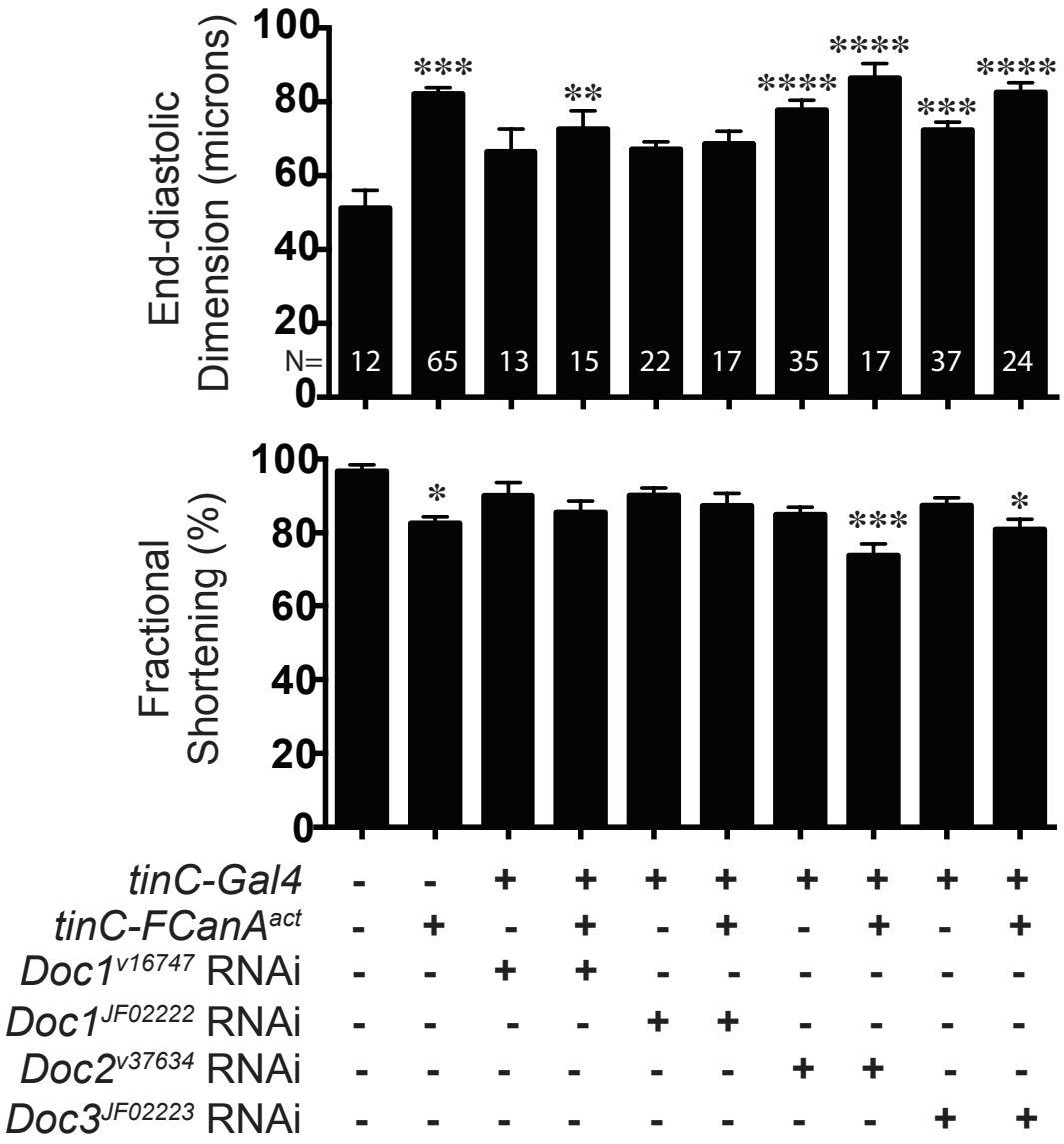

Figure 13: Knocking down the *dorsocross* genes did not rescue CanA^{act}-induced cardiac enlargement.

Summary data of end-diastolic dimensions and fractional shortenings for w^{1118} control, heterozygous *tinC-FCanA*^{act} or fly lines expressing the corresponding RNAi to *dorsocross* (*Doc*) genes. Knocking down *Doc2* and *Doc3* genes caused cardiac enlargement, and did not rescue *tinC-FCanA*^{act}-induced cardiac enlargement. *Doc1*^{v16746}

RNAi= *P{GD4334}v16746*; *Doc1*^{JF02222} RNAi= *P{TRiP.JF02222}*; *Doc2*^{v37634} RNAi= *P{GD4335}v37634*; *Doc3*^{JF02223} RNAi= *P{TRiP.JF02223}attP2*. All transgenes were heterozygous. (*p<0.05, **P<0.01, ***P<0.001, ****P<0.0001 compared to control w^{1118}. End-diastolic dimension and fractional shortening of flies expressing RNAi to the *Doc* genes were not significantly different from *tinC-FCanA*^{act} flies. These results indicate that *Doc* did not modify CanA^{act}-induced cardiac enlargement. One-way ANOVA with Bonferroni correction for multiple comparisons. Data represent mean ±SEM.)

4.3.2 *Arginine kinase* (*Argk*)

Arginine kinase (*Argk*) was one of the genes highly expressed in the adult fly heart according to FlyAtlas (Table 2). Therefore, I examined how the disruption of Argk would influence *tinC-YCanA*^{act}-induced cardiac enlargement. I used the piggyback insertion in *Argk*, *PBac{PB}Argk*^{f05255}. Results from OCT imaging show that disruption of *Argk* did not rescue *tinC-YCanA*^{act}-induced cardiac enlargement (Figure 14), suggesting that *Argk* is not the causal phenotype in the deficiency region. However, the disruption only caused 30% reduction in gene expression and protein expression was not tested. It is possible that the lack of modification by disruption of *ArgK* was due to incomplete knock-down of expression.

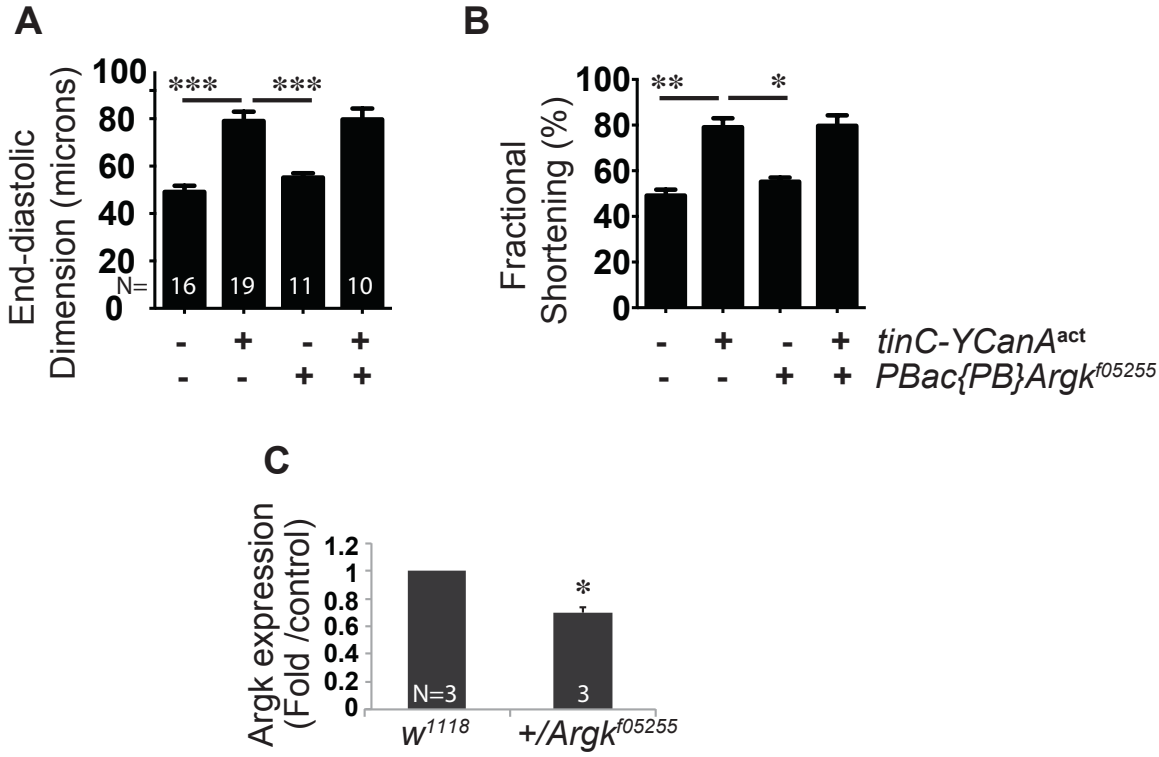

Figure 14: Transposable element insertion in *Argk* did not suppress CanA^{act}-induced cardiac enlargement.

A) End-diastolic dimensions and B) fractional shortenings quantified from OCT m-mode images of control w^{1118}, heterozygous *tinC-YCanA*^{act}, heterozygous *PBac{PB}Argk*^{f05255}, or heterozygous *PBac{PB}Argk*^{f05255} in the context of *tinC-YCanA*^{act}. *PBac{PB}Argk*^{f05255} insertion in *Argk* did not rescue *tinC-YCanA*^{act}-induced cardiac enlargement. (*P<0.05; **P<0.01; ***P<0.0001, one-way ANOVA with Bonferroni correction for multiple comparisons.) C) Real-time RT-PCR of *Argk* expression in flies heterozygous for the piggyback insertion in *Argk*, *PBac{PB}Argk*^{f05255}. Expression level of *Argk* is downregulated in *PBac{PB}Argk*^{f05255} flies. (*P<0.05, student's t test. All data represent mean ±SEM.)

4.3.3 *Galactokinase* (*Galk*)

Galactokinase (*Galk*) was another one of the genes highly expressed in the adult fly heart according to FlyAtlas (Table 2). Galk phosphorylates galactose and N-acetyl-galactosamine (Galactose/GalNAc), allowing further utilization in either metabolism (energy production) or glycosylation (protein modification) [214]. To date, no studies have directly investigated the function of Galk in the heart.

4.3.3.1 Transposable elements in *Galk* rescue *tinC-YCanA^{act}*-induced cardiac enlargement

I tested the hypothesis that *Galk* was the causative modifier in the suppressor region for CanA^{act} cardiac enlargement. I obtained flies with transposable element insertions in *Galk* (*PBac{PB}Galk^{c03848}* and *Mi{ET1}Galk^{MB10638}*) and analyzed the effect of having a heterozygous transposable element allele in the context of *tinC-YCanA^{act}*. Results show that both transposable elements in *Galk* rescued the CanA^{act}-induced cardiac contractility phenotype (Figure 15A-B). *Mi{ET1}Galk^{MB10638}* rescued both end-diastolic dimension and fractional shortening while *PBac{PB}Galk^{c03848}* rescued the fractional shortening to a lesser extent and did not significantly rescue increased end-diastolic dimension. This may be due to the lesser extent of gene knock-down as shown with real-time RT-PCR (Figure 15C). These results show that transposable elements in

Galk rescue CanA^{act}-induced cardiac enlargement, revealing *Galk* as a potential modifier gene.

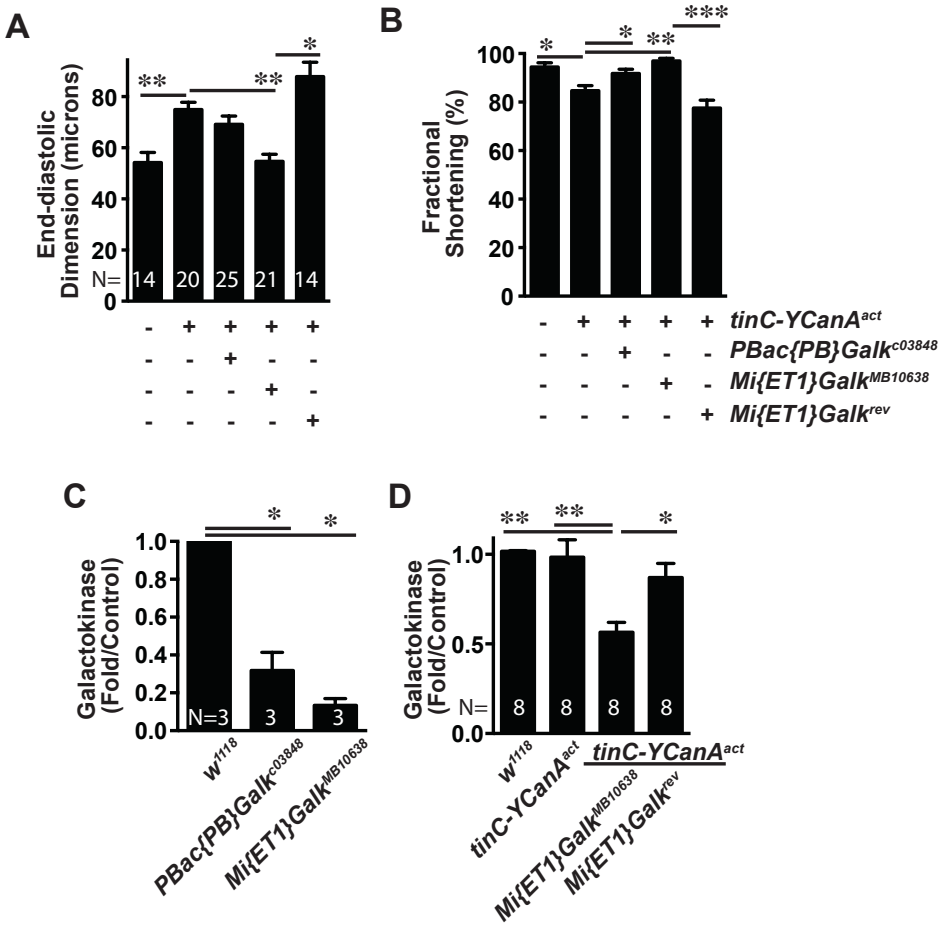

Figure 15: Transposable elements in galactokinase rescued CanA^{act}-induced cardiac enlargement.

(A-B) Summary data for (A) end-diastolic dimensions and (B) fractional shortenings of flies expressing w^{1118} control, heterozygous *tinC-YCanA^{act}*, the transposable elements *PBac{PB}Galk^{c03848}*, *Mi{ET1}Galk^{MB10638}*, or precise excision of

Mi{ET1}Galk^{MB10638} (*Mi{ET1}Galk*^{rev}), in the context of *tinC-YCanA*^{act}. The two transposable elements in *Galk* rescued *tinC-YCanA*^{act}-mediated cardiac contractility, *Mi{ET1}Galk*^{MB10638} rescued cardiac enlargement, while a precise excision reverted the rescue. (A: *P<0.05, **P<0.01; B: *P<0.05, **P<0.001, ***P<0.0001 compared to *tinC-YCanA*^{act} or *Mi{ET1}Galk*^{MB10638} as indicated with an over bar.) (C) qRT-PCR for *Galk* expression of w^{1118} control, homozygous *PBac{PB}Galk*^{c03848}, or homozygous *Mi{ET1}Galk*^{MB10638}. Galk expression is downregulated by transposable element insertions (*P<0.001 compared to w^{1118} control). (D) qRT-PCR of *Galk* expression in w^{1118} control flies, flies heterozygous for *tinC-YCanA*^{act} alone, in the context of heterozygous *Mi{ET1}Galk*^{MB10638}, or a precise excision of *Mi{ET1}Galk*^{MB10638}, *Mi{ET1}Galk*^{rev} (*P<0.05, **P<0.001 compared to heterozygous *tinC-YCanA*^{act}/*Mi{ET1}Galk*^{MB10638}). One-way ANOVA with Bonferroni correction for multiple comparisons, all data represent mean ±SEM.

4.3.3.2 RNAi to *Galk* rescued *tinC-YCanA*^{act}-induced cardiac enlargement

To further confirm that the *tinC-CanA*^{act} cardiac phenotype is rescued by deficiency of *Galk* instead of non-target effects from transposable elements, flies expressing RNAi against *Galk* were utilized. *Drosophila* expressing shRNA that is converted into siRNA by Dicer protein to degrade *Galk* mRNA was used (*P{KK107801}VIE-260B*). Control w^{1118}, driver alone, RNAi transgene no driver, RNAi

expression alone, *tinC-YCanA^{act}* alone, or *Galk* RNAi rescue of *tinC-YCanA^{act}* were generated according to the crosses in Figure 16A. Results show that RNAi to *Galk* rescued *tinC-YCanA^{act}*-induced cardiac enlargement and driver alone, RNAi transgene alone, and RNAi expression alone controls did not cause a cardiac phenotype (Figure 16B-C). Real-time RT-PCR confirmed that gene expression was knocked down in RNAi expressing flies (Figure 16D). These results further confirm that deficiency of Galk suppresses CanA^{act}-induced cardiac enlargement.

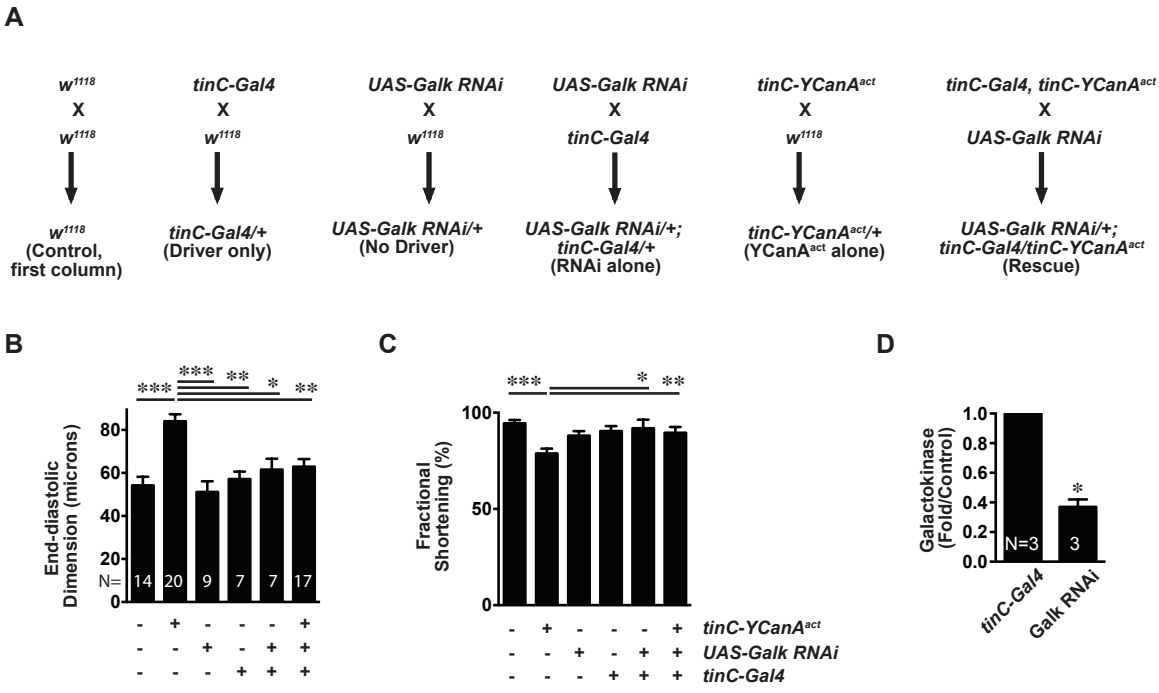

Figure 16: RNAi against Galk rescued *tinC-CanA^{act}*-induced cardiac enlargement.

A) Experimental design of fly crosses set up for RNAi rescue experiment. B) End-diastolic dimensions and C) fractional shortenings from OCT m-mode images of F1 progeny from the crosses made in (A). Compared to control w^{1118}, driver or RNAi alone do not result in an enlargement phenotype and expressing RNAi rescued the *tinC-YCanA*^{act} cardiac enlargement phenotype. (*P<0.05, **P<0.001, ***P<0.0001, one-way ANOVA with Bonferroni correction.) D) Real-time RT-PCR confirmed that *Galk* mRNA levels were down-regulated in flies expressing Galk RNAi. (*P<0.001, student's t test. All data represent mean ±SEM.)

Chapter 5. Characterizing *galactokinase* (*Galk*) as a modifier of CanA^{act}-induced cardiac enlargement

Results in the previous chapter established a suppressor region which encompasses genes that modify CanA^{act}-induced cardiac enlargement and revealed *galactokinase* (*Galk*) as a potential modifier. I proceeded to further characterize this novel finding using the *tinC-Gal4>UAS-CanA^{act}* fly as a model. I used multiple driver lines to express *UAS-CanA^{act}* in different tissues and analyzed additional phenotypes including life span, wing, and lethality. In addition, I examined the effect of knocking down mammalian *Galk* orthologues on calcineurin signaling using siRNA in cell culture.

5.1 Deficiency in Galk also rescued tinC-Gal4>UAS-YCanA^{act}-induced phenotypes

I had used multiple methods to confirm that deficiency of *Galk* rescued the *tinC-YCanA^{act}*-induced cardiac enlargement phenotype. I generated another *UAS-YCanA^{act}* fly to utilize the *Gal4*/*UAS* system for two main purposes: 1) to further demonstrate that deficiency of *Galk* rescues CanA^{act}-induced cardiac enlargement using another system; and 2) to examine the effect of *Galk* deficiency in other tissues. This first section describes the phenotype of *tinC-Gal4>UAS-YCanA^{act}* and rescue by deficiency of *Galk*.

5.1.1 The *tinC-Gal4>UAS-YCanA^{act}* fly displayed cardiac enlargement that was rescued by deficiencies encompassing *Galk* and known modifiers of calcineurin signaling

The *UAS-YCanA^{act}* line was crossed with a *tinC-Gal4* line to express YCanA^{act} in the heart. Cardiac enlargement was also displayed in *tinC-Gal4>UAS-YCanA^{act}* flies: end-diastolic dimension was enlarged and fractional shortening was decreased (Figure 17). In the context of *tinC-Gal4>UAS-YCanA^{act}*, the deficiencies incorporating Galk previously found to rescue *tinC-YCanA^{act}*-induced cardiac enlargement (*Df(3L)ED4416* and *Df(3L)BSC130*) also rescued cardiac enlargement, further demonstrating Galk deficiency as a suppressor of CanA^{act}-induced cardiac enlargement. In addition, known modifiers of CanA^{act} (*Mef2*, *sprouty*, and *CanB2*) were tested for rescue of the cardiac enlargement phenotype to assay the consistency of the system for detecting modifiers. Deficiency of

Mef2 (*Df(2R)X1,Mef2*^{X1}), *sprouty* (*sty*$^{\Delta 5}$), and *CanB2* (*P{EP}CanB2*^{EP774}), also rescued *tinC-Gal4>UAS-YCanA*^{act} -induced cardiac enlargement (Figure 17).

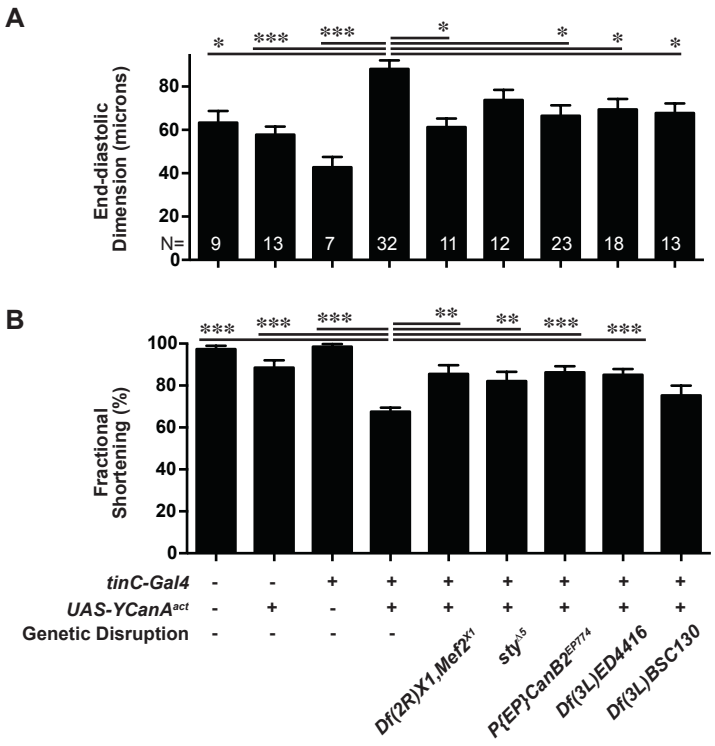

Figure 17: Deficiency of *Galk* also rescued *tinC-Gal4>UAS-YCanA*^{act}-induced cardiac enlargement.

A) End-diastolic dimensions and B) fractional shortenings for *w*^{1118} control (first column), *UAS-YCanA*^{act} alone (no driver), *tinC-Gal4* alone (driver only), *tinC-Gal4>UAS-YCanA*^{act} (CanA^{act} only), and *tinC-Gal4>UAS-YCanA*^{act} in the context of deficiencies in the known calcineurin modifiers: *Mef2*, *sprouty*, or *CanB2*, or the deficiencies encompassing *Galk*: *Df(3L)ED4416* or *Df(3L)BSC130*. In agreement with previous results, *tinC-*

Gal4>UAS-YCanA^{act} also induced a significant cardiac enlargement phenotype. This is rescued by the known modifiers of calcineurin: *Mef2*, *sprouty*, and *CanB2*, and deficiencies encompassing *Galk*: *Df(3L)ED4416* and *Df(3L)BSC130*. (*P<0.05, **P<0.01, ***P<0.0001. One-way ANOVA with Bonferroni correction. All data represent mean ±SEM.)

5.1.2 The *tinC-Gal4>UAS-YCanA*^{act} fly displayed thickening of the cardiac chamber wall that is rescued by disruption of *Galk*

To further characterize the *tinC-Gal4>UAS-YCanA*^{act} fly, histology of the fly hearts was examined. Examining the hearts of *tinC-Gal4* (driver alone) or *tinC-Gal4>UAS-YCanA*^{act} flies in histological sections, wall thickness was significantly increased in *tinC-Gal4>UAS-YCanA*^{act} flies (Figure 18). This was consistent with the cardiac hypertrophy observed in mice; though distinct from the *tinC-YCanA*^{act} phenotype which displayed cardiac enlargement without a thickening of the cardiac chamber wall. The higher expression level of CanA^{act} with the *Gal4/UAS* bipartite system may have caused sarcomeric structures to be added in parallel as well as in series. The effect of disrupting *Galk* with *Mi{ET1}Galk*^{MB10638} was also examined for *tinC-Gal4>UAS-YCanA*^{act} flies. Results showed that disruption of *Galk* with *Mi{ET1}Galk*^{MB10638} rescued the increase in wall thickness induced by *tinC-Gal4>UAS-YCanA*^{act} (Figure 18).

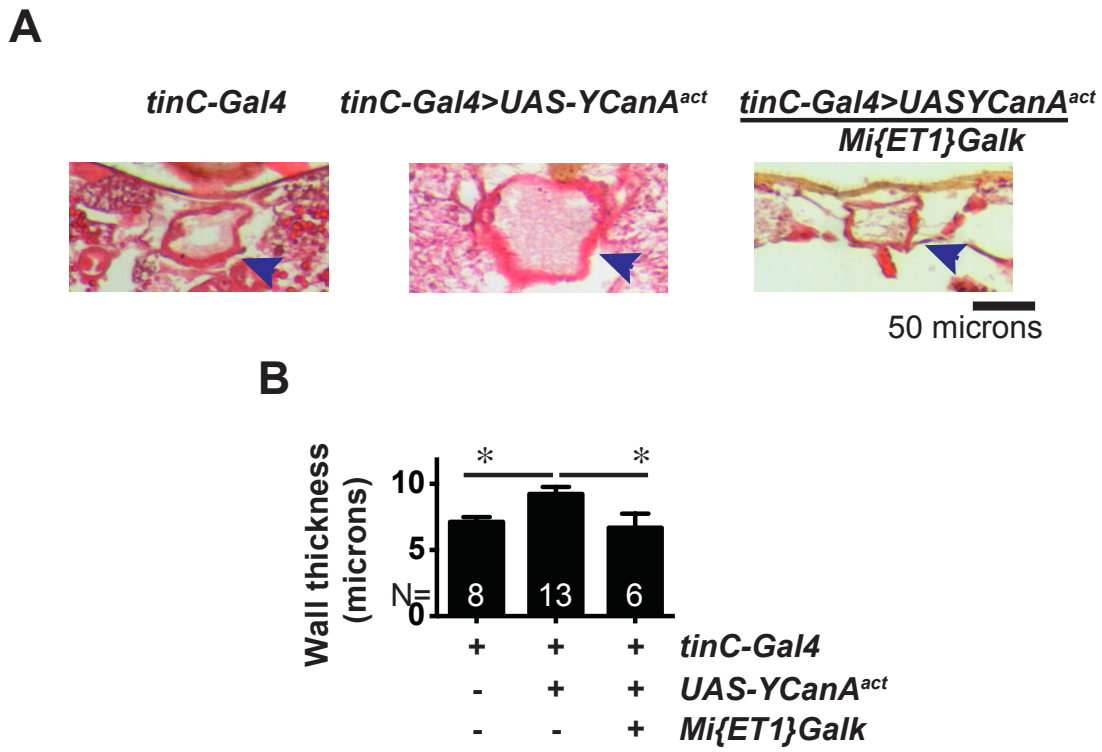

Figure 18: Wall thickness is increased in *tinC-Gal4>UAS-YCanA^{act}* fly hearts and is rescued by disruption of *Galk*.

A) Paraffin sections 8μm thick with H&E stain for *tinC-Gal4* (driver alone), *tinC-Gal4>UAS-YCanA^{act}*, or *tinC-Gal4>UAS-YCanA^{act}* in the context of *Mi{ET1}Galk^{MB10638}* (*Mi{ET1}Galk*) flies. Arrow heads point to the heart wall. B) Quantitative results measured from images of histological sections in image J. Measurements were made from the dorsal, ventral, left and right of the heart, excluding the dorsal longitudinal muscle underlying the heart tube. Compared to control flies, *tinC-Gal4>UAS-YCanA^{act}* flies display a significantly thicker heart wall which is rescued in the context of *Mi{ET1}Galk^{MB10638}*. (*P<0.05, one-way ANOVA with Bonferroni correction, data represent mean ±SEM.)

5.2 Deficiency in Galk also rescued decreased life span of tinC-YCanA^{act} flies

I further characterized the nature of the *Galk* disruption-mediated rescue of *tinC-YCanA^{act}* phenotypes. The life span of *tinC-YCanA^{act}* flies relative to control was examined. Compared to flies only expressing a transposable element in *Galk*, *Mi{ET1}Galk^{MB10638}*, which displayed a normal end-diastolic dimension and fractional shortening, *tinC-YCanA^{act}* flies displayed a much shorter life span, with 98% of the progeny not surviving past 80 days post-eclosion. *tinC-CanA^{act}* in the context of *Mi{ET1}Galk^{MB10638}* rescued this shortening of life span (Figure 19). These results show that rescuing cardiac function in cardiac-CanA^{act} flies also rescued survival. However, a caveat to this result is the possibility of genetic background confounding the survival data.

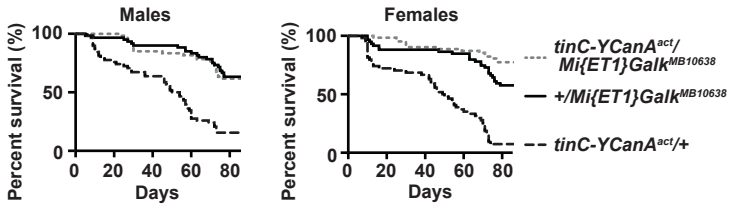

Figure 19: Transposable element insertion in Galk rescued *tinC-YCanA^{act}*-induced decrease in life span.

Survival curve of male and female flies heterozygous for *Mi{ET1}Galk*^{MB10638}, *tinC-YCanA*^{act}, or *Mi{ET1}Galk*^{MB10638} in the context of *tinC-YCanA*^{act}. *Mi{ET1}Galk*^{MB10638} significantly rescued the *tinC-YCanA*^{act} survival phenotype. ($P<0.0001$ for both male and female groups comparing *tinC-YCanA*^{act} with *tinC-YCanA*^{act}/*Mi{ET1}Galk*^{MB10638}, Mantel-Cox log rank test. N=60 in each group.)

5.3 Disruption of Galk does not rescue cardiac enlargement of hdp2 flies.

I then tested whether *Mi{ET1}Galk*^{MB10638} could rescue a non calcineurin-mediated cardiomyopathy of the troponin I mutant (*hdp2*) that shows a flight muscle abnormality and cardiac dilation [189, 203]. *Mi{ET1}Galk*^{MB10638} did not rescue the cardiac dilation phenotype of heterozygous *hdp2* flies (Figure 20), indicating that Galk involvement is specific to CanA^{act}-induced cardiomyopathy.

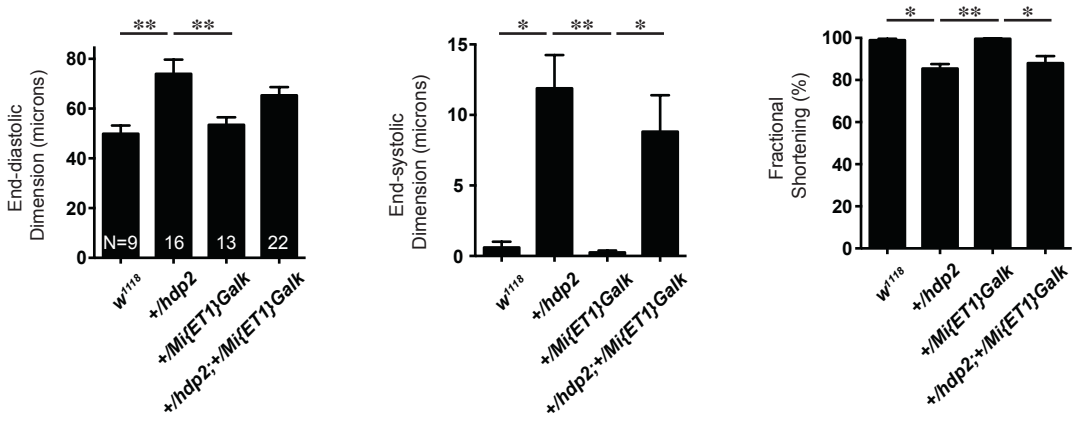

Figure 20: Disruption of *Galk* did not rescue cardiac enlargement of *hdp2* flies

Quantified results from OCT m-mode images of end-diastolic dimension, end-systolic dimensions, and fractional shortenings of w^{1118} control, heterozygous *hdp2* (+/*hdp2*), heterozygous $Mi\{ET1\}Galk^{MB10638}$ (+/*Mi{ET1}Galk*), and *hdp2* in the context of $Mi\{ET1\}Galk^{MB10638}$ (+/*hdp2;+/Mi{ET1}Galk*). Heterozygous *hdp2* induced a mild cardiac enlargement phenotype that was not rescued by $Mi\{ET1\}Galk^{MB10638}$. *hdp2* is a fly with a null mutation of troponin I. *P<0.05, **P<0.01, one-way ANOVA with Bonferroni correction. All data represent mean ±SEM.

5.4 Galk is not sufficient to induce cardiac enlargement.

I further characterized the nature of Galk in the heart by engineering a fly to overexpress Galk in the heart. A transgenic fly was made expressing *UAS-Galk*. This was crossed with the *tinC-Gal4* line and progeny overexpressing *tinC-Gal4>UAS-Galk* for

cardiac enlargement. Compared to controls, *tinC-YCanA^{act}* fly hearts were enlarged measuring OCT images for end-diastolic dimension and fractional shortening while *tinC-Gal4>UAS-Galk* fly hearts are not (Figure 21). These results indicate that expressing Galk is not sufficient to induce cardiac enlargement without CanA^{act}.

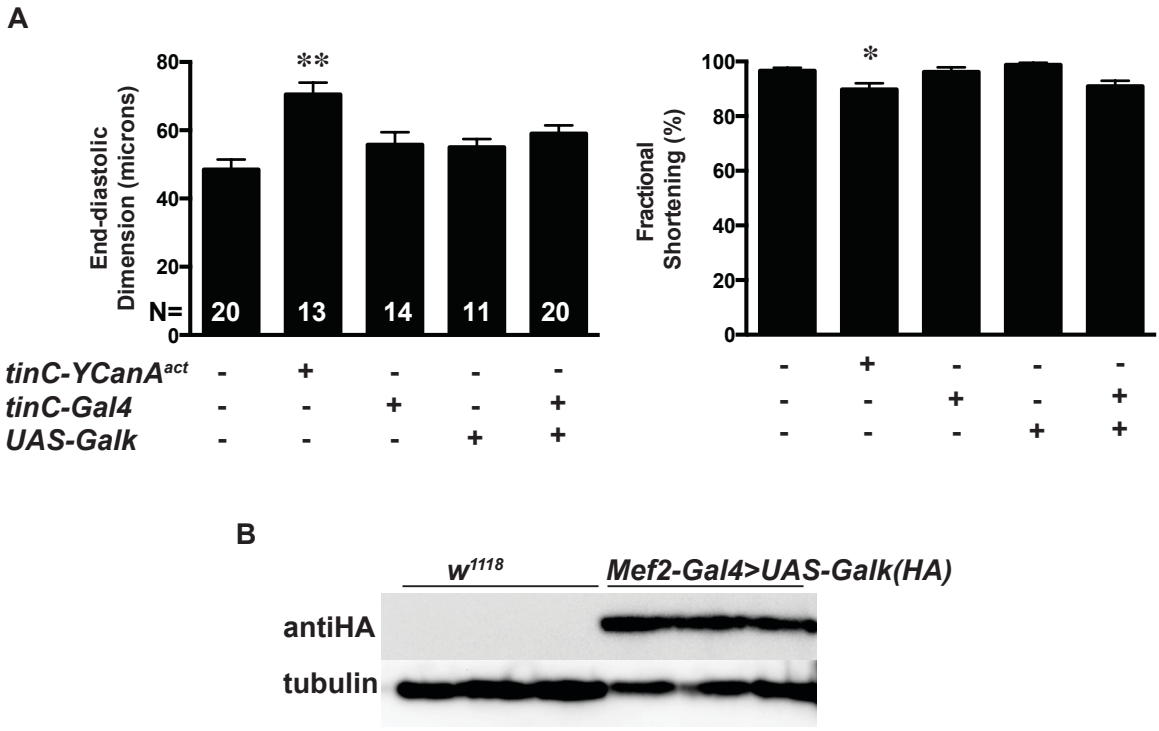

Figure 21: Overexpressing Galk in the fly heart did not induce cardiac enlargement.

A) Quantification for m-mode OCT images measuring end-diastolic dimensions and fractional shortenings in control *w^{1118}*, heterozygous *tinC-YCanA^{act}*, *tinC-Gal4* (driver alone), *UAS-Galk* (no driver), or flies expressing *tinC-Gal4>UAS-Galk*. Expressing Galk in the heart of *tinC-Gal4>UAS-Galk* flies did not induce cardiac enlargement. (*P<0.05,

**P<0.0001 compared to control, one-way ANOVA with Bonferroni correction.) B) Western blots demonstrating expression of HA-tagged Galk in w^{1118} and heterozygous *Mef2-Gal4>UAS-Galk* flies. Tubulin is used as an internal control.

5.5 Galk modified expression of UAS-CanA^{act} in a tissue-specific manner

I expressed *UAS-YCanA^{act}* in different tissues including ectoderm, mesoderm, and posterior compartment of the imaginal wing disc, using corresponding *-Gal4* driver lines to further characterize the nature of the *Galk* rescue of *YCanA^{act}* phenotypes outside of the heart.

5.5.1 Genetic disruption of *Galk* rescued *e16E>UAS-YCanA^{act}*-induced wing vein abnormality

According to previous studies, driving CanA^{act} in the wing with an engrailed driver causes wing vein abnormality [10]. *UAS-YCanA^{act}* expressed under the control of an *e16E-Gal4* engrailed driver produced a variable wing vein phenotype: abnormality in the posterior crossveins (PCV) and the longitudinal wing vein L5 (Figure 22). *Df(3L)ED4416* and *Mi{ET1}Galk^{MB10638}* significantly rescued the *e16E-Gal4>UAS-YCanA^{act}*-induced abnormal wing vein phenotype. The percentage of normal wing vein flies significantly increased from 11% to 44%, and the percentage of flies with abnormal wing vein phenotypes decreased from 89% to 56% with a genetic deficiency encompassing

Galk. The rescue with *Mi{ET1}Galk*^{MB10638} was significant but less pronounced, with an increase of 5% normal to 31% normal wing vein flies, and a decrease of 95% to 69% abnormal wing vein flies (Figure 22). This difference could be explained by residual expression of Galk in the Minos insertion mutant or interference by other genes within the deficiency region.

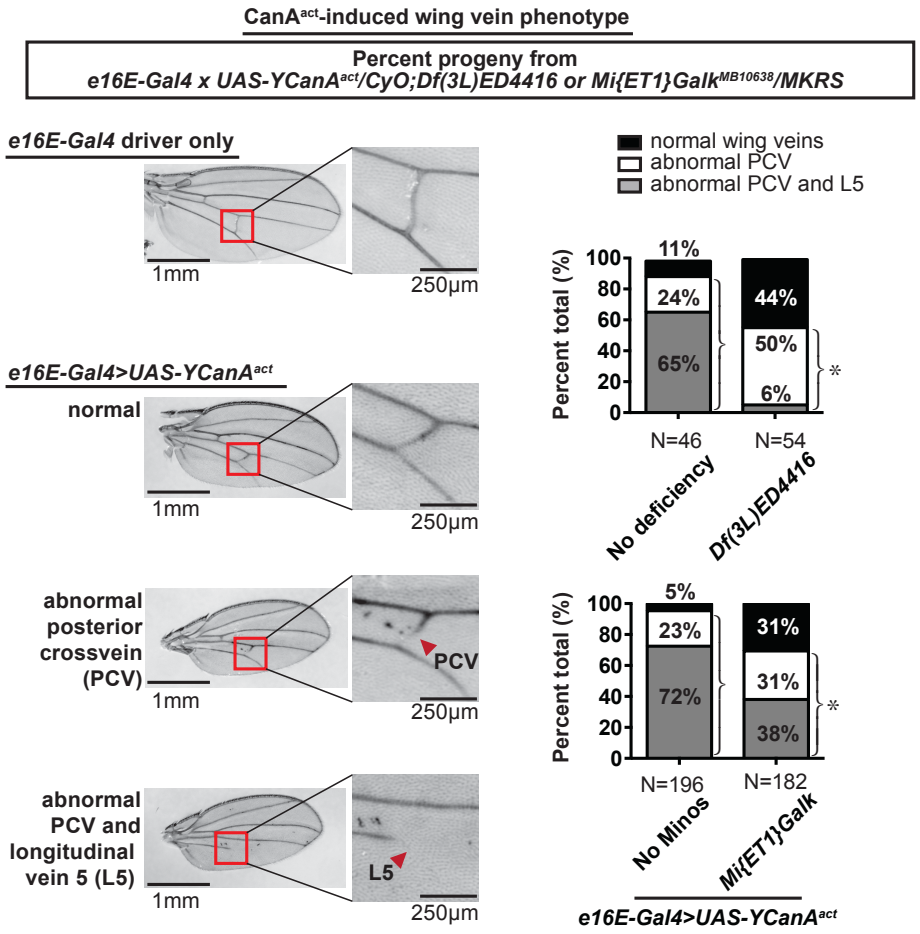

Figure 22: Disruption of Galk rescued *e16E>UAS-YCanA*^{act}-induced wing vein abnormality.

Wings of progeny from the cross *e16E-Gal4* x *UAS-YCanA^{act}/CyO;Df(3L)ED4416/MKRS*. Homozygous *e16E-Gal4* (driver only), or wings of flies expressing *e16E-Gal4>UAS-YCanA^{act}* were imaged. A range of phenotypes were observed in flies: normal, abnormality of the posterior cross vein (PCV), or abnormality of both the PCV and longitudinal wing vein 5 (L5). Bar graphs on the right show percentages of flies displaying the corresponding wing vein phenotypes. Results show that genetic deficiency or disruption of Galk by *Df(3L)ED4416* or *Mi{ET1}Galk^{MB10638}* significantly rescued the wing vein phenotype. (*P<0.0001, Fisher's exact test comparing percentage of normal versus abnormal winged flies.)

5.5.2 Deficiency of *Galk* did not rescue *Act5C-Gal4>UAS-YCanA^{act}*-induced lethality

The effect of driving *UAS-YCanA^{act}* ubiquitously with the *Act5C-Gal4* driver was evaluated. Ubiquitous *Act5C-Gal4>UAS-YCanA^{act}* caused lethality. These flies died at the 1st instar larval stage. Progeny from the cross *Act5C-Gal4/CyO* x *YCanA^{act}/CyO;Df(3L)ED4416/TM2* was analyzed. Since *Act5C-Gal4>UAS-YCanA^{act}* caused lethality, if progeny was produced in the context of *Df(3L)ED4416*, this would signify a rescue. However, results showed that out of 324 total progeny, no flies were detected either with or without the deficiency. This demonstrates that deficiency of Galk did not rescue the *Act5C-Gal4>UAS-YCanA^{act}* lethality phenotype. The rescue of the CanA^{act} phenotype by deficiency of *Galk* was not universal (Figure 23). However, these results

do not rule out the possibility that the level of *Galk* disruption was not sufficient to rescue the lethality due to the severity of the phenotype.

CanA^{act}-induced lethality

Recovered progeny from *Act5C-Gal4/CyO x UAS-YCanA^{act}/CyO;Df(3L)ED4416/TM2*		
Genotype	**No deficiency**	***Df(3L)ED4416***
No *UAS-YCanA^{act}* expression	130	194
Act5C-Gal4>UAS-YCanA^{act}	0	0 (No rescue)

Figure 23: Deficiency of Galk rescued *Act5C-Gal4>UAS-YCanA^{act}*-induced lethality.

Number of progeny expressing the respective phenotypes from the cross. No progeny were produced expressing *Act5C-Gal4>UAS-YCanA^{act}*, showing that deficiency of *Galk* did not rescue *Act5C-Gal4>UAS-YCanA^{act}* -induced lethality. (Fisher's exact test comparing percentage of viable flies expressing *Act5C-Gal4>UAS-YCanA^{act}* with deficiency to without deficiency.)

5.5.3 Deficiency of *Galk* did not rescue *dpp-Gal4>UAS-YCanA^{act}*-induced wing abnormality

The effect of driving *UAS-YCanA^{act}* ectodermally with the *dpp-Gal4* driver was evaluated. Ectodermal *dpp-Gal4>UAS-YCanA^{act}* caused an abnormal wing phenotype where the wing was unable to expand (Figure 24). Progeny from the cross *dpp-Gal4/TM6B* x *YCanA^{act}/CyO;Df(3L)ED4416/TM2* was analyzed; if the percentage of

normal winged progeny expressing *dpp-Gal4>UAS-YCanA^{act}* was increased in the context of *Df(3L)ED4416*, this would signify a rescue. Results showed that there was no significant increase in normal-winged progeny. These results suggest that Galk does not modify CanA^{act} in ectodermal tissue. However, it is possible that the level of Galk disruption was not sufficient to rescue the phenotype even if Galk does play a role downstream to CanA^{act} in ectodermal tissue.

CanA^{act}-induced wing phenotype

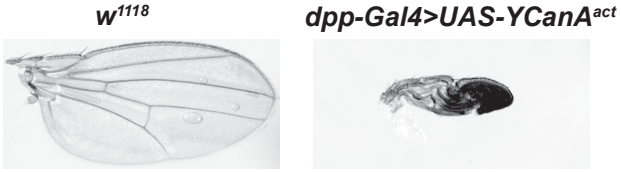

Percent abnormal winged progeny from *dpp-Gal4/TM6B x UAS-YCanA^{act}/CyO;Df(3L)ED4416/TM2*		
Genotype	**No deficiency**	***Df(3L)ED4416***
No *UAS-YCanA^{act}* expression	**0% (N=0/20)**	**0% (N=0/14)**
dpp-Gal4>UAS-YCanA^{act}	**72.22% (N=8/11)**	**69.59% (N=16/23) (No rescue)**

Figure 24: Deficiency encompassing *Galk* did not rescue *dpp-Gal4>UAS-YCanA^{act}*-induced abnormal wing phenotype.

Images show the wing of control *w^{1118}* and *dpp-Gal4>UAS-YCanA^{act}* flies. Flies expressing *dpp-Gal4>UAS-YCanA^{act}* show an abnormal wing phenotype where the wing fails to expand after eclosion. Bottom figure shows the percentage and number of total abnormal winged progeny expressing the respective genotypes from the cross *dpp-Gal4/CyO* x *YCanA^{act}/CyO;Df(3L)ED4416/TM2*. Deficiency encompassing *Galk*,

Df(3L)ED4416, did not rescue wing abnormality of *dpp-Gal4>UAS-YCanA^{act}* flies. (Fisher's exact test comparing the percentage of abnormal winged flies expressing *dpp-Gal4>UAS-YCanA^{act}* between groups with or without deficiency. All transgenes were heterozygous.)

5.5.4 Deficiency of *Galk* did not rescue *Mef2-Gal4>UAS-YCanA^{act}*-induced lethality

The above experiments showed that *Galk* modified *UAS-YCanA^{act}* phenotypes in a tissue-specific manner. I next examined the effect of driving *UAS-YCanA^{act}* with a mesodermal *Mef2-Gal4* driver. Driving CanA^{act} expression in the mesoderm with *Mef2-Gal4>UAS-YCanA^{act}* led to late pupal lethality where pharate adults failed to emerge from the pupa. This result was consistent with the observations of Gajewski *et al*, who reported that ectopic expression of CanA^{act} with the *24B-* driver also causes pupal lethality due to defects of flight muscle development. If disruption of *Galk* rescued *Mef2-Gal4>UAS-YCanA^{act}*-induced pupal lethality, viable progeny will be recovered in the context of disruption of *Galk* with *Mi{ET1}Galk^{MB10638}* or *Df{3L}ED4416*. *Mi{ET1}Galk^{MB10638}* or *Df{3L}ED4416* was put into the context of *Mef2* by crossing *Mef2-Gal4* flies with *UAS-YCanA^{act}/CyO;Mi{ET1}Galk^{MB10638}/MKRS* or *UAS-YCanA^{act}/CyO;Df{3L}ED4416/MKRS* flies. No viable progeny expressing *Mef2-Gal4>UAS-YCanA^{act}* were recovered in the context of either *Mi{ET1}Galk^{MB10638}* or *Df{3L}ED4416*, indicating that disruption of *Galk* did not

rescue the *Mef2-Gal4>UAS-YCanA^{act}* -induced pupal lethality (Figure 25). Whether this result correlates to Galk not effecting CanA^{act} in mesodermal tissue remains to be confirmed.

A) CanA^{act}-induced lethality

Recovered progeny from *Mef2-Gal4 x UAS-YCanA^{act}/CyO;Df{3L}ED4416/MKRS*		
Genotype	**No deficiency**	***Df(3L)ED4416***
No *UAS-YCanA^{act}* expression	52	49
Mef2-Gal4>UAS-YCanA^{act}	0	0 (No rescue)

B)

Recovered progeny from *Mef2-Gal4 x UAS-YCanA^{act}/CyO;Mi{ET1}Galk^{MB10638}/MKRS*		
Genotype	**No Minos**	***Mi{ET1}Galk^{MB10638}***
No *UAS-YCanA^{act}* expression	104	107
Mef2-Gal4>UAS-YCanA^{act}	0	0 (No rescue)

Figure 25: Disruption of *Galk* did not rescue *Mef2-Gal4>UAS-YCanA^{act}*-induced pupal lethality.

Experiments were performed to determine if disruption of *Galk* rescues *Mef2-Gal4>UAS-YCanA^{act}*-induced lethality. Flies expressing *Mef2-Gal4* were crossed to either *UAS-YCanA^{act}/CyO* flies with A) *Df{3L}ED4416* or B) *Mi{ET1}Galk^{MB10638}* over the MKRS balancer on the third chromosome. The number of resulting progeny expressing the corresponding genotypes was counted. No progeny expressing *Mef2-Gal4>UAS-YCanA^{act}* were recovered from the cross, indicating that deficiency *Df{3L}ED4416* encompassing *Galk* and disruption of *Galk* with *Mi{ET1}Galk^{MB10638}* did not rescue the *Mef2-Gal4>UAS-YCanA^{act}* lethality phenotype. (Fisher's exact test comparing percentage

of viable flies expressing *Mef2-Gal4>UAS-YCanA^{act}* with or without deficiency or insertion.)

5.6 Knocking down Galk1 in H9c2 and NIH-3T3 cells did not affect calcineurin-induced NFAT translocation

I went on to further explore the role of *Galk* in calcineurin signaling in mammalian cell lines. Ionomycin is an ionophore which increases calcium concentration in the cell, thereby activating calcineurin by calcium/calmodulin and CanB binding. NFAT-GFP was transfected into cells to examine NFAT translocation. NFAT-GFP translocation was activated downstream of ionomycin-induced calcineurin activation. An siRNA to a mammalian homologue of *Galk*, *Galk1*, was found to effectively knock down *Galk1* expression and was used to investigate the role of Galk1 on calcineurin-induced NFAT translocation. If Galk1 played a role in modifying the calcineurin/NFAT pathway, NFAT translocation would be altered with siRNA to Galk1. Results showed that NFAT translocation was not altered by knocking down *Galk1* in the NIH-3T3 mouse fibroblast cell line or the H9c2 rat cardiomyoblast cell line (Figure 26).

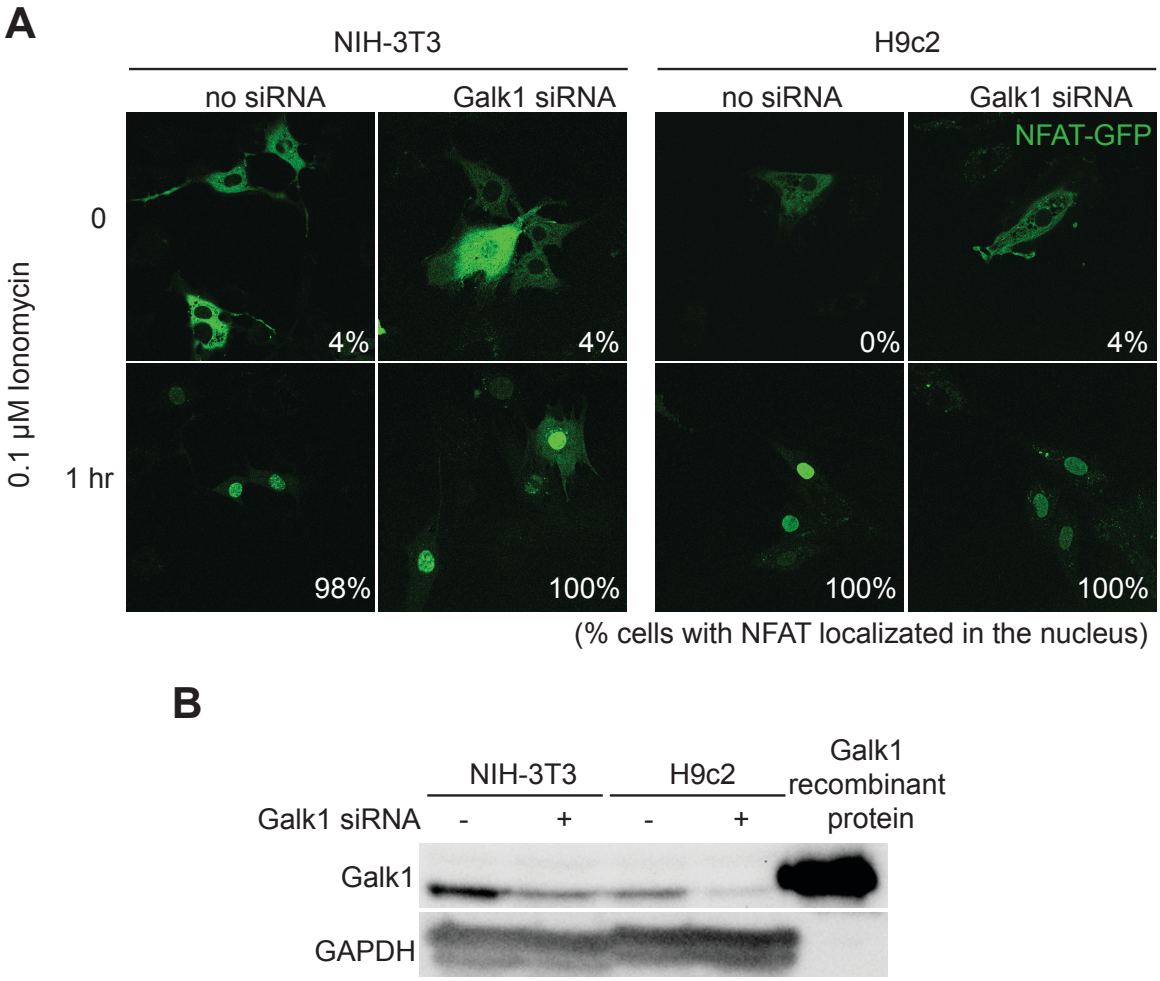

Figure 26: Knocking down Galk with siRNA in NIH-3T3 fibroblast and H9c2 cells did not alter calcineurin-activated NFAT translocation.

A) Transiently transfected NFAT-GFP localization with or without the calcineurin activator ionomycin (0.1 μM) or siRNA to Galk1. Ionomycin induces NFAT translocation into the cell nucleus in NIH-3T3 mouse fibroblasts and H9c2 rat cardiomyoblasts. This translocation is not inhibited by knocking down Galk1 with siRNA. (N=50 in each group, Fisher's exact test comparing the percentage of cells with

translocated NFAT between control and siRNA groups.) B) Western blot showed that siRNA to Galk1 reduced Galk1 protein expression in both NIH-3T3 and H9c2 cells.

Chapter 6. A deficiency region on chromosome 2L rescued CanA^{act}-induced cardiac enlargement

Previous results in this study established a feasible method for screening for novel modifiers of CanA^{act}-induced cardiac enlargement. Utilizing this method, another region on chromosome 2L in the *Drosophila* genome was screened for rescue of CanA^{act}-induced cardiac enlargement. This was a region based on Gajewski *et al* in their screen for modifiers of the *24B-Gal4*-driven lethality phenotype. Another deficiency region and candidate gene was identified to modify CanA^{act}-induced cardiac enlargement.

6.1 A deficiency region on chromosome 2L rescued tinC-YCanA^{act}-induced cardiac enlargement.

Another deficiency region that was previously found to rescue *24B-Gal4 >CanA^{act}-*induced lethality was tested (Table 1). A deficiency region encompassing 31 genes was analyzed. Two deficiency lines from the Bloomington deficiency kit were used: *Df(2L)ED50001* and *Df(2L)ED5857*. As the results show, *Df(2L)ED5857* rescued *tinC-CanA^{act}*-induced cardiac enlargement while *Df(2L)ED50001* did not (Figure 27). This revealed another deficiency region on chromosome 2L encompassing 21 genes. As described in Table 3, several genes in this region appear to have high expression in the heart and may be potential candidate genes for modifiers of calcineurin-induced cardiac enlargement.

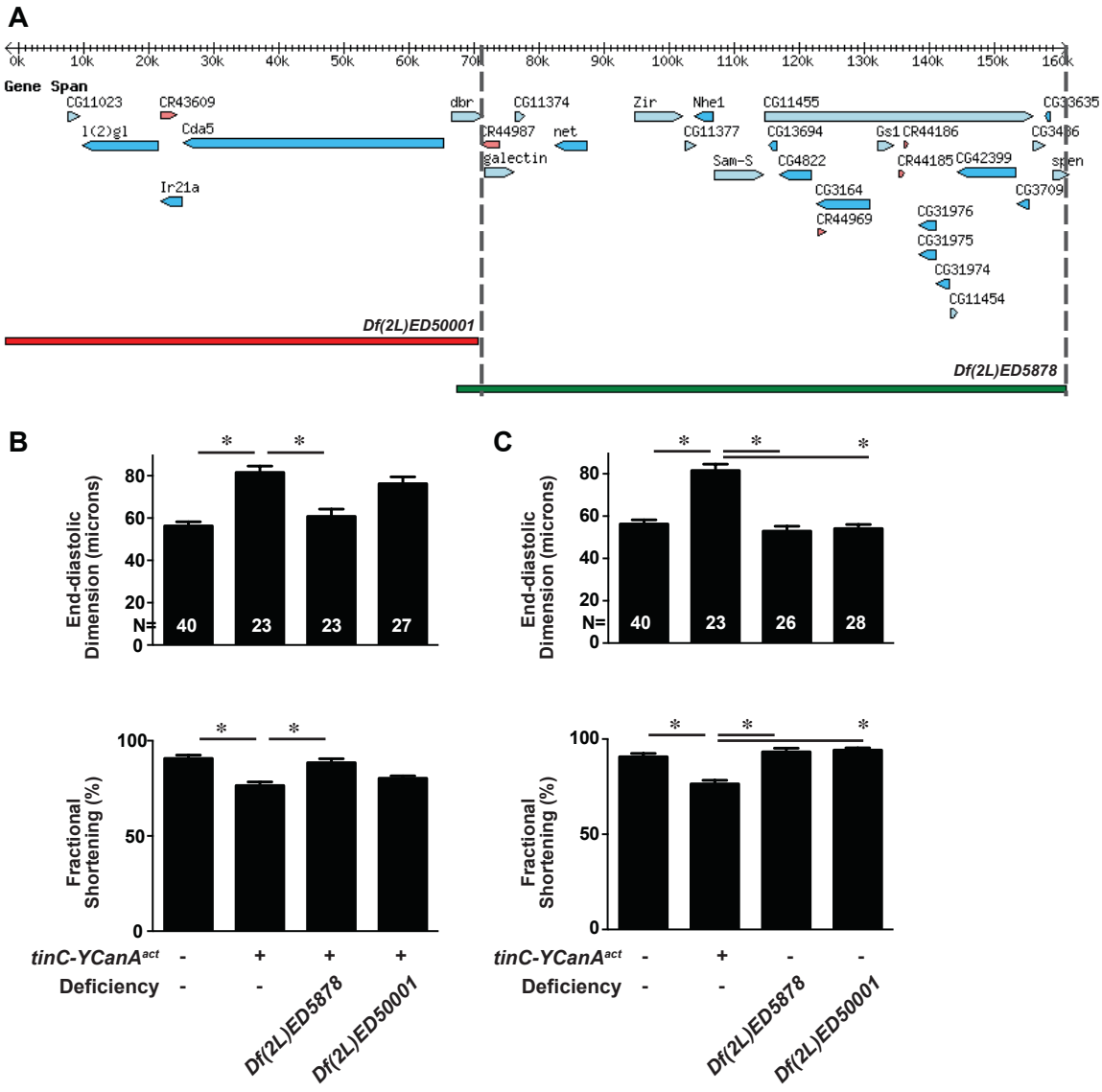

Figure 27: A deficiency region on chromosome 2L rescued *tinC-YCanA^{act}*-induced cardiac enlargement.

A) Chromosomal region covered by the deficiency lines *Df(2L)ED50001* and *Df(2L)ED5878*. (Adapted from Gbrowse, http://flybase.org/cgi-bin/gbrowse/dmel) B) End-diastolic dimension and fractional shortenings from OCT m-mode images of w^{1118} control, *tinC-YCanA^{act}*, and *tinC-YCanA^{act}* in the context of the *Df(2L)ED5878* or

Df(2L)ED50001. *Df(2L)ED5878* rescued *tinC-YCanA^{act}* cardiac enlargement while *Df(2L)ED50001* did not. The deficiency region delineated is outlined in grey dashed lines in (A). C) End-diastolic dimension and fractional shortenings of deficiency lines on their own without *tinC-YCanA^{act}*. The deficiency lines alone did not cause cardiac enlargement. (*P<0.0001, one-way ANOVA with Bonferroni correction. All data represent mean ±SEM. All transgenes were heterozygous.)

Table 3: Genes in the suppressor region on chromosome 2L

Gene	Possible function	Human orthologue	Expression in adult heart
galectin	Galactoside binding	LGALS9	High
CG11374	Galactoside binding	None	No
net	transcription.	None	Low
Zizimin-relatd	Rho GEF	None	Moderate
CG11377	Calcium binding	CRELD2	Moderate
Nhe1	Sodium/hydrogen exchanger	SLC9A8	Moderate
S-adenosylmethionine trasnsferase	Methionine adenosyltransferase	MAT2A	High
CG11455	NADH dehydrogenase	None	High
CG13694	unknown	None	No
CG4822	transporter	None	High
CG3164	transporter	None	High
Glutamine synthetase 1	Glutamine synthetase	None	High

CG31976	unknown	None	No
CG31974	transferase	None	High
CG11454	mRNA binding	None	Moderate
CG42399	unknown	None	No

Gene information obtained from flybase.org; expression data obtained from flyatlas.org

6.2 Transposable element insertion in galectin rescued tinC-YCanA^{act}-induced cardiac enlargement

Galectin, a galactoside-binding lectin, is known to facilitate protein-protein interactions through binding to galactosides on cell surface proteins. Interestingly, galectin stood out as a candidate because one possible mechanism by which Galk may exert its function is by facilitating glycosylation of glycoproteins with galactosides. I analyzed the effect of transposable elements in galectin. A P-element insertion in galectin, *P{wHy}galectin^{DG25505}*, rescued *tinC-YCanA^{act}*-induced cardiac enlargement (Figure 28). From these results, it is postulated that galectin may be a candidate modifier gene within the second region for CanA^{act}-induced cardiac enlargement. Whether or not additional genes are involved requires further experimentation.

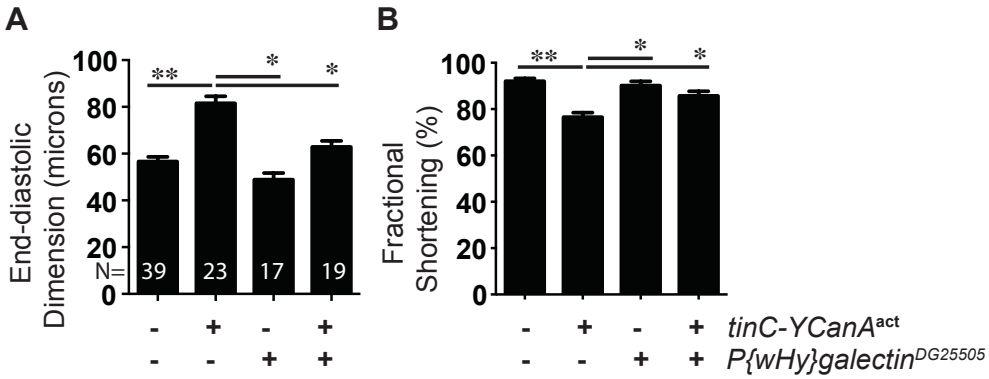

Figure 28: P-element insertion in *galectin* rescued *tinC-YCanA^{act}*-induced cardiac enlargement.

A) End-diastolic dimensions and B) Fractional shortenings measured from OCT m-mode images of *w^{1118}* control or *Drosophila* expressing heterozygous *tinC-YCanA^{act}*, a P-element insertion in galectin (*P{wHy}galectin^{DG25505}*), and *tinC-YCanA^{act}* in the context of *P{wHy}galectin^{DG25505}*. Genetic disruption of galectin rescued *tinC-YCanA^{act}*-induced cardiac enlargement. (*P<0.05, **P<0.0001, one-way ANOVA with Bonferroni correction. All data represent mean ±SEM.)

7. Discussion

Calcineurin has been shown to regulate mammalian cardiac hypertrophy; understanding factors associated with calcineurin signaling can lead to novel targets for treating cardiac disease. My study utilizes the advantages of the *Drosophila melanogaster* system to screen for modifiers of constitutively active calcineurin ($CanA^{act}$)-induced cardiac enlargement. I generated $CanA^{act}$-expressing sensitized *Drosophila* lines, which display cardiac enlargement and screened for modifiers of $CanA^{act}$-induced cardiac enlargement. From this study, I have 1) demonstrated that $CanA^{act}$ induces a significant cardiac phenotype despite the lack of calcineurin-regulated NFAT in *Drosophila*, 2) established a feasible method for discovering novel modifiers of $CanA^{act}$ in the heart, 3) discovered and characterized galactokinase as a novel modifier of $CanA^{act}$-induced cardiac enlargement, and 4) discovered galectin as a potential modifier of $CanA^{act}$-induced cardiac enlargement from a deficiency region on chromosome 2L.

7.1 Using Drosophila as a model to discover novel calcineurin modifiers in the heart

My results demonstrate a significant cardiac enlargement when overexpressing $CanA^{act}$ in the *Drosophila* heart. A substantial amount of research has accumulated regarding calcineurin-induced cardiac hypertrophy in mice [9, 19, 28, 73, 81, 82, 91, 94, 215-217]. Many modifiers of calcineurin-induced cardiac hypertrophy have been discovered, including NFAT [9], Mef2 [61], MCIP1 [71], Cain, and AKAP79 [72]. These include factors that signal downstream of calcineurin and factors that regulate calcineurin activity. These aspects of the calcineurin signaling pathway are under active investigation; however, it is clear that additional regulatory factors are involved. In fact, a recent study discovered that interferon regulatory factor 8 (IRF8), previously unknown to regulate calcineurin signaling, negatively regulates cardiac hypertrophy by inhibiting NFAT [216]. The fact that many of these known factors are absent from the *Drosophila* genome and that powerful genetic tools are available for large scale screening in the fly indicate that *Drosophila* provides a system to investigate essential components downstream of $CanA^{act}$, which may not be discovered in a mammalian system. This is evidenced by the discovery of two novel regulators of calcineurin-mediated cardiac hypertrophy in my study: Galk and galectin.

Multiple signaling pathways crosstalk and form a complex signaling pathway during the onset of cardiac hypertrophy, with calcineurin serving as one branch of this system. Many of these pathways may have dual functionality and multiple pathways

may converge to induce the phenotype. For example, the upregulation of calcium/calmodulin induces activation of PKC, CaMK, and calcineurin [94, 218]; ERK activates NFAT while inhibiting apoptosis; Mef2 is necessary but not sufficient to induce a cardiac hypertrophic phenotype [61]; and MEK1 to ERK signaling is necessary but not sufficient to induce concentric cardiac hypertrophy [96]. To add to the complexity, when comparing the genes upregulated in several different cardiac hypertrophy models, the downstream activated genes did not overlap, indicating that the same hypertrophic phenotype can be elicited by the expression of distinct sets of genes [103]. These data indicate that cardiac hypertrophy is a complex disease induced by multiple redundant signaling pathways that may be differentially regulated in different patients, and discovering novel pathways has the potential to benefit patients that are not responsive to current treatments. In addition, more complete knowledge of the signaling pathways will provide insight regarding the most beneficial combination of genes and proteins to target for therapy.

In my study, I have established the use of *Drosophila* as a model enabling large scale screening for novel genes that modify calcineurin-induced cardiomyopathy. I have also identified two novel genes that modify calcineurin-induced cardiac enlargement. Further exhaustive deficiency screening will provide great insight into the regulation and signaling of calcineurin in the heart.

7.2 Comparing the CanA^{act}-induced cardiac enlargement phenotype in the fly to mammalian cardiac hypertrophy

Ultimately, the goal is to discover novel genes that also regulate mammalian cardiac calcineurin. Both the fly and mammalian models displayed significant phenotypes in the heart. However, the specific phenotypes were distinct from each other: the *α-MHC-CanA^{act}* mouse displayed eccentric and concentric cardiac hypertrophy with significant myofibrillar disarray, collagen deposition, and premature death, while the *tinC-CanA^{act}* fly displayed eccentric cardiac hypertrophy, and decreased life span with no obvious myofibrillar disarray or collagen deposition. These descrepancies may be due to the distinct cardiac structures and genetic compositions of the mammalian and fly hearts.

7.2.1 Eccentric cardiac hypertrophy (increased lumen area)

The mouse model of cardiac CanA^{act} displayed several hypertrophy phenotypes including eccentric cardiac hypertrophy, which is the dilation of the cardiac chamber due to the addition of sarcomeres in series [9]. This is the main phenotype that was observed in *tinC-YCanA^{act}* and *tinC-Gal4>UAS-YCanA^{act} Drosophila*. *Drosophila* do not express calcineurin-mediated NFAT; it can be postulated that a mechanism involving a different downstream transcription factor may be involved, possibly Mef2. Interestingly, studies involving overexpressing Mef2 in mice show that Mef2 may

regulate this distinct aspect of the cardiac phenotype: CanA^{act} mice still display concentric hypertrophy (wall thickness increase), while eccentric hypertrophy (dilation) and cardiac function are rescued by expressing dominant negative Mef2. In addition, overexpressing Mef2 on its own causes cardiac dilation instead of concentric cardiac hypertrophy [61]. In my study, disrupting Mef2 rescued *tinC-YCanA^{act}* and *tinC-Gal4>UAS-YCanA^{act}*-induced cardiac enlargement. This suggests that calcineurin/Mef2 may induce downstream signaling that leads towards eccentric cardiac hypertrophy, adding sarcomeres in series, in the fly. In agreement with this, overexpressing Mef2 in the *Drosophila* heart induced cardiac enlargement similar to the *tinC-CanA^{act}* cardiac enlargement phenotype (Figure 29). Interestingly, overexpressing Mef2 in the heart did not reduce fractional shortening, indicating that additional mechanisms may be involved in controlling contractility. The disruption of *Galk* with *Mi{ET1}Galk^{MB10638}* partially rescued the *tinC-Gal4>UAS-Mef2*-induced cardiac enlargement, suggesting that Galk modifies cardiac enlargement downstream of Mef2. The incomplete rescue indicates that there are additional pathways downstream of Mef2 that are not regulated by Galk. In relation to calcineurin, the rescue of the *tinC-CanA^{act}* cardiac enlargement phenotype by *Mi{ET1}Galk^{MB10638}* (98% EDD rescue, Figure 15) was much greater than that of *tinC-Gal4>UAS-Mef2* (48% EDD rescue, Figure 29), suggesting that Galk also regulates pathways downstream of CanA^{act} independent from Mef2.

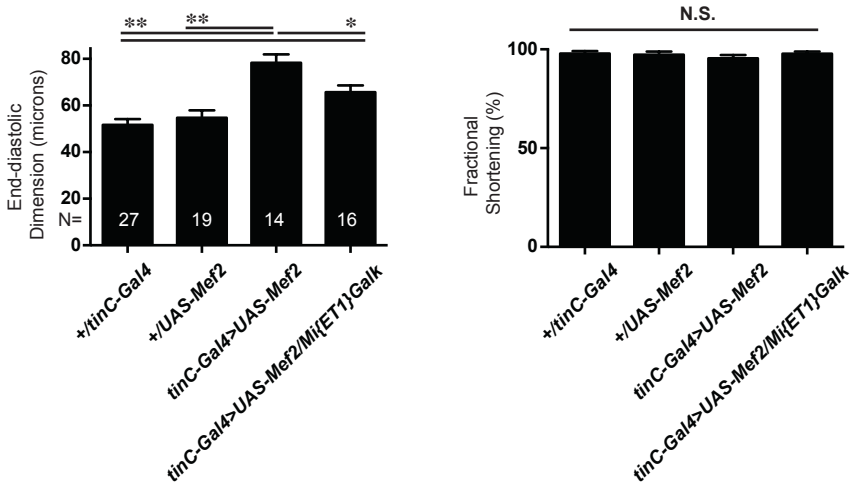

Figure 29: Overexpressing Mef2 in the heart causes cardiac enlargement which is partially rescued by Minos insertion in *Galk*.

Quantification of the m-mode OCT images of end-diastolic dimensions and fractional shortenings for heterozygous *tinC-Gal4* (driver only), *UAS-Mef2* (no driver), *tinC-Gal4>UAS-Mef2*, and *tinC-Gal4>UAS-Mef2* in the context of *Mi{ET1}Galk*^{MB10638} (*Mi{ET1}Galk*) fly hearts. The results show that overexpressing Mef2 in the heart with *tinC-Gal4>UAS-Mef2* induces cardiac enlargement and did not decrease contractility. *Mi{ET1}Galk*^{MB10638} partially rescued *tinC-Gal4>UAS-Mef2*-induced cardiac enlargement. *P<0.01, **P<0.0001, one-way ANOVA with Bonferroni correction. Data represent the mean ±SEM.

7.2.2 Concentric cardiac hypertrophy (increased wall thickness)

The mouse model of cardiac CanA^{act} displayed severe concentric cardiac hypertrophy where the ventricular wall was 2-3 times thicker than in control mice [9]. The *tinC-YCanA^{act}* fly did not replicate this wall thickness phenotype; however, compared to control, the *tinC-Gal4>UAS-YCanA^{act}* fly did display a 2-fold increase in wall thickness. The discrepancy between the *tinC-YCanA^{act}* and *tinC-Gal4>UAS-YCanA^{act}* fly models is most likely due to increased expression level using the *Gal4/UAS* bipartite system. Concentric cardiac hypertrophy results from the induction of signaling cascades leading to the addition of sarcomeres in parallel [219]. I postulate that this higher level of expression induced sarcomere formation in parallel as a result of excessive signaling. However, studies specifically examining the number of sarcomeres making up the cardiac wall are required to confirm this notion.

7.2.3 Cardiac contractility

Decreased contractility was observed in CanA^{act} transgenic mouse hearts as was observed in *tinC-CanA^{act}* fly hearts [215]. However, overexpressing Mef2 in the fly heart with *tinC-Gal4>UAS-Mef2* did not induce a decrease in cardiac contractility (fractional shortening, Figure 29). This data suggests that the cardiac enlargement phenotype can be separated from the contractility phenotype and may be regulated through distinct factors. Previous examples support this case: the ablation of phospholamban and

overexpression of S100A1 increase contractility without affecting hypertrophy, while S100A1 null mice display decreased contractile function after pressure-overload with no effect on hypertrophy [220-222]. However, this result also shows that the fly contractility phenotype cannot be completely correlated with the mouse contractility phenotype since overexpressing Mef2 in the mouse heart does decrease cardiac contractility [217].

7.2.4 Heart failure

Heart failure is defined as the condition where cardiac function is insufficient to sustain normal bodily functions. This is not easily monitored in the fly. In an RNAi screen in *Drosophila* heart to identify genes relevant to cardiac disease, Penninger *et al.* discovered that knock-down of *Not3* results in increased end-systolic dimension and decreased fractional shortening. In this study, $Not3^{+/-}$ mice displayed heart failure with arrhythmia and sudden death, suggesting an example where decreased fractional shortening in flies can correlate to mammalian heart failure [182]. In addition, Wessells and Bodmer utilized screening of arrhythmia or arrest with response to electrical pacing stress as an indication of heart failure [199]. Even though my study did not directly address heart failure, $tinC\text{-}CanA^{act}$ flies display significantly shorter life spans, implying that the cardiac function of $tinC\text{-}CanA^{act}$ flies was insufficient to maintain a normal life

span. This is also similar to the findings by Molkentin *et al*, where cardiac CanA^{act} expressing mice experienced sudden premature death [9].

7.2.5 Myofibrillar disarray and fibrosis

In addition to the above-mentioned phenotypes, the mouse model of cardiac CanA^{act} displayed myofibrillar disarray and fibrosis. Although not rigorously tested, these phenotypes were not observed in the fly model. This may be due to the difference in cardiac structure between flies and mammals.

The mammalian heart is constituted by multiple layers of cardiomyocytes that are elongated, branching fibers, organized in tandem to facilitate contraction while *Drosophila* hearts are one cell layer thick, organized in a tube structure with one cell on each side, two opposing cells interconnecting to form a tube. It is plausible that the simplified structure of the *Drosophila* cardiac tube allows for more uniform enlargement with the addition of sarcomeres that does not cause disarray due to lack of multiple cell layers. As for fibrosis, fibroblast cells are present in mammalian hearts to produce extracellular matrix and facilitate wound healing; however, they are not present in the fly heart. Thus, it is conceivable that fibrosis is not evident in *Drosophila* hearts.

7.3 Disruption of Doc and Argk did not rescue CanA^{act}-induced cardiac enlargement.

Several potential genes were ruled out as modifiers from our original candidate region. The *Doc* genes are known to regulate *Drosophila* cardiac development [213]. Our study showed that RNAi against *Doc2* and *Doc3* caused cardiac enlargement and did not rescue *tinC-CanA*^{act}. This implies that Doc genes are important for cardiac development but are not regulated by calcineurin activation. Interestingly, deficiencies encompassing all three *Doc* genes did not cause cardiac enlargement. This may be due to the different *Doc* genes playing different roles during cardiac development. Decreasing expression to less than half of the normal amount induced a phenotype, while decreasing all three, each at 50% the normal amount, did not cause a phenotype. Alternatively, there may be a nearby modifier gene that inhibits the cardiac enlargement caused by *Doc* deficiency.

Argk has high expression in the adult *Drosophila* heart. Argk is an enzyme that transfers the phosphate on ATP to arginine, creating an energy rich buffer for maintaining ATP concentration [223]. Even though Argk does not have close mammalian orthologs, the function is analogous to that of mammalian creatine kinase. While it is conceivable that Argk functions to provide sufficient energy for the fly myocardium, our results showed that disrupting *Argk* with a transposable element did not produce a phenotype and did not rescue calcineurin-induced cardiac enlargement. These results suggest that *Argk* does not regulate calcineurin-induced cardiac enlargement. Although a caveat to this conclusion is that the transposable element

insertion *PBac{PB}ArgK*^{f05255} displayed only a 30% decrease in expression, and this may have interfered with the ability to rescue the cardiac enlargement phenotype.

7.4 Genetic disruption of Galk rescued UAS-CanA^{act}*-induced phenotypes tissue specifically*

The screen I performed was based on two previous screens for calcineurin modifiers performed using two different tissues, including one expressing CanA^{act} in the eye and one expressing CanA^{act} mesodermally with a 24B driver. A total of 70,000 X-ray or EMS mutagenized flies were examined for both enhancers and suppressors of the *GMR-Gal4>UAS-CanA*^{act}-induced rough eye phenotype [10]; in the other study, deficiency kits spanning chromosomes 2 and 3 maximally were screened for suppressors of the *24B-Gal4>UAS-CanA*^{act}-induced lethality phenotype [11]. Interestingly, the modifier regions rarely overlapped between these two studies: both studies found *canB2* as a modifier and 66F5 on chromosome 3L to span potential modifiers (Table 1). The eye phenotype mutagenesis screen discovered a suppressor and enhancer region that was much larger in span, and I initiated my screen with a broader region than initially discovered by Gajewski *et al*. *Galk* does not lie within but adjacent to the Gajewski *et al.* suppressor region. My data also indicated that *Mef2-Gal4>UAS-CanA*^{act} lethality was not rescued by *Galk* disruption. Taken together, it may be suggested that Galk does not modify mesodermally driven lethality phenotypes. I had attempted over-expressing *GMR-Gal4>UAS-CanA*^{act} in the eye to see if Galk may be a candidate modifier gene for

the region described by Sullivan and Rubin. However, difficulties were encountered due to a subtle rough eye phenotype in the driver alone flies and variation in the eye phenotype with CanA^{act}. Further experiments with a more robust driver line may facilitate in determining whether Galk corresponds to a modifier in the eye screen performed by Sullivan and Rubin.

In my study, genetic disruption of *Galk* rescued the CanA^{act} phenotypes induced by *tinC-Gal4* in the heart and *e16E-Gal4* in the posterior wing imaginal disc, but the phenotypes induced by expression with several other drivers were not rescued. These included ubiquitous *Act5C-Gal4*, ectodermal *dpp-Gal4*, and mesodermal *Mef2-Gal4* drivers. Table 4 summarizes the expression pattern of the different drivers investigated. Each of these drivers induces expression in a separate set of tissues. Even though both *e16E-* and *dpp*-driving CanA^{act} induced wing phenotypes, *e16E-* drives expression in the posterior wing, while *dpp-* drives expression anterior to the anterior-posterior boundary during imaginal disc development at the third instar larva stage [224, 225]. Many signaling factors are differentially expressed during wing development in these two separate compartments to guide correct patterning. For example, *engrailed* and *hedgehog* are expressed posteriorly, guiding formation of the posterior wing veins [224, 226], while *dpp* and the EGFR inhibitor *knot* are expressed specifically in the anterior wing imaginal disc [225, 227]. It is possible that *Galk* modification of calcineurin signaling is regulated by these differentially expressed factors.

In addition, *dpp-Gal4*, *Mef2-Gal4*, and *Act5C-Gal4* all induce expression in a broad band of cells, which further differentiate to form a wide range of tissues. It is possible that these three genes are expressed in an overlapping region that causes the corresponding CanA^{act} phenotype, and Galk does not regulate CanA^{act} in that tissue. However, this is less plausible by analyzing expression patterns in Table 4, *dpp-Gal4* and *Mef2-Gal4* do not seem to have overlapping expression. It is more likely that *Galk* disruption did not rescue the CanA^{act} phenotypes because of the lack of Galk modulation in separate tissues corresponding to each driver. For example, it appears that the *dpp-Gal4>UAS-YCanA^{act}* fly displays a fully developed wing that fails to expand upon eclosion. The expansion of the *Drosophila* wing after eclosion is an integrated process that involves programed cell death in the wing, following the induction of a neuroendocrine cascade and epithelial-mesenchymal transition after eclosion [228, 229]. It is plausible that CanA^{act} disrupts one of these processes, and this is not regulated by Galk. The *dpp-Gal4*, *Mef2-Gal4*, and *Act5C-Gal4* driven phenotypes are also more severe all-or-none phenotypes compared to *tinC-* and *e16E-Gal4* phenotypes that display a range of abnormalities where a lower level of disruption will result in a quantifiable rescue. It is possible that the level of Galk disruption was not sufficient to rescue these more severe phenotypes even if Galk was acting in these tissues.

Table 4: Expression pattern of Gal4 lines driving expression of *UAS-YCanA^{act}* in the current study

Driver for YCanA^{act}	*Expression pattern*	*Stage of expression*	*Galk suppression?*
tinC-Gal4 (*tinman*)	Cardioblasts	Stage 12-adult[1]	Yes
e16E-Gal4 (*engrailed*)	Segmentally repeated stripes, ectoderm and mesoderm anlage	Stage 4-larval[2]	Partial
	Posterior wing disc	3rd instar larval-pupal[3]	
Dpp-Gal4 (*decapentaplegic*)	Dorsal	Stage 4[4]	No
	Dorsal ectoderm stripes	Stage 5-10[5]	
	Dorsal ectoderm	Stage 11-13[5]	
	Anterior-posterior boundary	Larval[6]	
	Wing vein primordia	Pupal [6]	
Mef2-Gal4 (*mef2*)	Mesoderm primordium All muscles, heart	Stage 5[7] Stage 11 -adult[7]	No
Act5C-Gal4 (*actin*)	Ubiquitous	Stage 1- adult (BDGP insitu)	No

[1] 211. Yin, Z., X.L. Xu, and M. Frasch, *Regulation of the twist target gene tinman by modular cis-regulatory elements during early mesoderm development.* Development, 1997. **124**(24): p. 4971-82.

[2] 230. Karr, T.L., et al., *Patterns of engrailed protein in early Drosophila embryos.* Ibid.1989. **105**(3): p. 605-12.

[3] 231. Drees, B., et al., *The transcription unit of the Drosophila engrailed locus: an unusually small portion of a 70,000 bp gene.* EMBO J, 1987. **6**(9): p. 2803-9, 232. Blair, S.S., *Engrailed expression in the anterior lineage compartment of the developing wing blade of Drosophila.* Development, 1992. **115**(1): p. 21-33.

[4] 233. Chang, T., et al., *Dpp and Hh signaling in the Drosophila embryonic eye field.* Ibid.2001. **128**(23): p. 4691-704.

[5] 234. Jackson, P.D. and F.M. Hoffmann, *Embryonic expression patterns of the Drosophila decapentaplegic gene: separate regulatory elements control blastoderm expression and lateral ectodermal expression.* Dev Dyn, 1994. **199**(1): p. 28-44.

[6] 235. Yu, K., et al., *The Drosophila decapentaplegic and short gastrulation genes function antagonistically during adult wing vein development.* Development, 1996. **122**(12): p. 4033-44.

[7] 49. Nguyen, H.T., et al., *D-mef2: a Drosophila mesoderm-specific MADS box-containing gene with a biphasic expression profile during embryogenesis.* Proc Natl Acad Sci U S A, 1994. **91**(16): p. 7520-4.

7.5 Galactokinase in mammals

My study has concluded that galactokinase may be involved in calcineurin-induced cardiomyopathy. There is limited literature regarding the relevance of Galk to calcineurin signaling or cardiomyopathy. Two Galk homologs are expressed in mammals, Galk1 and Galk2. The major defect of humans and mice deficient for Galk1 is cataracts and mental and/or motor neurological disorders [236, 237]. Cardiac defects have not been specifically observed in these studies and no known mutations in Galk2 have been studied. In addition, my data showed that Galk itself may not affect cardiac function on its own without calcineurin. Further studies are pending to investigate whether or not Galk modifies calcineurin in the mammalian heart.

Also affecting glycosylation, a phosphoglucomutase 1 (PGM1) mutation was found in humans to cause cardiac abnormalities including dilated cardiomyopathy and cardiac arrest [238]. In this study, supplementing fibroblast cells with galactose alleviated glycosylation defects from PGM1 mutation. This study demonstrates that galactoside modifications are important for cardiac function. Another study found that overexpressing the Galβ1,3GalNAc α2,3-sialyltransferase II (ST3Gal-II), inducing abnormal protein glycosylation, induced dilated cardiomyopathy in transgenic mice [239]. These studies corroborate that Galk and glycosylation are important for normal cardiac function.

7.6 Galactokinase as a novel modifier of calcineurin: possible mechanisms

Galactokinase belongs to the GHMP ATP-dependent kinase family (named after the four representative kinases in this family: galactokinase, homoserine kinase, mevalonate kinase, and phosphomevalonate kinase) [214]. In the fly, galactokinase phosphorylates galactose and N-acetyl-galactosamine, allowing further utilization in either metabolism (energy production) or glycosylation (protein modification) [214]. These pathways potentially lead to cardiac enlargement: either galactokinase promotes a higher level of phosphorylated galactose, galactose-1-p, leading to a diseased state, or downstream reactions involving UDP-galactose incorporation into glycosylated proteins promotes cardiac enlargement, or both mechanisms may be required. These possible pathways are summarized in Figure 30. A previous screen examining *Drosophila* cardiac development discovered that mutations in HMG-CoA reductase (the rate-limiting enzyme in the mevalonate pathway) induces a cardiac phenotype by geranylgeranylation of the G protein Gγ1, suggesting a pathway by which post-translational modifications can alter the fly heart [240].

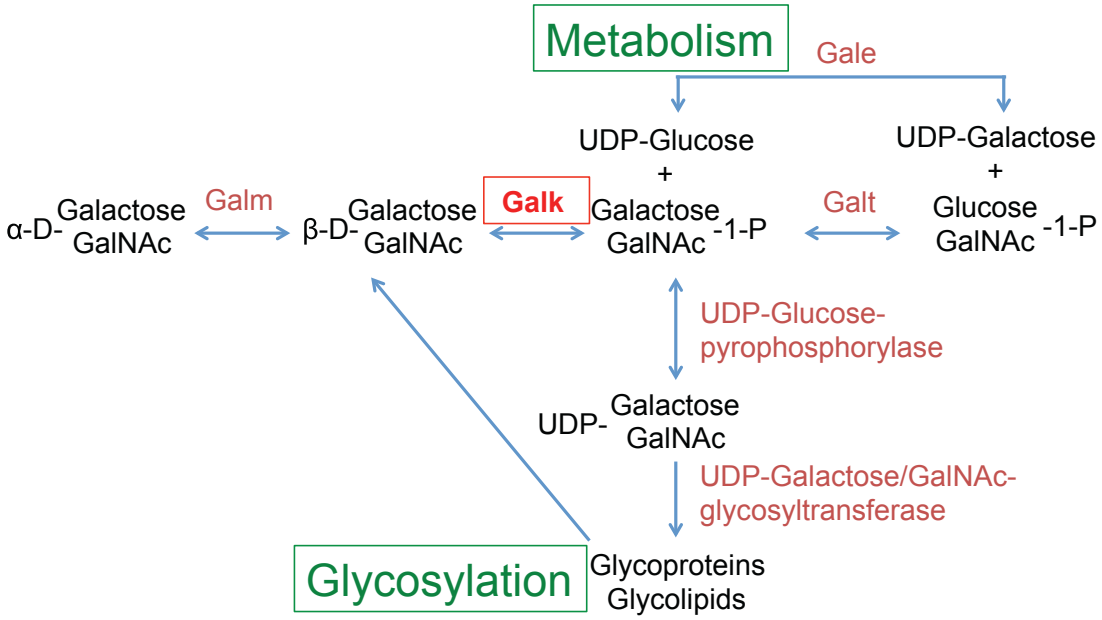

Figure 30: Galactokinase-related pathways

Galactokinase (Galk), in the red box, catalyzes the phosphorylation of β-D-Galactose/GalNAc into Galactose/GalNAc-1-Phosphate. This potentially influences metabolism by conversion into UDP-Glucose and utilization for ATP production, or conversion into UDP-Galactose/GalNAc, facilitating glycosylation through respective glycosyltransferases. (Abbreviations: GalNAc= N-Acetyl-Galactosamine; Galm= Galactose mutarotase; Galk= Galactokinase; Gale= UDP-Galactose-4-epimerase; Galt= Galactose-1-P-uridylyltransferase.)

In addition to the well known affects of galactokinase related to galactose/GalNAc metabolism, the yeast homologue of Galk, Gal3p, has been found to act as a transcriptional activator by interacting with Gal80p [241]; transcriptional regulation is activated with the binding of galactose and ATP to Gal3p. This suggests the possibility that Galk may act as a modifier of transcription for known pathways including Mef2. Whether Galk functions as part of the transcriptional machinery remains to be determined. Co-immunoprecipitation experiments for Galk- Mef2 interaction and luciferase assay for Mef2-luciferase reporter gene activation with RNAi to Galk in the context of $CanA^{act}$ can be performed to determine this.

7.7 Galectin is a possible downstream regulator of Galk in $CanA^{act}$-induced cardiac enlargement.

The function of Galk is to phosphorylate Galactose/N-Acetyl-Galactosamine (GalNAc) to form Galactose/GalNAc-1-P. Both Galactose and GalNAc are commonly found in glycoproteins and is important for normal function. My study shows that a transposable element insertion in galectin (a galactoside-binding lectin) suppressed the *tinC-$CanA^{act}$* cardiac phenotype. Mammalian Galectin3 has been shown to bind to the N-acetyllactosamine on EGFR, preventing endocytosis and enhancing signaling of isolated mouse mammary cells [242]. Driving activated EGFR in the *Drosophila* heart has been

shown to induce a cardiac hypertrophy phenotype while dominant negative EGFR induces a dilation phenotype [194] and *sprouty*, a negative regulator of EGFR signaling, has been shown to modify calcineurin-induced rough eye [10]. Although speculation, one potential mechanism by which galactokinase functions to modulate calcineurin-induced cardiac enlargement is by influencing co-translational glycosylation of EGFR or another yet unidentified cell surface protein that is bound by galectin.

Based on these findings and previously published literature, I propose a possible mechanism for Galk modification of calcineurin-induced cardiac enlargement (Figure 31). I propose that calcineurin indirectly activates Galk, regulating glycosylation of a cell surface receptor (possibly EGFR), which is bound by galectin. Galectin facilitates dimerization and activation of downstream signaling factors which regulate either unknown transcription factors or Mef2 activation, leading to cardiac enlargement.

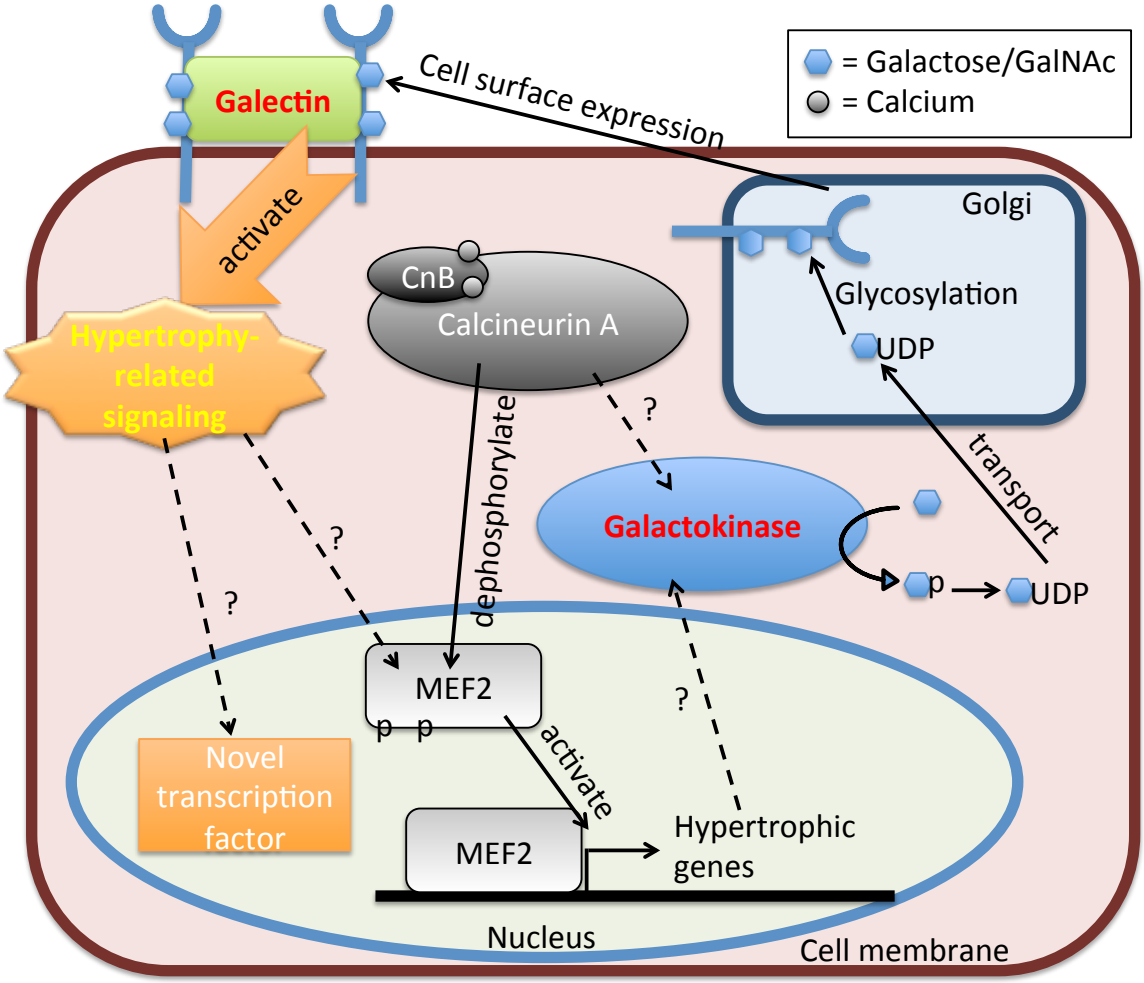

Figure 31: Possible mechanism for Galk regulation of calcineurin-induced hypertrophy.

Galactokinase and galectin may cooperate in modifying calcineurin downstream activation of hypertrophy. Pathways with possibly indirect effects are shown with dashed lines. CnB= Calcineurin B; p= phosphate. While speculative, a possible mechanism that links Galk and galectin is by their action on galactose/GalNAc. Galactokinase regulates the phosphorylation of galactose/GalNAc, allowing for conversion of phosphorylated galactose/GalNAc into UDP-galactose/GalNAc. UDP-

galactose/GalNAc is then transferred on to cell surface receptor proteins that are recognized and bound by galectin, possibly altering signal transduction downstream of the receptor proteins to modify downstream cardiac enlargement.

7.8 Therapeutic possibilities

Cardiac hypertrophy is a complex disease involving multiple signaling pathways. Previous studies have not examined the effects of *Galk* in the mammalian heart. My studies show that *Galk* is a modifier downstream of calcineurin. This implies that pharmacological inhibition of Galk may be beneficial to treating cardiac hypertrophy. Even though Galk inhibitors are not commonly administered, previous studies have tested multiple small molecular compounds that specifically inhibit Galk1 [243]. Out of 50,000 compounds, 150 compounds were found to inhibit Galk1, and 34 of these were further characterized. Less research has been conducted examining Galk2. However, since Galk1 and Galk2 share similar domain structures, it is plausible that a portion of these inhibitors may inhibit Galk2. In addition, the Galk1 inhibitors discovered had common characteristics including multiple carbon ring structures, at least one aromatic ring structure, and at least 2 hydrogen-bond acceptor sites. Examining similar small molecular structures may reveal compounds specific to Galk2 as well.

7.9 Conclusions and impact

In conclusion, I have 1) characterized CanA^{act}-induced cardiomyopathy in the fly; 2) established a reliable model for discovering novel modifiers of calcineurin-mediated cardiac enlargement and through this screen; 3) identified galactokinase as a modifier of constitutively active calcineurin-induced cardiomyopathy, shortened life span, and wing vein abnormality in adult *Drosophila*; and 4) identified galectin as a potential modifier of constitutively active calcineurin-induced cardiomyopathy. My study has provided a basis for performing unbiased and exhaustive studies for understanding calcineurin signaling in the *Drosophila* heart and novel insight into downstream regulation of calcineurin-induced cardiomyopathy. Identification of galactokinase and galectin as modifiers of calcineurin-induced cardiomyopathy bring light to the importance of galactose metabolism and glycosylation in cardiomyopathy. These findings have the potential to further our understanding of cardiac hypertrophy and heart failure by revealing novel pathways that may be targeted in combination with other treatments for more effective therapy.

7.10 Future directions

This study provides the basis for future research, including more rigorous characterization of the calcineurin fly, further screening for novel modifiers of calcineurin signaling, and characterization of the role of Galk in calcineurin signaling.

7.10.1 Characterization of the cardiac CanA^{act}-induced phenotypes

I have established that the *tinC-CanA^{act}* fly displays significant cardiac enlargement. This enlargement is due to hypertrophy of individual cells and not to proliferation. It was preliminarily noted by confocal imaging that no significant alterations in fiber structure is visible. However, this has not been rigorously tested. Further studies using electron microscopy (EM) will provide more detailed information regarding the sarcomeric structure of *tinC-CanA^{act}* versus wildtype flies. Phalloidin staining followed by fluorescence microscopy will also be potentially useful in determining the fiber structure. In addition, examining the mitochondria of *tinC-CanA^{act}* flies by EM will be helpful in further determining the phenotype of the calcineurin fly and the comparison to mammalian cardiomyopathy phenotypes. The mammalian heart displays a decrease in mitochondria with pressure-overload cardiac hypertrophy [244-246].

My study showed that the *tinC-CanA^{act}* fly displays a decrease in life span. It is postulated that this decrease in life span is due to an inability of the heart to pump normally, reducing the amount of oxygen and nutrients provided to essential organs.

However, the relation between cardiac enlargement of *tinC-CanA^{act}* flies and decreased hemolymph flow was not rigorously tested. This has been achieved through Doppler OCT with injection of a contrast agent (830nm red polysterene beads) to visualize hemolymph [247].

7.10.2 Identification of novel modifiers of calcineurin-induced cardiomyopathy

I have established a reliable model for detecting modifiers of CanA^{act}-induced cardiac enlargement in *Drosophila*. An exhaustive screen can be performed using the Bloomington deficiency kit which consists of 462 fly stocks that maximally cover the fly genome [212, 248]. This will potentially identify all of the key molecules involved in regulation of CanA^{act}-induced cardiomyopathy. Of note, this will bring out many key molecules, but we should keep in mind that deficiency screening will not detect genes that only exert effects when the transcript level is decreased to less than half the normal amount, and larger deficiency regions potentially contain multiple modifiers that may interfere with the outcome. Many resources are available and continuously being developed and refined for targeting specific genes in *Drosophila*. For knocking down or disrupting gene expression, transposable element insertions, RNAi, and more recent techniques with CRISPR/Cas9 and TALENs systems are available [163-168]. These resources will prove useful in determining candidate molecules to fill in gaps in the pathways discovered and generate a complete calcineurin signaling network.

Within the current suppressor region, Argk cannot be completely ruled out as a modifier due to the incomplete reduction of transcript by *PBac{PB}Argk*^{f05255}. Many systems are available to generate knock-down or knock-out of gene expression including RNAi, CRISPR, and TALEN systems. The emerging CRISPR system has been utilized in several studies and reported to have less off-target effects than RNAi [163-165]. The TALEN system is more specific but requires more specialized techniques [166-168]. The logical next step would be to generate genetic null mutations with the CRISPR system to effectively target Argk.

7.10.3 Delineation of the role of Galk in calcineurin-induced cardiomyopathy and signaling

I have found that Galk modifies CanA^{act}-induced cardiomyopathy. The mechanism by which Galk may modify signaling has not been investigated. It is not known whether Galk interacts with known pathways downstream of calcineurin, or if it is an independent factor. Several approaches may be employed to clarify the role of Galk in calcineurin signaling.

The most well documented role for Galk is its role in phosphorylating galactose/GalNAc, enabling utilization for glycolysis or glycosylation. Several downstream molecules are involved in either pathway (Figure 30). For example, conversion into glucose-1-phosphate and UDP-galactose/GalNAc is mediated by galactose-1-phosphate uridyltransferase (Galt) [249]. Glucose-1-phosphate is then

converted into glucose-6-phosphate with phosphoglucomutase [250], which is utilized in glycolysis to generate ATP [251]. On the glycosylation side, UDP-glucose-transferase and UDP-galactose/GalNAc glycosyltransferases regulate glycosylation downstream of galactokinase [252]. Overexpressing these downstream enzymes controlling either glycolysis or glycosylation in the context of *tinC-CanA*^{act} and *Mi{ET1}Galk*^{MB10638} will provide insight into which of these pathways is primarily influencing the phenotype.

It is not known whether Galk interacts with known pathways downstream of calcineurin signaling. Currently, Mef2 is the most direct and well characterized modifier of calcineurin signaling. Examining the effects of Galk overexpression in the context of Mef2 deficiency, or Mef2 overexpression with Galk deficiency in *tinC-CanA*^{act} flies will provide insight into whether these molecules interact. Another possible function of Galk is in the transcriptional machinery. Determining whether Galk binds to Mef2 via immunoprecipitation and if transcription activation is altered in Galk deficient flies using a Mef2-luciferase or IL-2 reporter construct will provide further insight into the role of Galk in the induction of transcription.

7.10.4 Confirmation and characterization of galectin as a modifier of calcineurin-induced cardiomyopathy

Galectin was discovered to modify *tinC-CanA*^{act}-induced cardiac enlargement. However, these results should be further confirmed with RNAi knock-down to ensure specificity of the results. Also, interaction of galectin with Galk by over-expressing

galectin in Galk disrupted flies in the context of *tinC-CanA*^{act} will provide insight as to whether Galk and galectin are part of the same pathway for inducing cardiomyopathy downstream of calcineurin. Overexpressing galectin will provide insight as to whether galectin is sufficient to induce cardiac enlargement.

Further studies can be performed to determine the mechanism by which galectin influences calcineurin-induced cardiomyopathy. Candidate receptor genes including EGFR and FGFR can be targeted and analyzed in the context of galectin deficient or overexpressing flies to assess for interaction between the pathways. In addition, whether or not calcineurin stimulation induces galectin-mediated changes in receptor recycling can be analyzed in cell culture using H9c2 or NIH-3T3 cells. If calcineurin induces alterations in receptor expression or recycling, siRNA to galectin can be utilized to determine if this process is regulated by galectin.

7.10.5 Examining the importance of galactose regulation for calcineurin-induced cardiac hypertrophy in mammalian systems

Preliminary results indicate that Galk1 is not involved in calcineurin-induced NFAT translocation. However, whether Galk1 knock-down affects calcineurin-induced Mef2 transcription activation remains to be elucidated. This can be accomplished using Mef2-luciferase reporter constructs in cellular systems. I have demonstrated efficient Galk1 knock-down and calcineurin activation using H9c2 and NIH-3T3 cells. These cell systems can be further utilized to perform luciferase assays to determine if Galk1

regulates Mef2 promoter activation. In addition, an appropriate system for Galk2 remains to be discovered. Galk2 is expressed highly in liver and heart tissue. HL-1 cells derived from primary cultured cardiomyocytes of mice expressing ANF driving SV40 large T antigen is a potential candidate for future investigation since primary cultured cardiomyocytes are difficult to culture and manipulate [253]. Rat neonatal cardiomyocytes are also available for culturing and have been used to study cardiac hypertrophy [9].

Limited information on Galk knock-out mice is available. Two isoforms of Galk are present in mouse, Galk1 and Galk2. The Galk1 mouse is available and shows neurological and eye phenotypes related to galactokinase deficiency [237], the Galk2 knock-out mouse is currently available through the International Knock-out Mouse Consortium (IKMC). No studies have been performed on these mice so far. Examining the effect of Galk1 or Galk2 knock-out on pressure overload or calcineurin overexpression-induced hypertrophy will demonstrate whether our discoveries in the fly system translate to the mammalian system.

References

1. Brown, L., M.X. Chen, and P.T. Cohen, *Identification of a cDNA encoding a Drosophila calcium/calmodulin regulated protein phosphatase, which has its most abundant expression in the early embryo.* FEBS Lett, 1994. **339**(1-2): p. 124-8.

2. Adams, M.D., et al., *The genome sequence of Drosophila melanogaster.* Science, 2000. **287**(5461): p. 2185-95.

3. Guerini, D., C. Montell, and C.B. Klee, *Molecular cloning and characterization of the genes encoding the two subunits of Drosophila melanogaster calcineurin.* J Biol Chem, 1992. **267**(31): p. 22542-9.

4. Warren, W.D., A.M. Phillips, and A.J. Howells, *Drosophila melanogaster contains both X-linked and autosomal homologues of the gene encoding calcineurin B.* Gene, 1996. **177**(1-2): p. 149-53.

5. Schulz, R.A. and K.E. Yutzey, *Calcineurin signaling and NFAT activation in cardiovascular and skeletal muscle development.* Dev Biol, 2004. **266**(1): p. 1-16.

6. Klee, C.B., T.H. Crouch, and M.H. Krinks, *Calcineurin: a calcium- and calmodulin-binding protein of the nervous system.* Proc Natl Acad Sci U S A, 1979. **76**(12): p. 6270-3.

7. Klee, C.B., G.F. Draetta, and M.J. Hubbard, *Calcineurin.* Adv Enzymol Relat Areas Mol Biol, 1988. **61**: p. 149-200.

8. Shibasaki, F., U. Hallin, and H. Uchino, *Calcineurin as a multifunctional regulator.* J Biochem, 2002. **131**(1): p. 1-15.

9. Molkentin, J.D., et al., *A calcineurin-dependent transcriptional pathway for cardiac hypertrophy.* Cell, 1998. **93**(2): p. 215-28.

10. Sullivan, K.M. and G.M. Rubin, *The Ca(2+)-calmodulin-activated protein phosphatase calcineurin negatively regulates EGF receptor signaling in Drosophila development.* Genetics, 2002. **161**(1): p. 183-93.

11. Gajewski, K., et al., *Requirement of the calcineurin subunit gene canB2 for indirect flight muscle formation in Drosophila.* Proc Natl Acad Sci U S A, 2003. **100**(3): p. 1040-5.

12. Musaro, A., et al., *IGF-1 induces skeletal myocyte hypertrophy through calcineurin in association with GATA-2 and NF-ATc1.* Nature, 1999. **400**(6744): p. 581-5.

13. Semsarian, C., et al., *Skeletal muscle hypertrophy is mediated by a Ca2+-dependent calcineurin signalling pathway.* Nature, 1999. **400**(6744): p. 576-81.

14. Chin, E.R., et al., *A calcineurin-dependent transcriptional pathway controls skeletal muscle fiber type.* Genes Dev, 1998. **12**(16): p. 2499-509.

15. Wu, H., et al., *MEF2 responds to multiple calcium-regulated signals in the control of skeletal muscle fiber type.* EMBO J, 2000. **19**(9): p. 1963-73.

16. Klee, C.B., H. Ren, and X. Wang, *Regulation of the calmodulin-stimulated protein phosphatase, calcineurin.* J Biol Chem, 1998. **273**(22): p. 13367-70.

17. Parsons, S.A., et al., *Genetic loss of calcineurin blocks mechanical overload-induced skeletal muscle fiber type switching but not hypertrophy.* J Biol Chem, 2004. **279**(25): p. 26192-200.

18. Watanabe, Y., et al., *Identification in the calcineurin A subunit of the domain that binds the regulatory B subunit.* J Biol Chem, 1995. **270**(1): p. 456-60.

19. Schaeffer, P.J., et al., *Impaired contractile function and calcium handling in hearts of cardiac-specific calcineurin b1-deficient mice.* Am J Physiol Heart Circ Physiol, 2009. **297**(4): p. H1263-73.

20. Maillet, M., et al., *Heart-specific deletion of CnB1 reveals multiple mechanisms whereby calcineurin regulates cardiac growth and function.* J Biol Chem, 2010. **285**(9): p. 6716-24.

21. Shaw, J.P., et al., *Identification of a putative regulator of early T cell activation genes.* Science, 1988. **241**(4862): p. 202-5.

22. Ranger, A.M., et al., *The nuclear factor of activated T cells (NFAT) transcription factor NFATp (NFATc2) is a repressor of chondrogenesis.* J Exp Med, 2000. **191**(1): p. 9-22.

23. Bales, J.W., et al., *Regional calcineurin subunit B isoform expression in rat hippocampus following a traumatic brain injury.* Brain Res, 2010. **1358**: p. 211-20.

24. Bales, J.W., et al., *Expression of protein phosphatase 2B (calcineurin) subunit A isoforms in rat hippocampus after traumatic brain injury.* J Neurotrauma, 2010. **27**(1): p. 109-20.

25. Youn, H.D., et al., *Apoptosis of T cells mediated by Ca2+-induced release of the transcription factor MEF2.* Science, 1999. **286**(5440): p. 790-3.

26. de la Pompa, J.L., et al., *Role of the NF-ATc transcription factor in morphogenesis of cardiac valves and septum.* Nature, 1998. **392**(6672): p. 182-6.

27. Graef, I.A., et al., *Signals transduced by Ca(2+)/calcineurin and NFATc3/c4 pattern the developing vasculature.* Cell, 2001. **105**(7): p. 863-75.

28. Molkentin, J.D., *Calcineurin and beyond: cardiac hypertrophic signaling.* Circ Res, 2000. **87**(9): p. 731-8.

29. Lopez-Rodriguez, C., et al., *NFAT5, a constitutively nuclear NFAT protein that does not cooperate with Fos and Jun.* Proc Natl Acad Sci U S A, 1999. **96**(13): p. 7214-9.

30. Miyakawa, H., et al., *Tonicity-responsive enhancer binding protein, a rel-like protein that stimulates transcription in response to hypertonicity.* Proc Natl Acad Sci U S A, 1999. **96**(5): p. 2538-42.

31. Rao, A., C. Luo, and P.G. Hogan, *Transcription factors of the NFAT family: regulation and function.* Annu Rev Immunol, 1997. **15**: p. 707-47.

32. Beals, C.R., et al., *Nuclear localization of NF-ATc by a calcineurin-dependent, cyclosporin-sensitive intramolecular interaction.* Genes Dev, 1997. **11**(7): p. 824-34.

33. Beals, C.R., et al., *Nuclear export of NF-ATc enhanced by glycogen synthase kinase-3.* Science, 1997. **275**(5308): p. 1930-4.

34. Sheridan, C.M., et al., *Protein kinase A negatively modulates the nuclear accumulation of NF-ATc1 by priming for subsequent phosphorylation by glycogen synthase kinase-3.* J Biol Chem, 2002. **277**(50): p. 48664-76.

35. Chow, C.W., et al., *Nuclear accumulation of NFAT4 opposed by the JNK signal transduction pathway.* Science, 1997. **278**(5343): p. 1638-41.

36. Yang, T.T., et al., *Phosphorylation of NFATc4 by p38 mitogen-activated protein kinases.* Mol Cell Biol, 2002. **22**(11): p. 3892-904.

37. Macian, F., C. Lopez-Rodriguez, and A. Rao, *Partners in transcription: NFAT and AP-1.* Oncogene, 2001. **20**(19): p. 2476-89.

38. Tsai, E.Y., et al., *Tumor necrosis factor alpha gene regulation in activated T cells involves ATF-2/Jun and NFATp.* Mol Cell Biol, 1996. **16**(2): p. 459-67.

39. Iniguez, M.A., et al., *An essential role of the nuclear factor of activated T cells in the regulation of the expression of the cyclooxygenase-2 gene in human T lymphocytes.* J Biol Chem, 2000. **275**(31): p. 23627-35.

40. Hodge, M.R., et al., *NF-AT-Driven interleukin-4 transcription potentiated by NIP45.* Science, 1996. **274**(5294): p. 1903-5.

41. Horsley, V., et al., *IL-4 acts as a myoblast recruitment factor during mammalian muscle growth.* Cell, 2003. **113**(4): p. 483-94.

42. Pan, S., et al., *Molecular cloning and functional characterization of murine cDNA encoding transcription factor NFATc.* Biochem Biophys Res Commun, 1997. **240**(2): p. 314-23.

43. Duncliffe, K.N., et al., *A T cell-specific enhancer in the interleukin-3 locus is activated cooperatively by Oct and NFAT elements within a DNase I-hypersensitive site.* Immunity, 1997. **6**(2): p. 175-85.

44. Oukka, M., et al., *The transcription factor NFAT4 is involved in the generation and survival of T cells.* Immunity, 1998. **9**(3): p. 295-304.

45. Gwack, Y., et al., *A genome-wide Drosophila RNAi screen identifies DYRK-family kinases as regulators of NFAT.* Nature, 2006. **441**(7093): p. 646-50.

46. Wu, H., et al., *Activation of MEF2 by muscle activity is mediated through a calcineurin-dependent pathway.* EMBO J, 2001. **20**(22): p. 6414-23.

47. Potthoff, M.J. and E.N. Olson, *MEF2: a central regulator of diverse developmental programs.* Development, 2007. **134**(23): p. 4131-40.

48. Edmondson, D.G., et al., *Mef2 gene expression marks the cardiac and skeletal muscle lineages during mouse embryogenesis.* Development, 1994. **120**(5): p. 1251-63.

49. Nguyen, H.T., et al., *D-mef2: a Drosophila mesoderm-specific MADS box-containing gene with a biphasic expression profile during embryogenesis.* Proc Natl Acad Sci U S A, 1994. **91**(16): p. 7520-4.

50. Black, B.L., et al., *Cooperative transcriptional activation by the neurogenic basic helix-loop-helix protein MASH1 and members of the myocyte enhancer factor-2 (MEF2) family.* J Biol Chem, 1996. **271**(43): p. 26659-63.

51. Fickett, J.W., *Quantitative discrimination of MEF2 sites.* Mol Cell Biol, 1996. **16**(1): p. 437-41.

52. Gossett, L.A., et al., *A new myocyte-specific enhancer-binding factor that recognizes a conserved element associated with multiple muscle-specific genes.* Mol Cell Biol, 1989. **9**(11): p. 5022-33.

53. Molkentin, J.D. and E.N. Olson, *Combinatorial control of muscle development by basic helix-loop-helix and MADS-box transcription factors.* Proc Natl Acad Sci U S A, 1996. **93**(18): p. 9366-73.

54. Bertos, N.R., A.H. Wang, and X.J. Yang, *Class II histone deacetylases: structure, function, and regulation.* Biochem Cell Biol, 2001. **79**(3): p. 243-52.

55. McKinsey, T.A., C.L. Zhang, and E.N. Olson, *Control of muscle development by dueling HATs and HDACs.* Curr Opin Genet Dev, 2001. **11**(5): p. 497-504.

56. Shen, H., et al., *The Notch coactivator, MAML1, functions as a novel coactivator for MEF2C-mediated transcription and is required for normal myogenesis.* Genes Dev, 2006. **20**(6): p. 675-88.

57. Yang, C.C., et al., *Interaction of myocyte enhancer factor 2 (MEF2) with a mitogen-activated protein kinase, ERK5/BMK1.* Nucleic Acids Res, 1998. **26**(20): p. 4771-7.

58. Molkentin, J.D., L. Li, and E.N. Olson, *Phosphorylation of the MADS-Box transcription factor MEF2C enhances its DNA binding activity.* J Biol Chem, 1996. **271**(29): p. 17199-204.

59. Zhao, M., et al., *Regulation of the MEF2 family of transcription factors by p38.* Mol Cell Biol, 1999. **19**(1): p. 21-30.

60. Passier, R., et al., *CaM kinase signaling induces cardiac hypertrophy and activates the MEF2 transcription factor in vivo.* J Clin Invest, 2000. **105**(10): p. 1395-406.

61. van Oort, R.J., et al., *MEF2 activates a genetic program promoting chamber dilation and contractile dysfunction in calcineurin-induced heart failure.* Circulation, 2006. **114**(4): p. 298-308.

62. Sakuma, K., et al., *Cyclosporin A modulates cellular localization of MEF2C protein and blocks fiber hypertrophy in the overloaded soleus muscle of mice.* Acta Neuropathol, 2008. **115**(6): p. 663-74.

63. Li, J., et al., *Regulation of MEF2 transcriptional activity by calcineurin/mAKAP complexes.* Exp Cell Res, 2013. **319**(4): p. 447-54.

64. Bour, B.A., et al., *Drosophila MEF2, a transcription factor that is essential for myogenesis.* Genes Dev, 1995. **9**(6): p. 730-41.

65. Lilly, B., et al., *Requirement of MADS domain transcription factor D-MEF2 for muscle formation in Drosophila.* Science, 1995. **267**(5198): p. 688-93.

66. Ranganayakulu, G., et al., *A series of mutations in the D-MEF2 transcription factor reveal multiple functions in larval and adult myogenesis in Drosophila.* Dev Biol, 1995. **171**(1): p. 169-81.

67. Lin, M.H., et al., *Ectopic expression of MEF2 in the epidermis induces epidermal expression of muscle genes and abnormal muscle development in Drosophila.* Dev Biol, 1997. **182**(2): p. 240-55.

68. Rothermel, B., et al., *A protein encoded within the Down syndrome critical region is enriched in striated muscles and inhibits calcineurin signaling.* J Biol Chem, 2000. **275**(12): p. 8719-25.

69. Lai, M.M., et al., *Cain, a novel physiologic protein inhibitor of calcineurin.* J Biol Chem, 1998. **273**(29): p. 18325-31.

70. Kashishian, A., et al., *AKAP79 inhibits calcineurin through a site distinct from the immunophilin-binding region.* J Biol Chem, 1998. **273**(42): p. 27412-9.

71. Rothermel, B.A., et al., *Myocyte-enriched calcineurin-interacting protein, MCIP1, inhibits cardiac hypertrophy in vivo.* Proc Natl Acad Sci U S A, 2001. **98**(6): p. 3328-33.

72. Taigen, T., et al., *Targeted inhibition of calcineurin prevents agonist-induced cardiomyocyte hypertrophy.* Proc Natl Acad Sci U S A, 2000. **97**(3): p. 1196-201.

73. Bueno, O.F., et al., *Impaired cardiac hypertrophic response in Calcineurin Abeta -deficient mice.* Proc Natl Acad Sci U S A, 2002. **99**(7): p. 4586-91.

74. Goldspink, P.H., et al., *Angiotensin II induced cardiac hypertrophy in vivo is inhibited by cyclosporin A in adult rats.* Mol Cell Biochem, 2001. **226**(1-2): p. 83-8.

75. Lim, H.W. and J.D. Molkentin, *Calcineurin and human heart failure.* Nat Med, 1999. **5**(3): p. 246-7.

76. Sussman, M.A., et al., *Prevention of cardiac hypertrophy in mice by calcineurin inhibition.* Science, 1998. **281**(5383): p. 1690-3.

77. Liu, J., et al., *Calcineurin is a common target of cyclophilin-cyclosporin A and FKBP-FK506 complexes.* Cell, 1991. **66**(4): p. 807-15.

78. Okamura, H., et al., *Concerted dephosphorylation of the transcription factor NFAT1 induces a conformational switch that regulates transcriptional activity.* Mol Cell, 2000. **6**(3): p. 539-50.

79. Clipstone, N.A. and G.R. Crabtree, *Identification of calcineurin as a key signalling enzyme in T-lymphocyte activation.* Nature, 1992. **357**(6380): p. 695-7.

80. Keyser, P., K. Borge-Renberg, and D. Hultmark, *The Drosophila NFAT homolog is involved in salt stress tolerance.* Insect Biochem Mol Biol, 2007. **37**(4): p. 356-62.

81. Wilkins, B.J. and J.D. Molkentin, *Calcineurin and cardiac hypertrophy: where have we been? Where are we going?* J Physiol, 2002. **541**(Pt 1): p. 1-8.

82. Wilkins, B.J., et al., *Calcineurin/NFAT coupling participates in pathological, but not physiological, cardiac hypertrophy.* Circ Res, 2004. **94**(1): p. 110-8.

83. Levy, D., et al., *Prognostic implications of echocardiographically determined left ventricular mass in the Framingham Heart Study.* N Engl J Med, 1990. **322**(22): p. 1561-6.

84. Messerli, F.H. and R. Ketelhut, *Left ventricular hypertrophy: an independent risk factor.* J Cardiovasc Pharmacol, 1991. **17 Suppl 4**: p. S59-66; discussion S66-7.

85. Levy, D., et al., *Risk of ventricular arrhythmias in left ventricular hypertrophy: the Framingham Heart Study.* Am J Cardiol, 1987. **60**(7): p. 560-5.

86. Drazner, M.H., et al., *Increased left ventricular mass is a risk factor for the development of a depressed left ventricular ejection fraction within five years: the Cardiovascular Health Study.* J Am Coll Cardiol, 2004. **43**(12): p. 2207-15.

87. Smith, S.H. and S.P. Bishop, *Regional myocyte size in compensated right ventricular hypertrophy in the ferret.* J Mol Cell Cardiol, 1985. **17**(10): p. 1005-11.

88. van Berlo, J.H., M. Maillet, and J.D. Molkentin, *Signaling effectors underlying pathologic growth and remodeling of the heart.* J Clin Invest, 2013. **123**(1): p. 37-45.

89. Gerdes, A.M., S.E. Campbell, and D.R. Hilbelink, *Structural remodeling of cardiac myocytes in rats with arteriovenous fistulas.* Lab Invest, 1988. **59**(6): p. 857-61.

90. Calderone, A., et al., *Pressure- and volume-induced left ventricular hypertrophies are associated with distinct myocyte phenotypes and differential induction of peptide growth factor mRNAs.* Circulation, 1995. **92**(9): p. 2385-90.

91. Heineke, J. and J.D. Molkentin, *Regulation of cardiac hypertrophy by intracellular signalling pathways.* Nat Rev Mol Cell Biol, 2006. **7**(8): p. 589-600.

92. Rockman, H.A., W.J. Koch, and R.J. Lefkowitz, *Seven-transmembrane-spanning receptors and heart function.* Nature, 2002. **415**(6868): p. 206-12.

93. Lu, J., et al., *Signal-dependent activation of the MEF2 transcription factor by dissociation from histone deacetylases.* Proc Natl Acad Sci U S A, 2000. **97**(8): p. 4070-5.

94. Wilkins, B.J. and J.D. Molkentin, *Calcium-calcineurin signaling in the regulation of cardiac hypertrophy.* Biochem Biophys Res Commun, 2004. **322**(4): p. 1178-91.

95. Sugden, P.H. and A. Clerk, *"Stress-responsive" mitogen-activated protein kinases (c-Jun N-terminal kinases and p38 mitogen-activated protein kinases) in the myocardium.* Circ Res, 1998. **83**(4): p. 345-52.

96. Bueno, O.F., et al., *The MEK1-ERK1/2 signaling pathway promotes compensated cardiac hypertrophy in transgenic mice.* EMBO J, 2000. **19**(23): p. 6341-50.

97. Molkentin, J.D. and G.W. Dorn, 2nd, *Cytoplasmic signaling pathways that regulate cardiac hypertrophy.* Annu Rev Physiol, 2001. **63**: p. 391-426.

98. Hunter, J.J., et al., *Ventricular expression of a MLC-2v-ras fusion gene induces cardiac hypertrophy and selective diastolic dysfunction in transgenic mice.* J Biol Chem, 1995. **270**(39): p. 23173-8.

99. Sheng, Z., et al., *Cardiotrophin 1 (CT-1) inhibition of cardiac myocyte apoptosis via a mitogen-activated protein kinase-dependent pathway. Divergence from downstream CT-1 signals for myocardial cell hypertrophy.* J Biol Chem, 1997. **272**(9): p. 5783-91.

100. Parrizas, M., A.R. Saltiel, and D. LeRoith, *Insulin-like growth factor 1 inhibits apoptosis using the phosphatidylinositol 3'-kinase and mitogen-activated protein kinase pathways.* J Biol Chem, 1997. **272**(1): p. 154-61.

101. Sanna, B., et al., *Direct and indirect interactions between calcineurin-NFAT and MEK1-extracellular signal-regulated kinase 1/2 signaling pathways regulate cardiac gene expression and cellular growth.* Mol Cell Biol, 2005. **25**(3): p. 865-78.

102. Nicol, R.L., et al., *Activated MEK5 induces serial assembly of sarcomeres and eccentric cardiac hypertrophy.* EMBO J, 2001. **20**(11): p. 2757-67.

103. Aronow, B.J., et al., *Divergent transcriptional responses to independent genetic causes of cardiac hypertrophy.* Physiol Genomics, 2001. **6**(1): p. 19-28.

104. Seidman, C.E. and J.G. Seidman, *Identifying sarcomere gene mutations in hypertrophic cardiomyopathy: a personal history.* Circ Res, 2011. **108**(6): p. 743-50.

105. Enriquez, A.D. and M.E. Goldman, *Management of Hypertrophic Cardiomyopathy.* Ann Glob Health, 2014. **80**(1): p. 35-45.

106. Marian, A.J. and R. Roberts, *The molecular genetic basis for hypertrophic cardiomyopathy.* J Mol Cell Cardiol, 2001. **33**(4): p. 655-70.

107. Maron, B.J. and M.S. Maron, *Hypertrophic cardiomyopathy.* Lancet, 2013. **381**(9862): p. 242-55.

108. Kirschner, S.E., et al., *Hypertrophic cardiomyopathy-related beta-myosin mutations cause highly variable calcium sensitivity with functional imbalances among individual muscle cells.* Am J Physiol Heart Circ Physiol, 2005. **288**(3): p. H1242-51.

109. Lowey, S., *Functional consequences of mutations in the myosin heavy chain at sites implicated in familial hypertrophic cardiomyopathy.* Trends Cardiovasc Med, 2002. **12**(8): p. 348-54.

110. Colan, S.D., *Mechanics of left ventricular systolic and diastolic function in physiologic hypertrophy of the athlete's heart.* Cardiol Clin, 1997. **15**(3): p. 355-72.

111. Daniels, S.R., et al., *Effect of lean body mass, fat mass, blood pressure, and sexual maturation on left ventricular mass in children and adolescents. Statistical, biological, and clinical significance.* Circulation, 1995. **92**(11): p. 3249-54.

112. Lorell, B.H. and B.A. Carabello, *Left ventricular hypertrophy: pathogenesis, detection, and prognosis.* Circulation, 2000. **102**(4): p. 470-9.

113. Mesa, A., et al., *Left ventricular diastolic function in normal human pregnancy.* Circulation, 1999. **99**(4): p. 511-7.

114. Oudit, G.Y., et al., *The role of phosphoinositide-3 kinase and PTEN in cardiovascular physiology and disease.* J Mol Cell Cardiol, 2004. **37**(2): p. 449-71.

115. McMullen, J.R. and G.L. Jennings, *Differences between pathological and physiological cardiac hypertrophy: novel therapeutic strategies to treat heart failure.* Clin Exp Pharmacol Physiol, 2007. **34**(4): p. 255-62.

116. Chobanian, A.V., et al., *Seventh report of the Joint National Committee on Prevention, Detection, Evaluation, and Treatment of High Blood Pressure.* Hypertension, 2003. **42**(6): p. 1206-52.

117. *Guidelines for the evaluation and management of heart failure. Report of the American College of Cardiology/American Heart Association Task Force on Practice Guidelines (Committee on Evaluation and Management of Heart Failure).* Circulation, 1995. **92**(9): p. 2764-84.

118. Calhoun, D.A., et al., *Resistant hypertension: diagnosis, evaluation, and treatment: a scientific statement from the American Heart Association Professional Education Committee of the Council for High Blood Pressure Research.* Circulation, 2008. **117**(25): p. e510-26.

119. Moon, A., *Mouse models of congenital cardiovascular disease.* Curr Top Dev Biol, 2008. **84**: p. 171-248.

120. Ng, W.A., et al., *Cardiac myosin heavy chain mRNA expression and myocardial function in the mouse heart.* Circ Res, 1991. **68**(6): p. 1742-50.

121. Lompre, A.M., et al., *Species- and age-dependent changes in the relative amounts of cardiac myosin isoenzymes in mammals.* Dev Biol, 1981. **84**(2): p. 286-90.

122. Yazaki, Y., et al., *Cardiac atrial myosin adenosine triphosphatase of animals and humans: distinctive enzymatic properties compared with cardiac ventricular myosin.* Circ Res, 1979. **45**(4): p. 522-7.

123. Lopez, J.E., et al., *beta-myosin heavy chain is induced by pressure overload in a minor subpopulation of smaller mouse cardiac myocytes.* Circ Res, 2011. **109**(6): p. 629-38.

124. Lowes, B.D., et al., *Changes in gene expression in the intact human heart. Downregulation of alpha-myosin heavy chain in hypertrophied, failing ventricular myocardium.* J Clin Invest, 1997. **100**(9): p. 2315-24.

125. Rockman, H.A., et al., *Segregation of atrial-specific and inducible expression of an atrial natriuretic factor transgene in an in vivo murine model of cardiac hypertrophy.* Proc Natl Acad Sci U S A, 1991. **88**(18): p. 8277-81.

126. Colomer, J.M., et al., *Pressure overload selectively up-regulates Ca2+/calmodulin-dependent protein kinase II in vivo.* Mol Endocrinol, 2003. **17**(2): p. 183-92.

127. Naga Prasad, S.V., et al., *Gbetagamma-dependent phosphoinositide 3-kinase activation in hearts with in vivo pressure overload hypertrophy.* J Biol Chem, 2000. **275**(7): p. 4693-8.

128. Zhang, S., et al., *The role of the Grb2-p38 MAPK signaling pathway in cardiac hypertrophy and fibrosis.* J Clin Invest, 2003. **111**(6): p. 833-41.

129. Saadane, N., L. Alpert, and L.E. Chalifour, *Expression of immediate early genes, GATA-4, and Nkx-2.5 in adrenergic-induced cardiac hypertrophy and during regression in adult mice.* Br J Pharmacol, 1999. **127**(5): p. 1165-76.

130. Friddle, C.J., et al., *Expression profiling reveals distinct sets of genes altered during induction and regression of cardiac hypertrophy.* Proc Natl Acad Sci U S A, 2000. **97**(12): p. 6745-50.

131. D'Angelo, D.D., et al., *Transgenic Galphaq overexpression induces cardiac contractile failure in mice.* Proc Natl Acad Sci U S A, 1997. **94**(15): p. 8121-6.

132. Gomez, A.M., et al., *Defective excitation-contraction coupling in experimental cardiac hypertrophy and heart failure.* Science, 1997. **276**(5313): p. 800-6.

133. Sato, Y., et al., *Cardiac-specific overexpression of mouse cardiac calsequestrin is associated with depressed cardiovascular function and hypertrophy in transgenic mice.* J Biol Chem, 1998. **273**(43): p. 28470-7.

134. Zou, Y., et al., *Protein kinase C, but not tyrosine kinases or Ras, plays a critical role in angiotensin II-induced activation of Raf-1 kinase and extracellular signal-regulated protein kinases in cardiac myocytes.* J Biol Chem, 1996. **271**(52): p. 33592-7.

135. Takeishi, Y., et al., *In vivo phosphorylation of cardiac troponin I by protein kinase Cbeta2 decreases cardiomyocyte calcium responsiveness and contractility in transgenic mouse hearts.* J Clin Invest, 1998. **102**(1): p. 72-8.

136. Takeishi, Y., et al., *Transgenic overexpression of constitutively active protein kinase C epsilon causes concentric cardiac hypertrophy.* Circ Res, 2000. **86**(12): p. 1218-23.

137. Mochly-Rosen, D., et al., *Cardiotrophic effects of protein kinase C epsilon: analysis by in vivo modulation of PKCepsilon translocation.* Circ Res, 2000. **86**(11): p. 1173-9.

138. Feldman, A.M., et al., *Selective changes in cardiac gene expression during compensated hypertrophy and the transition to cardiac decompensation in rats with chronic aortic banding.* Circ Res, 1993. **73**(1): p. 184-92.

139. Ito, N., et al., *Remodelling of microvessels by coronary hypertension or cardiac hypertrophy in rats.* J Mol Cell Cardiol, 1994. **26**(1): p. 49-59.

140. Brown, L., et al., *Cardiac responses after norepinephrine-induced ventricular hypertrophy in rats.* J Cardiovasc Pharmacol, 1992. **20**(2): p. 316-23.

141. Cutilletta, A.F., et al., *Regression of myocardial hypertrophy. I. Experimental model, changes in heart weight, nucleic acids and collagen.* J Mol Cell Cardiol, 1975. **7**(10): p. 761-80.

142. Mertens, M.J., et al., *Depressed inotropic response to beta-adrenoceptor agonists in the presence of advanced cardiac hypertrophy in hearts from rats with induced aortic stenosis and from spontaneously hypertensive rats.* J Hypertens, 1992. **10**(11): p. 1361-8.

143. Toffolo, R.L. and C.D. Ianuzzo, *Myofibrillar adaptations during cardiac hypertrophy.* Mol Cell Biochem, 1994. **131**(2): p. 141-9.

144. Zheng, S., et al., *Retake the center stage--new development of rat genetics.* J Genet Genomics, 2012. **39**(6): p. 261-8.

145. Bohm, M., et al., *Beta-adrenergic neuroeffector mechanisms in cardiac hypertrophy of renin transgenic rats.* Hypertension, 1994. **24**(6): p. 653-62.

146. Hasenfuss, G., *Animal models of human cardiovascular disease, heart failure and hypertrophy.* Cardiovasc Res, 1998. **39**(1): p. 60-76.

147. Stainier, D.Y., *Zebrafish genetics and vertebrate heart formation.* Nat Rev Genet, 2001. **2**(1): p. 39-48.

148. Chico, T.J., P.W. Ingham, and D.C. Crossman, *Modeling cardiovascular disease in the zebrafish.* Trends Cardiovasc Med, 2008. **18**(4): p. 150-5.

149. Poss, K.D., *Getting to the heart of regeneration in zebrafish.* Semin Cell Dev Biol, 2007. **18**(1): p. 36-45.

150. Poss, K.D., L.G. Wilson, and M.T. Keating, *Heart regeneration in zebrafish.* Science, 2002. **298**(5601): p. 2188-90.

151. Chen, Y.H., et al., *Inactivation of Myosin binding protein C homolog in zebrafish as a model for human cardiac hypertrophy and diastolic dysfunction.* J Am Heart Assoc, 2013. **2**(5): p. e000231.

152. Sun, X., et al., *Cardiac hypertrophy involves both myocyte hypertrophy and hyperplasia in anemic zebrafish.* PLoS One, 2009. **4**(8): p. e6596.

153. Wolf, M.J. and H.A. Rockman, *Drosophila melanogaster as a model system for genetics of postnatal cardiac function.* Drug Discov Today Dis Models, 2008. **5**(3): p. 117-123.

154. Wolf, M.J. and H.A. Rockman, *Drosophila, genetic screens, and cardiac function.* Circ Res, 2011. **109**(7): p. 794-806.

155. Mohr, S.E., et al., *Resources for functional genomics studies in Drosophila melanogaster.* Genetics, 2014. **197**(1): p. 1-18.

156. Bellen, H.J., et al., *The Drosophila gene disruption project: progress using transposons with distinctive site specificities.* Genetics, 2011. **188**(3): p. 731-43.

157. Parks, A.L., et al., *Systematic generation of high-resolution deletion coverage of the Drosophila melanogaster genome.* Nat Genet, 2004. **36**(3): p. 288-92.

158. Thibault, S.T., et al., *A complementary transposon tool kit for Drosophila melanogaster using P and piggyBac.* Nat Genet, 2004. **36**(3): p. 283-7.

159. Rubin, G.M. and A.C. Spradling, *Genetic transformation of Drosophila with transposable element vectors.* Science, 1982. **218**(4570): p. 348-53.

160. Spradling, A.C. and G.M. Rubin, *Transposition of cloned P elements into Drosophila germ line chromosomes.* Science, 1982. **218**(4570): p. 341-7.

161. Handler, A.M., *Use of the piggyBac transposon for germ-line transformation of insects.* Insect Biochem Mol Biol, 2002. **32**(10): p. 1211-20.

162. Metaxakis, A., et al., *Minos as a genetic and genomic tool in Drosophila melanogaster.* Genetics, 2005. **171**(2): p. 571-81.

163. Bassett, A.R., et al., *Highly efficient targeted mutagenesis of Drosophila with the CRISPR/Cas9 system.* Cell Rep, 2013. **4**(1): p. 220-8.

164. Sebo, Z.L., et al., *A simplified and efficient germline-specific CRISPR/Cas9 system for Drosophila genomic engineering.* Fly (Austin), 2014. **8**(1): p. 52-7.

165. Yu, Z., et al., *Highly efficient genome modifications mediated by CRISPR/Cas9 in Drosophila.* Genetics, 2013. **195**(1): p. 289-91.

166. Katsuyama, T., et al., *An efficient strategy for TALEN-mediated genome engineering in Drosophila.* Nucleic Acids Res, 2013. **41**(17): p. e163.

167. Kondo, T., et al., *TALEN-induced gene knock out in Drosophila.* Dev Growth Differ, 2014. **56**(1): p. 86-91.

168. Liu, J., et al., *Efficient and specific modifications of the Drosophila genome by means of an easy TALEN strategy.* J Genet Genomics, 2012. **39**(5): p. 209-15.

169. Gratz, S.J., et al., *Highly specific and efficient CRISPR/Cas9-catalyzed homology-directed repair in Drosophila.* Genetics, 2014. **196**(4): p. 961-71.

170. Xue, Z., et al., *Efficient gene knock-out and knock-in with transgenic Cas9 in Drosophila.* G3 (Bethesda), 2014. **4**(5): p. 925-9.

171. Brand, A.H. and N. Perrimon, *Targeted gene expression as a means of altering cell fates and generating dominant phenotypes.* Development, 1993. **118**(2): p. 401-15.

172. O'Kane, C.J. and W.J. Gehring, *Detection in situ of genomic regulatory elements in Drosophila.* Proc Natl Acad Sci U S A, 1987. **84**(24): p. 9123-7.

173. Morin, X., et al., *A protein trap strategy to detect GFP-tagged proteins expressed from their endogenous loci in Drosophila.* Proc Natl Acad Sci U S A, 2001. **98**(26): p. 15050-5.

174. Kelso, R.J., et al., *Flytrap, a database documenting a GFP protein-trap insertion screen in Drosophila melanogaster.* Nucleic Acids Res, 2004. **32**(Database issue): p. D418-20.

175. Monier, B., et al., *Steroid-dependent modification of Hox function drives myocyte reprogramming in the Drosophila heart.* Development, 2005. **132**(23): p. 5283-93.

176. Lemaitre, B. and I. Miguel-Aliaga, *The digestive tract of Drosophila melanogaster.* Annu Rev Genet, 2013. **47**: p. 377-404.

177. Chapman, R.F., et al., *The insects structure and function*, 2013, Cambridge University Press,: Cambridge. p. 1 online resource (xxxi, 929 p.).

178. Williams, M.J., *Drosophila hemopoiesis and cellular immunity.* J Immunol, 2007. **178**(8): p. 4711-6.

179. Burmester, T. and T. Hankeln, *The respiratory proteins of insects.* J Insect Physiol, 2007. **53**(4): p. 285-94.

180. Wasserthal, L.T., *Drosophila flies combine periodic heartbeat reversal with a circulation in the anterior body mediated by a newly discovered anterior pair of ostial valves and 'venous' channels.* J Exp Biol, 2007. **210**(Pt 21): p. 3707-19.

181. Wasserthal, L.T., *Periodic heartbeat reversals cause cardiogenic inspiration and expiration with coupled spiracle leakage in resting blowflies, Calliphora vicina.* J Exp Biol, 2014. **217**(Pt 9): p. 1543-54.

182. Neely, G.G., et al., *A global in vivo Drosophila RNAi screen identifies NOT3 as a conserved regulator of heart function.* Cell, 2010. **141**(1): p. 142-53.

183. Lehmacher, C., B. Abeln, and A. Paululat, *The ultrastructure of Drosophila heart cells.* Arthropod Struct Dev, 2012. **41**(5): p. 459-74.

184. Yu, L., et al., *Affecting Rhomboid-3 function causes a dilated heart in adult Drosophila.* PLoS Genet, 2010. **6**(5): p. e1000969.

185. Vogler, G. and K. Ocorr, *Visualizing the beating heart in Drosophila.* J Vis Exp, 2009(31).

186. Paternostro, G., et al., *Age-associated cardiac dysfunction in Drosophila melanogaster.* Circ Res, 2001. **88**(10): p. 1053-8.

187. Ocorr, K., et al., *Semi-automated Optical Heartbeat Analysis of small hearts.* J Vis Exp, 2009(31).

188. Ocorr, K., et al., *KCNQ potassium channel mutations cause cardiac arrhythmias in Drosophila that mimic the effects of aging.* Proc Natl Acad Sci U S A, 2007. **104**(10): p. 3943-8.

189. Wolf, M.J., et al., *Drosophila as a model for the identification of genes causing adult human heart disease.* Proc Natl Acad Sci U S A, 2006. **103**(5): p. 1394-9.

190. Bodmer, R. and T.V. Venkatesh, *Heart development in Drosophila and vertebrates: conservation of molecular mechanisms.* Dev Genet, 1998. **22**(3): p. 181-6.

191. Cripps, R.M. and E.N. Olson, *Control of cardiac development by an evolutionarily conserved transcriptional network.* Dev Biol, 2002. **246**(1): p. 14-28.

192. Zaffran, S. and M. Frasch, *Early signals in cardiac development.* Circ Res, 2002. **91**(6): p. 457-69.

193. Zaffran, S., et al., *Cardiogenesis in the Drosophila model: control mechanisms during early induction and diversification of cardiac progenitors.* Cold Spring Harb Symp Quant Biol, 2002. **67**: p. 1-12.

194. Yu, L., et al., *Raf-mediated cardiac hypertrophy in adult Drosophila.* Dis Model Mech, 2013. **6**(4): p. 964-76.

195. Allikian, M.J., et al., *Reduced life span with heart and muscle dysfunction in Drosophila sarcoglycan mutants.* Hum Mol Genet, 2007. **16**(23): p. 2933-43.

196. Goldstein, J.A., et al., *SMAD signaling drives heart and muscle dysfunction in a Drosophila model of muscular dystrophy.* Hum Mol Genet, 2011. **20**(5): p. 894-904.

197. Wolf, M.J., *Modeling dilated cardiomyopathies in Drosophila.* Trends Cardiovasc Med, 2012. **22**(3): p. 55-61.

198. Fink, M., et al., *A new method for detection and quantification of heartbeat parameters in Drosophila, zebrafish, and embryonic mouse hearts.* Biotechniques, 2009. **46**(2): p. 101-13.

199. Wessells, R.J. and R. Bodmer, *Screening assays for heart function mutants in Drosophila.* Biotechniques, 2004. **37**(1): p. 58-60, 62, 64 passim.

200. Wessells, R.J., et al., *Insulin regulation of heart function in aging fruit flies.* Nat Genet, 2004. **36**(12): p. 1275-81.

201. Yin, Z. and M. Frasch, *Regulation and function of tinman during dorsal mesoderm induction and heart specification in Drosophila.* Dev Genet, 1998. **22**(3): p. 187-200.

202. Gunthorpe, D., K.E. Beatty, and M.V. Taylor, *Different levels, but not different isoforms, of the Drosophila transcription factor DMEF2 affect distinct aspects of muscle differentiation.* Dev Biol, 1999. **215**(1): p. 130-45.

203. Beall, C.J. and E. Fyrberg, *Muscle abnormalities in Drosophila melanogaster heldup mutants are caused by missing or aberrant troponin-I isoforms.* J Cell Biol, 1991. **114**(5): p. 941-51.

204. Barolo, S., L.A. Carver, and J.W. Posakony, *GFP and beta-galactosidase transformation vectors for promoter/enhancer analysis in Drosophila.* Biotechniques, 2000. **29**(4): p. 726, 728, 730, 732.

205. Tokoyoda, K., et al., *Synergism between the calmodulin-binding and autoinhibitory domains on calcineurin is essential for the induction of their phosphatase activity.* J Biol Chem, 2000. **275**(16): p. 11728-34.

206. Burkard, N., et al., *Targeted proteolysis sustains calcineurin activation.* Circulation, 2005. **111**(8): p. 1045-53.

207. Kang, Y.J., et al., *Calcineurin negatively regulates TLR-mediated activation pathways.* J Immunol, 2007. **179**(7): p. 4598-607.

208. Ashburner, M., *Drosophila*. 1989, Cold Spring Harbor, N.Y.: Cold Spring Harbor Laboratory.

209. Arca, B., et al., *Mobilization of a Minos transposon in Drosophila melanogaster chromosomes and chromatid repair by heteroduplex formation.* Genetics, 1997. **145**(2): p. 267-79.

210. Lo, P.C. and M. Frasch, *A role for the COUP-TF-related gene seven-up in the diversification of cardioblast identities in the dorsal vessel of Drosophila.* Mech Dev, 2001. **104**(1-2): p. 49-60.

211. Yin, Z., X.L. Xu, and M. Frasch, *Regulation of the twist target gene tinman by modular cis-regulatory elements during early mesoderm development.* Development, 1997. **124**(24): p. 4971-82.

212. Cook, R.K., et al., *The generation of chromosomal deletions to provide extensive coverage and subdivision of the Drosophila melanogaster genome.* Genome Biol, 2012. **13**(3): p. R21.

213. Reim, I. and M. Frasch, *The Dorsocross T-box genes are key components of the regulatory network controlling early cardiogenesis in Drosophila.* Development, 2005. **132**(22): p. 4911-25.

214. Holden, H.M., et al., *Galactokinase: structure, function and role in type II galactosemia.* Cell Mol Life Sci, 2004. **61**(19-20): p. 2471-84.

215. Chu, G., et al., *Enhanced myocyte contractility and Ca2+ handling in a calcineurin transgenic model of heart failure.* Cardiovasc Res, 2002. **54**(1): p. 105-16.

216. Jiang, D.S., et al., *IRF8 suppresses pathological cardiac remodelling by inhibiting calcineurin signalling.* Nat Commun, 2014. **5**: p. 3303.

217. Xu, J., et al., *Myocyte enhancer factors 2A and 2C induce dilated cardiomyopathy in transgenic mice.* J Biol Chem, 2006. **281**(14): p. 9152-62.

218. Wu, X., et al., *Local InsP3-dependent perinuclear Ca2+ signaling in cardiac myocyte excitation-transcription coupling.* J Clin Invest, 2006. **116**(3): p. 675-82.

219. Gjesdal, O., D.A. Bluemke, and J.A. Lima, *Cardiac remodeling at the population level--risk factors, screening, and outcomes.* Nat Rev Cardiol, 2011. **8**(12): p. 673-85.

220. Du, X.J., et al., *Impaired cardiac contractility response to hemodynamic stress in S100A1-deficient mice.* Mol Cell Biol, 2002. **22**(8): p. 2821-9.

221. Frank, K. and E.G. Kranias, *Phospholamban and cardiac contractility.* Ann Med, 2000. **32**(8): p. 572-8.

222. Most, P., et al., *S100A1: a regulator of myocardial contractility.* Proc Natl Acad Sci U S A, 2001. **98**(24): p. 13889-94.

223. Newsholme, E.A., et al., *The role of creatine kinase and arginine kinase in muscle.* Biochem J, 1978. **172**(3): p. 533-7.

224. Brower, D.L., *Engrailed gene expression in Drosophila imaginal discs.* EMBO J, 1986. **5**(10): p. 2649-56.

225. de Celis, J.F., *Expression and function of decapentaplegic and thick veins during the differentiation of the veins in the Drosophila wing.* Development, 1997. **124**(5): p. 1007-18.

226. Lee, J.J., et al., *Secretion and localized transcription suggest a role in positional signaling for products of the segmentation gene hedgehog.* Cell, 1992. **71**(1): p. 33-50.

227. Mohler, J., et al., *Activation of knot (kn) specifies the 3-4 intervein region in the Drosophila wing.* Development, 2000. **127**(1): p. 55-63.

228. Johnson, S.A. and M.J. Milner, *The final stages of wing development in Drosophila melanogaster.* Tissue Cell, 1987. **19**(4): p. 505-13.

229. Kiger, J.A., Jr., et al., *Tissue remodeling during maturation of the Drosophila wing.* Dev Biol, 2007. **301**(1): p. 178-91.

230. Karr, T.L., et al., *Patterns of engrailed protein in early Drosophila embryos.* Development, 1989. **105**(3): p. 605-12.

231. Drees, B., et al., *The transcription unit of the Drosophila engrailed locus: an unusually small portion of a 70,000 bp gene.* EMBO J, 1987. **6**(9): p. 2803-9.

232. Blair, S.S., *Engrailed expression in the anterior lineage compartment of the developing wing blade of Drosophila.* Development, 1992. **115**(1): p. 21-33.

233. Chang, T., et al., *Dpp and Hh signaling in the Drosophila embryonic eye field.* Development, 2001. **128**(23): p. 4691-704.

234. Jackson, P.D. and F.M. Hoffmann, *Embryonic expression patterns of the Drosophila decapentaplegic gene: separate regulatory elements control blastoderm expression and lateral ectodermal expression.* Dev Dyn, 1994. **199**(1): p. 28-44.

235. Yu, K., et al., *The Drosophila decapentaplegic and short gastrulation genes function antagonistically during adult wing vein development.* Development, 1996. **122**(12): p. 4033-44.

236. Bosch, A.M., et al., *Clinical features of galactokinase deficiency: a review of the literature.* J Inherit Metab Dis, 2002. **25**(8): p. 629-34.

237. Ai, Y., et al., *A mouse model of galactose-induced cataracts.* Hum Mol Genet, 2000. **9**(12): p. 1821-7.

238. Tegtmeyer, L.C., et al., *Multiple phenotypes in phosphoglucomutase 1 deficiency.* N Engl J Med, 2014. **370**(6): p. 533-42.

239. Suzuki, O., et al., *Adult onset cardiac dilatation in a transgenic mouse line with Galbeta1,3GalNAc alpha2,3-sialyltransferase II (ST3Gal-II) transgenes: a new model for dilated cardiomyopathy.* Proc Jpn Acad Ser B Phys Biol Sci, 2011. **87**(8): p. 550-62.

240. Yi, P., et al., *The mevalonate pathway controls heart formation in Drosophila by isoprenylation of Ggamma1.* Science, 2006. **313**(5791): p. 1301-3.

241. Zenke, F.T., et al., *Activation of Gal4p by galactose-dependent interaction of galactokinase and Gal80p.* Science, 1996. **272**(5268): p. 1662-5.

242. Partridge, E.A., et al., *Regulation of cytokine receptors by Golgi N-glycan processing and endocytosis.* Science, 2004. **306**(5693): p. 120-4.

243. Wierenga, K.J., et al., *High-throughput screening for human galactokinase inhibitors.* J Biomol Screen, 2008. **13**(5): p. 415-23.

244. Caulfield, J.B., *Fine structure of normal and diseased heart.* Prog Cardiovasc Dis, 1963. **5**: p. 610-30.

245. Anversa, P., et al., *Experimental cardiac hypertrophy: a quantitative ultrastructural study in the compensatory stage.* J Mol Cell Cardiol, 1971. **3**(3): p. 213-27.

246. Page, E. and L.P. McCallister, *Quantitative electron microscopic description of heart muscle cells. Application to normal, hypertrophied and thyroxin-stimulated hearts.* Am J Cardiol, 1973. **31**(2): p. 172-81.

247. Choma, M.A., et al., *Heart wall velocimetry and exogenous contrast-based cardiac flow imaging in Drosophila melanogaster using Doppler optical coherence tomography.* J Biomed Opt, 2010. **15**(5): p. 056020.

248. Roote, J. and S. Russell, *Toward a complete Drosophila deficiency kit.* Genome Biol, 2012. **13**(3): p. 149.

249. Field, T.L., W.S. Reznikoff, and P.A. Frey, *Galactose-1-phosphate uridylyltransferase: identification of histidine-164 and histidine-166 as critical residues by site-directed mutagenesis.* Biochemistry, 1989. **28**(5): p. 2094-9.

250. Najjar, V.A., *The isolation and properties of phosphoglucomutase.* J Biol Chem, 1948. **175**(1): p. 281-90.

251. Depre, C., M.H. Rider, and L. Hue, *Mechanisms of control of heart glycolysis.* Eur J Biochem, 1998. **258**(2): p. 277-90.

252. Van den Steen, P., et al., *Concepts and principles of O-linked glycosylation.* Crit Rev Biochem Mol Biol, 1998. **33**(3): p. 151-208.

253. Claycomb, W.C., et al., *HL-1 cells: a cardiac muscle cell line that contracts and retains phenotypic characteristics of the adult cardiomyocyte.* Proc Natl Acad Sci U S A, 1998. **95**(6): p. 2979-84.

Biography

Teresa Ena Lee was born in Urbana-Champaign, Illinois, 1983 to Shuo-Jen and Huei-Ju Lee. She majored in Biology at National Cheng Kung University, Tainan, Taiwan 2001-2005, where she obtained her B.S. degree. She then attended National Yang Ming University, Taipei, Taiwan 2005-2007, where she obtained her M.S. degree in Physiology. She was admitted to Duke University through the program of Cell and Molecular Biology, 2007, and joined the department of Cell Biology, working in Dr. Howard Rockman's lab in 2008. She received a pre-doctoral fellowship from the American Heart Association 2011-2013.

Publications:

Yu, L., Lee, T.E. *et al*. Affecting Rhomboid-3 function causes a dilated heart in adult *Drosophila*. PLoS Genet. 6(5):e1000969 (2010)

Abraham, D.M., Lee, T.E. *et al*. TREK-1 mediates diastolic dysfunction after pressure overload. (2014, in preparation)

Lee, T.E., Yu, L., Wolf, M.J., and Rockman, H.A. Galactokinase is a novel modifier of calcineurin-induced cardiomyopathy in *Drosophila*. (2014 accepted, Genetics)